

JPRS-CST-85-008

27 March 1985

CHINA REPORT  
SCIENCE AND TECHNOLOGY

**DISTRIBUTION STATEMENT A**  
Approved for Public Release  
Distribution Unlimited

FBIS FOREIGN BROADCAST INFORMATION SERVICE

**DTIC QUALITY INSPECTED**

REPRODUCED BY  
NATIONAL TECHNICAL  
INFORMATION SERVICE  
U.S. DEPARTMENT OF COMMERCE  
SPRINGFIELD, VA. 22161

19990416 132

#### NOTE

JPRS publications contain information primarily from foreign newspapers, periodicals and books, but also from news agency transmissions and broadcasts. Materials from foreign-language sources are translated; those from English-language sources are transcribed or reprinted, with the original phrasing and other characteristics retained.

Headlines, editorial reports, and material enclosed in brackets [] are supplied by JPRS. Processing indicators such as [Text] or [Excerpt] in the first line of each item, or following the last line of a brief, indicate how the original information was processed. Where no processing indicator is given, the information was summarized or extracted.

Unfamiliar names rendered phonetically or transliterated are enclosed in parentheses. Words or names preceded by a question mark and enclosed in parentheses were not clear in the original but have been supplied as appropriate in context. Other unattributed parenthetical notes within the body of an item originate with the source. Times within items are as given by source.

The contents of this publication in no way represent the policies, views or attitudes of the U.S. Government.

#### PROCUREMENT OF PUBLICATIONS

JPRS publications may be ordered from the National Technical Information Service, Springfield, Virginia 22161. In ordering, it is recommended that the JPRS number, title, date and author, if applicable, of publication be cited.

Current JPRS publications are announced in Government Reports Announcements issued semi-monthly by the National Technical Information Service, and are listed in the Monthly Catalog of U.S. Government Publications issued by the Superintendent of Documents, U.S. Government Printing Office, Washington, D.C. 20402.

Correspondence pertaining to matters other than procurement may be addressed to Joint Publications Research Service, 1000 North Glebe Road, Arlington, Virginia 22201.

27 March 1985

# CHINA REPORT

## SCIENCE AND TECHNOLOGY

### CONTENTS

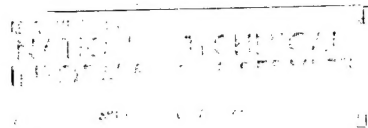
#### PEOPLE'S REPUBLIC OF CHINA

##### NATIONAL DEVELOPMENTS

- Large Input Into Training, Information Exchange Programs  
(Thomas Neumaier; FRANKFURTER ZEITUNG/BLICK DURCH DIE  
WIRTSCHAFT, 18 Jan 85) ..... 1
- Minister Jiang on Electronics Development  
(Jiang Zemin; Beijing Domestic Service, 10 Feb 85) ..... 5

##### APPLIED SCIENCES

- New Powered Glider Debuts Over Shenyang  
(LIAONING RIBAO, 8 Dec 84) ..... 10
- Research Wins Acclaim for 'Ion Doping' Technology  
(Wu Zhendong, Li Jinsheng; SHANXI RIBAO, 19 Sep 84) ..... 11
- Development of Sol-Gel-Sphere-Pac Fuel Element  
(Liu Naixin; HE DONGLI GONGCHENG, No 4, Aug 84) ..... 15
- Distance-Inertial Guidance of Launch Vehicle Described  
(Guo Xiaokuan, et al.; ZIDONGHUA XUEBAO, No 4, Oct 84) ..... 31
- Systems Research on 'China in Year 2000'  
(Wang Huijiang, Li Boxi; XITONG GONGCHENG LILUN YU SHIJIAN,  
No 2, 1984) ..... 37
- Potential at Atomic Boundaries in the TF (OR TFD) Model and  
Equations of States  
(Cheng Kaijia, et al.; WULI XUEBAO, No 2, Feb 84) ..... 51
- Waveform Control and Application of Detonation Wave in Explosives  
(Chen Weibo; LIXUE YU SHIJIAN, No 5, 1984) ..... 74



Briefs		
Recombinant Vaccine Virus		84
LIFE SCIENCES		
Application of YAG Laser to Otorhinolaryngology		
(Ru Yizhong, Meng Zhaohe; YINGYONG JIGUANG, No 4, Aug 84)		85
ABSTRACTS		
ACOUSTICS		
YINGYONG SHENGXUE [APPLIED ACOUSTICS], No 4, Oct 84 .....		88
AERODYNAMICS		
KONGQIDONGLIXUE XUEBAO [ACTA AERODYNAMICA SINICA], No 4, 1984		92
APPLIED MATHEMATICS		
YINGYONG SHUXUE XUEBAO [ACTA MATHEMATICAE APPLICATAE SINICA], No 4, Oct 84 .....		96
BIOCHEMISTRY		
SHENGWU HUAXUE YU SHENGWU WULIXUE JINZHAN [BIOCHEMISTRY AND BIOPHYSICS], No 5, Oct 84) .....		97
CHEMISTRY		
YOUJI HUAXUE [ORGANIC CHEMISTRY], No 3, Jun 84 .....		98
ELECTRONICS		
DIANZI XUEBAO [ACTA ELECTRONICA SINICA], No 4, Jul 84 .....		99
DIANZI KEXUE XUEKAN [JOURNAL OF ELECTRONICS], No 1, Jan 85 .....		102
ENGINEERING		
ZHONGGUO KEXUE JISHU DAXUE XUEBAO [JOURNAL OF CHINA UNIVERSITY OF SCIENCE AND TECHNOLOGY], No 3, Sep 84 .....		109
MECHANICS		
YINGYONG SHUXUE HE LIXUE [ACTA MATHEMATICS AND MECHANICS], No 5, Sep 84 .....		113



## MOLECULAR SCIENCE

- FENZI KEXUE YU HUAXUE YANJIU [JOURNAL OF MOLECULAR SCIENCE], No 1,  
Mar 84 ..... 116

## OCEANOLOGY

- NANHAI HAIYANG KEXUE JIKAN [NANHAI STUDIA MARINA SINICA], Nos 2,  
3, 5, various dates ..... 118
- SHANDONG HAIYANG XUEYUAN XUEBAO [JOURNAL OF SHANDONG COLLEGE OF  
OCEANOLOGY], No 3, 15 Sep 84 ..... 123

## OPTICS

- GUANGXUE XUEBAO [ACTA OPTICA SINICA], No 11, Nov 84 ..... 124

## PHARMACOLOGY

- YAOXUE XUEBAO [ACTA PHARMACEUTICA SINICA], Nos 10, 11, 20 Oct,  
29 Nov 84 ..... 129

## PHYSICS

- HEJUBIAN YU DENGLIZITI WULI [NUCLEAR FUSION AND PLASMA PHYSICS],  
No 4, 15 Dec 84 ..... 132

## VIROLOGY

- ZHONGGUO YIXUE KEXUEYUAN XUEBAO [ACTA ACADEMIAE MEDICINAE SINICAE],  
No 6, 15 Dec 84 ..... 138

## NATIONAL DEVELOPMENTS

### LARGE INPUT INTO TRAINING, INFORMATION EXCHANGE PROGRAMS

Frankfurt/Main FRANKFURTER ZEITUNG/BLICK DURCH DIE WIRTSCHAFT in German  
18 Jan 85 p 3

[Article by Engr Thomas Neumaier: "China Wants To Make More Use of German Know-How--Comprehensive Technical Cooperation Has Begun"]

[Text] The Far Eastern power of China is trying intensively today to meet its economic requirements with the aid of developmental millions from Bonn and with know-how from the Federal Republic. Twenty million DM of developmental aid reached the Middle Kingdom in 1983; a year later the amount was 25 million DM. And this year, 30 million DM is planned for Sino-German technical cooperation.

The extent of Chinese interest in such projects is seen from the multitude of project requests which have reached the Federal Government since 1980. Meanwhile, some 80 projects, including the so-called GTZ Measures, have been under discussion at the German Society for Technical Collaboration (GTZ) GmbH in Eschborn.

The most important areas in which the Eschborn federal enterprise is making German know-how available are: the entire area of institutions which are of great significance to the development of the economy such as the patent office; further, institutions similar to the TUeV [Technical Supervision Association], control, standardization and normative institutions, institutions for quality control--in other words, infrastructure institutions which are suitable to increase the quality of production and, thus, improve China's position in the world market.

The second most important area is the energy economy, particularly the coal industry. The third point of emphasis is agriculture. There are a number of agricultural pilot projects, such as, for example, insect control in forestry, reforestation with rapidly growing varieties or agricultural research projects. All of these are systematic steps which are intended to help promote the modernization of industry, to improve the energy bases of the country and, wherever possible, to utilize new knowledge toward improvement of agricultural production.

Following are four examples of Sino-German cooperation: following the end of the cultural revolution and the time that China, after the death of Mao, gradually opened up to Western markets the Chinese also decided to establish a national patent system. This was to be understood as an expression of the modification of the beginnings of planned economic moves during which economic self-initiatives would be called for in a stronger manner. With the introduction of a trademark system, technical progress is to be further developed as an important productive force of the Chinese economy.

On the basis of detailed consultations with German and other foreign patent authorities, a Chinese patent office was established in Beijing in 1980. In the spring of 1981, the Chinese requested German support. As early as the fall of 1981, the GTZ, together with the German Patent Office, undertook an inventory of all available personnel, institutional, and material resources. The GTZ then began its cooperation with the Chinese Patent Office in 1983. In July 1984 the first two German long-term experts moved to China.

The task of the German specialists is, on the one hand, advising the developing Chinese authority on questions of management, organization and personnel planning in administration. On the other hand, they will cooperate with the Chinese specialists in working out proposals for the patent granting procedure (formal testing, material-legal testing of patentability, appeals procedures), sample procedures, as well as legal procedures. The GTZ will be using some short-term experts in the following areas: patent procedure, publication activity, documentation, legal provisions, organization of automatic data processing and printing. Beyond that, Chinese counterparts (specialists) will receive training and postgraduate training in the Federal Republic of Germany (a total of 771 man-months).

The education and training of the Chinese specialists is currently in high gear. The Chinese are making efforts to complete the new buildings of the patent office soon, so that the German equipment can be delivered and installed rapidly. According to current plans, this is to take place in mid-1985. The Federal Republic of Germany is allocating a total of 12 million DM for this project (which will have a preliminary running time through 1988). The expenditures include 37 short-term experts for up to 110 man-months.

The Federal Ministry for Economic Cooperation and the Land Baden-Wuerttemberg are supporting the People's Republic of China through the GTZ with respect to the establishment of an industrial management training center (SIMTC) in Shanghai. On the basis of a Chinese project request, the GTZ was ordered by the Bonn Ministry for Development in fall of 1982 to work up recommendations regarding the decision and further steps. The GTZ also used the specialized knowledge of the German consulting industry in this event. Specialists determined that the management center in Shanghai would play an important role in passing on practical management knowledge and tested management procedures in the industrial arena to Chinese leaders. They furthermore determined that course programs involving enterprise management, production, sales, marketing and finances were required and would be augmented by brief branch-specific courses.

Following a Chinese-German examination of the project, the Chinese formally established the management center. Its development is to extend over a 5-year period. In mid-1984, the GTZ began the detailed planning and establishment of learning goals and course contents. In doing so, it worked with a team of specialists which have been dealing with similar tasks for many years in Germany. Within the framework of detailed planning a workshop was held in Shanghai in August 1984. It served the exchange of experiences between representatives of Chinese industry and practical experts of the German economy who were able to call on their experiences in collaboration between both countries in industry.

The planned 5-year German-Chinese cooperation encompasses four components, namely detailed project preparation, training of Chinese instructors, preparation of teaching material and the holding of training courses. During the course of German cooperation with the SIMTC, it is presumed that some 1,200 Chinese industrial managers would be trained in modern management principles.

The development of a national standardization system is indispensable with respect to the planned industrialization, particularly in light industry and in the consumer industry. Since international standardization does not yet exist in sufficient volume and since the country does not wish to become unilaterally dependent on any one industrial nation by taking on a ready-made foreign standardization system, China must develop a normative system of its own. In doing so, it is striving for intensive cooperation with the Federal Republic of Germany. The project is charged to the China Standards Information Center. The project, which is expected to run 4 to 5 years, has as its goal the establishment of an information center within the Chinese State Main Office for Standardization which would be in a position to pass national and international standards rapidly and precisely to users in China.

On the basis of a contract concluded between the Ministry of Economics of Baden-Wuerttemberg and the GTZ, dated 1983, the Chinese are to receive assistance in establishing a professional training center in Beijing. The purpose of the project--the supervising entity is the Ministry of Machinebuilding--is to establish a training facility with a capacity for 100 trainees and adequate training courses for young Chinese. The objective is to train specialized workers (apprentices), the continued training of specialized workers who have experience and the training of middle technical managers (master workers) in the professions of toolmaker and electrotechnician.

Baden-Wuerttemberg is assigning a total of 2 million DM from budgetary funds to this project. The Chinese partners have stated their willingness to contribute 25 percent of this amount for the project. As far as Germany is concerned, a total of some 4.7 million DM are available for this project which is planned for 1987. In the meantime, the GTZ was able to provide the equipment for the project; it is already in Beijing and has been installed by short-term experts. The training places have also been prepared. Eight Chinese specialists who were in the Federal Republic for advanced training have returned to their country. The first two German long-term experts were sent to China in October 1984.

The GTZ will, in the future, assign considerable significance to cooperation with China. It will, thus, primarily utilize the know-how of the German economy and of German consulting firms. Thus far, around 60 experts--primarily short-term experts--have traveled through the giant land between the Himalayas and the Sea of China in behalf of the GTZ. They have made expert studies, held seminars and made their initial contacts.

5911

CSO: 3620/260

27 March 1985

## NATIONAL DEVELOPMENTS

## MINISTER JIANG ON ELECTRONICS DEVELOPMENT

OW112317 Beijing Domestic Service in Mandarin 0630 GMT 10 Feb 85

[Address by Jiang Zemin, minister of electronics industry, entitled: "The Vigorous Development of China's Electronics Industry" in the "Sunday Lecture" program; date and place not given--recorded]

[Excerpts] People throughout the country are interested in the development of our country's electronics industry. Today, I want to introduce the situation in the development of China's electronics industry to the broad masses of listeners throughout the country.

China's electronics industry is a new industrial department, developed since the founding of new China. Before national liberation, our country's electronics industry was almost nonexistent. There were only about a dozen simple and small plants for repair and installation work.

After liberation, the party and state have paid great attention to the development of the electronics industry. Through 35 years of effort, we have built an electronics industry system on a relatively broad scale, which occupies a very important position in the national economy. The entire system has more than 2,600 electronics enterprises and related units with a total of 1.4 million staff members and workers, of which some 140,000 are engineers and technicians. The total annual output value has reached more than 20 billion yuan.

I shall introduce the road of development in our country's electronic industry and its prospects through the following three points:

1. Building Industry With Great Effort; Making Progress in a Tortuous Way

At the time of national liberation, we took over 11 small radio plants from bureaucratic capital. A telecommunications industry bureau was set up in 1950, running the electronics industry. This was the birth of China's electronics industry.

For 8 years, despite our country's economic difficulties, the state supported the building of a foundation for the electronics industry on a relatively large scale, and carried out technical transformation. We built, and put into operation 38 projects, and set up 9 electronics research institutes. We also carried out technical transformation for the old plants, and supported the development of the electronics industry in various localities. A number of

electronics enterprise groups were built centering on Beijing, Nanjing, Chengdu, Xian, Baoji, and other cities.

During the Great Cultural Revolution, the counterrevolutionary clique of Lin Biao and the gang of four seriously interfered with, and undermined, the major issues in the development of the electronics industry. Development of the industry suffered a serious setback. Nevertheless, due to the need for electronics products for national defense, and by dint of the great efforts of staff members and workers on the electronics industry front, we still made progress in some fields in the development of the industry.

## 2. Taking Positive Steps in Readjustment; Vigorously Developing the Industry

Since 1978, under the guidance of the line, principles, and policies formulated by the 3d Plenary Session of the 11th CPC Central Committee, our country's electronics industry has gradually taken on a stable and healthy development. In 1983, we reached the goal set for the last year of the Sixth 5-Year Plan 2 years ahead of schedule. In 1984, the total output value of the industry and profit realized both doubled those in 1980.

The development of the electronics industry during the above-mentioned period had the following special characteristics:

First, the industry developed at a fast pace. In 1984, its total output value increased by 45.4 percent, compared with 1983. The output of electronics products of various generations increased by a great margin in 1984. Compared with those in 1983, the output of miniature calculators increased 5.8 times, external parts for calculators 2.7 times, television sets 43.2 percent, of which the annual output of color television sets exceeded 1 million, an increase of 90.3 percent, recorders 45.7 percent, integrated circuits 66 percent, and electronic parts 47.1 percent. The output of many products increased several hundred times compared with the period before the convocation of the 3d Plenary Session of the 11th CPC Central Committee. For instance, the output of miniature calculators increased 400 times, television sets 17 times, of which color television sets increased 270 times, and recorders 142 times. This is a cheering situation.

Second, the industry has achieved good economic results. In 1984, both profit and tax to be turned over to the state and the industry's output value increased by 50 percent compared with 1983. We achieved success in both speed and economic results. Labor productivity in that year reached more than 16,000 yuan per person, an increase of 48 percent over the previous year. It should be pointed out that the above-mentioned good economic results were achieved in a situation in which the costs of energy and raw materials went up, while the price of electronics products steadily decreased.

Third, we have achieved significant results in scientific research. In recent years, the electronics industry departments carried out research, manufactured and provided large quantities of advanced electronics equipment for our country's launch of the carrier rocket across the Pacific Ocean, and launch of a submarine rocket. In April 1984, our country successfully launched the first



synchronous communications satellite. We again completed research and production of electronics equipment for new monitoring, control, and telecommunications system. We provided more than 1,500 sets of electronics equipment and large quantities of highly reliable parts and instruments. Those products functioned normally and insured the success of the launch and experiment.

Following the building of ground receiving stations in Nanjing, Beijing, Kunming, Urumqi, and Shijiazhuang, our country completed the building of a satellite ground receiving station in Lhasa on 1 October 1984. The people of Xizang for the first time saw the grand celebration of the 35th anniversary of the founding of the People's Republic of China live.

In the field of radar technology, the industry has designed China's own long-distance radar, which reached a very high level of performance in tracking, accurately detecting, and forecasting the Soviet Union's nuclear-powered satellite, and won a good reputation for our country.

In the manufacture of electronics, parts and equipment, the industry designed a 40 mm low-light [wei guang] pickup tube for man-made satellite's laser equipment, which could detect the smallest satellite launched by the United States.

Fourth, the industry has made progress in serving technical transformation of other industries. Technical transformation in various departments of the national economy urgently requires electronic products. We have provided more and more electronics equipment and facilities for various departments of the national economy, including petroleum, electric power, railways, shipbuilding, the metallurgical industry, textile industry, posts and telecommunications, radio and television, cultural and educational work, and public health work in order to serve the national economy. This has played an important role in promoting the technical progress of those departments.

Fifth, the quality of products has been raised significantly. Since the evaluation of outstanding products began in 1978, the electronics industry has received 15 gold and 121 silver prizes for its outstanding products.

Sixth, the industry has made significant improvements in its technical and economic foundation. During the period from 1978 to 1984, 55 projects were completed and put into operation. Completion of those projects has greatly raised the level of technology in our country's radio and television work and computer industry, and also increased production efficiency and self-sufficient capability. Fruitful results can already be seen. For instance, since completion of the Shaanxi Color Kinescope Plant, actual production capacity reached 960,000 tubes a year ahead of schedule. In 1984, the plant produced nearly a million kinescopes, and its profit exceeded 100 million yuan. It has made contributions to the development of our country's electronics industry.

### 3. Broad Prospects, Heavy Responsibility, and a Long Way to Go

In recent years, China has made considerable progress in developing its electronics industry. However, there are still many problems and shortcomings, which are mainly as follows: Both the production technology and research



methods used in our electronics industry are backward. Lacking a sound technological foundation, our electronics industry is far behind that of economically developed countries. Electronics products for use as means of production account for only a small portion of the total production, and have, as yet, to be widely applied. Although production of electronics consumer products has risen considerably in recent years, a relatively large portion of them are assembled with imported components. The output of many products cannot meet the ever-increasing demands of the people's daily life. Chinese-made electronics products are not competitive on the international market. The export market for our electronic products has not been really opened.

To implement the strategic plan and achieve the target for developing our electronics industry, we are prepared to grasp the following five major tasks in 1985 and for a certain period to come:

The first major task is to make further efforts to straighten our guiding thought, and speed up the two changes. The strategic plan for developing the electronics and information industries stipulates that two changes be made during the Seventh 5-Year Plan period. One change is that emphasis in this industry should be shifted to serving the needs of the national economy, the program of the four modernizations, and the daily life of people throughout society. The other change is that the electronics industry should be developed in such a way as to take microelectronics technology as the foundation, and computers and telecommunications equipment as the main products. The two changes are imperative in building an electronics industry structure with Chinese characteristics.

The second major task is to emancipate the mind and quicken the pace of reform in the economic structure of the electronics industry. The general concept of economic structural reform of this industry consists of the following: First, we should streamline administration, delegate power to lower levels, and further expand the decisionmaking power of various enterprises, to change the state of affairs in enterprises overly controlled by government organs, and to increase the vitality of enterprises. Two, we should let enterprises develop economic associations and socialized and specialized production, so as to radically solve such problems as big and complete enterprises, small but complete enterprises, barriers between departments and regions, and [words indistinct]. Three, we should change the administrative organizations of the electronics industry and the functions of these organizations, make a distinction between the governments' duties and responsibilities, and those of enterprises, and strengthen the management of various branches of this industry. The above concept is expected to be realized within 2 years.

The third major task is to further open to the outside world and accelerate the introduction of foreign capital and advanced technology into our country. Emphasis should be placed on implementing the principle of introducing foreign capital and advanced technology into our country, digesting them, making new developments, and creating our own new technology. Specifically, we should do four jobs: One, we should carry out a flexible policy and adopt flexible

measures to introduce capital and technology from abroad through numerous channels. More efforts should be made to develop joint ventures and cooperative production projects, and provide a still better condition and climate for the establishment and development of enterprises with Chinese and foreign investment. Two, we should raise the minimum level of technology to be imported from abroad, and increase the proportion of high and basic technology introduced into our country. Attention should be paid to introducing from abroad new product designs, technology which can be used for developing new products, and technology for modern production. Third, it is necessary to attach importance to the digestion and assimilation of imported technology, and go all out to make new developments and create our own new technology to increase our self-reliance. Four, we should give full play to the role of special economic zones as windows and stepping-stones in promoting the import of electronics technology and the export of electronics products on a large scale. We should strive to double, or treble, our exports by the year 1990.

The fourth major task is to formulate the Seventh 5-Year Development Plan well. We have preliminarily decided that the total output value of the electronics industry during the Seventh 5-Year Plan period should increase by more than 20 percent annually on an average, so that the total output value in 1990 will be 6.25 times that of 1980.

According to our preliminary plan, computers will be popularized among 80 percent or 90 percent of large enterprises, colleges, and major scientific research organizations, television sets be available to 45 percent of Chinese families, and color television sets be owned by a considerable number of families by 1990.

The fifth major task is to do a good job in scientific research, and continue to enhance the excellent situation. In 1985, which is the last year of the Sixth 5-Year Plan period, we should strive to accomplish our annual scientific research tasks in preparation for a greater development in the Seventh 5-Year Plan period. We plan to achieve a total industrial output value of 24 billion yuan in 1985, up 18 percent from 1984. We also plan to complete a number of new key construction and technical transformation projects, to further strengthen the technological foundation of the electronics industry.

The electronics industry has a bright future, but it shoulders heavy responsibilities. We shall surely not disappoint the concern shown by the party and the state for the electronics industry, nor shall we disappoint the hopes placed on the electronics industry by the people of the whole country. We shall strive to do our work well, create a new situation in the electronics industry, and make our due contributions to accomplishing the general tasks and objectives set by the 12th CPC National Congress.

CSO: 4008/248

## APPLIED SCIENCES

### NEW POWERED GLIDER DEBUTS OVER SHENYANG

Shenyang LIAONING RIBAO in Chinese 8 Dec 84 p 1

[Summary] On the morning of 7 December a silver and yellow aircraft--China's first powered glider--successfully completed its test flight over Shenyang.



The two-place powered glider was built by personnel of the Shenyang Glider Factory using a modified "Liberation-9" unpowered training glider built by the factory. Despite a wind speed of 12 meters per second on the day of the tests, the "Sea Swallow" performed exceptionally well in sustained powered and unpowered flight. Despite its light weight, it has a considerable payload capacity and is quite maneuverable. Fuel consumption is also quite low. It is capable of performing such roles as fighting forest fires, conducting geological surveys, crop dusting, etc.

CSO: 4008/252

APPLIED SCIENCES

RESEARCH WINS ACCLAIM FOR 'ION DOPING' TECHNOLOGY

Taiyuan SHANXI RIBAO in Chinese 19 Sep 84 pp 1, 2

[Article by Wu Zhendong [0702 2182 2639] and Li Jinsheng [2698 6955 5116]  
"For the Good of the Motherland--the Story of Xu Chong's Struggles and  
Success after He Developed the Ion Doping Technology"]

[Text] "The Xu Alloyage"

Wireless signals bringing good news from the United States on the east side of the Pacific Ocean to Shanxi, one of our key producing centers of energy and heavy chemical industries and to Taiyuan Industry University.

In late May 1983, the "ion doping" technology, successfully developed by him and his research group, obtained a patent application file number from the U.S. Patent and Trade Mark Office which also conferred upon the patenees the right of first choice for applying patent on this invention.

His "ion doping" technology had been named after him in the U.S. and is known as the "Xu Alloyage." Professor Schwartz, associate dean of the School of Engineering, South Carolina State University took the initiative to ask him to collaborate on a project to further study the "Xu Alloyage".

Two American professors, in their research proposal to the (U.S.) National Science Foundation, proposed to obtain his service as a consultant on their research project.

In 1984, The "ion doping" technology of his had obtained patent application file numbers and preferential rights to apply for patents in more than 10 countries: in order, Canada, West Germany, United Kingdom, France, Holland, Belgium, Japan, Australia, Brazil, Swiss etc. In the same year, the "Metal Steeping Process," jointly developed by him and two other American professors, was also granted an application file number by the U.S. Patent and Trade Mark Office.

This man, who had gained great honors for his country, is neither an esteemed professor nor a well-known scientist, he is just an instructor in Taiyuan Industry University. His name is Xu Chong [1776 6850]

The "ion doping" technology, successfully developed by Xu Chong, utilizes the electric discharge of bilayer luminosity phenomenon and ion bombardment method to introduce alloying elements into the top layer of carbon steel so as to form a high alloyed surface with prescribed characteristics. In cases, if only the metal surface properties are of practical importance, e.g. materials with corroding-resistant surface, instead of alloying the whole body of the material, the "ion doping" technology can be used for the surface treatment to meet the requirements. Thus, it saves energy and raw materials and reduces pollution.

#### Patent Application

Xu Chong went to South Carolina State University in the United States for further studies in September 1981. The High Pressure Technique Laboratory in the electric engineering department of this university is well-known for its achievements in America. In addition to 4 professors, there were 20 Ph.D and M.S. graduate students working in this laboratory. Xu Chong was invited to join the research team there as a full-time research associate. He was promised an equal share of the results achieved. The project he partook was the study of steeping solid metal surfaces in liquified metal and its application in high pressure processing. The development in this field was considered of national interest in the U.S.. During this study, Xu Chong submitted an overall research proposal, in which, he introduced the "ion doping" technology idea.

The professors from the South Carolina State University recognized the groundbreaking significance of this ion doping process, once it was proposed and suggested that Xu Chong should file an application to patent this ingenious idea.

However, Xu Chong, then, was not at all sure whether it's appropriate for a Chinese national to apply American patent for the results of his own study. In addition, he did not know how to initiate the application processes. To solve his dilemma, he sought the advice from our embassy in the U.S.. The answer came back: Yes, he may; however, he was the first of our scientists studying in America to apply for a U.S. patent and he should solicit advices and assistances from our friends to protect his legal rights.

A lot of people were there willing to offer their assistances in this matter. The South Carolina State University was ready to help, but the existing school policy demanded too high a percentage for royalty-sharing. There was also an Indian-American, Professor Sardasan offered to help with the condition that he got to claim part of Xu Chong's research results and achievements. But these were not the kind of help Xu Chong was looking for and he politely turned all of them down. Finally, with the approval of our embassy in Washington D.C., through the recommendation of a Chinese-American, Dr Liu Ledong, Xu Chong retained the service of a patent attorney to file for patent application on more favorable conditions.

Today, this Dr Liu Ledong has already had a sales agency set up to handle the business and of this new technology. It is to promote the applications

of this invention and conduct negotiations of the patent right transfers. A corporation is to be founded as well to further develop and study this new ion doping technology.

The study on "metal steeping" method, which Xu Chong collaborated with American professors, had also obtained good results; they applied and was issued a patent application file number on this new method. There was a little interlude in this second patent application process.

It again involved the scheming Professor Sardasan. Because Xu Chong had declined his offer of help in the ion doping patent application previously, he tried to get even this time by personally deleting Xu Chong's name as a patentee in the metal steeping patent application.

Deletion of his name from the patent application, in the legal sense, is to strip Xu Chong's rights to his own research results and to deny him his share of the royalty he deserved.

If the damage resulted from this kind of maneuver could have been limited to Xu Chong himself, he might have forgiven him and forgotten the whole incident, since Xu Chong's intentions were high; he did not devote himself to the research work solely for personal gains. He had gone ahead with the patent applications because he wanted to contribute the fruits of his research to the economic development of his motherland. He saved the stipend from South Carolina State University to pay the patent application expenses; he did not spend a cent on himself. However, being a Chinese and being a researcher from the People's Republic of China, one should carry oneself with dignity, protect his country's honor. Bearing in one's mind that we do not desire what we do not deserve, yet we do not yield what is rightfully ours. Xu Chong with the friendly support from his colleagues, Professors Foster and Schwartz and all the graduate students, appealed to the South Carolina State University authorities. The patent committee of the university, after two meetings, passed unanimously by an open balloting that Xu Chong was entitled to the ownership of the patent also. The senior vice president of the university personally notified Xu Chong the committee's decision.

#### Declined Job Offers and Returned Home

Xu Chong's tenure at the South Carolina State University expired in the latter half of 1983. When he was getting ready to come back, American research institutes and scientists asked him to stay to continue his study there. Professor Thompson, project leader of the High Pressure Technique Research Laboratory, South Carolina State University, promised him a handsome salary if he stayed on. Professors Thompson and Sardasan, in their research proposal submitted to the National Science Foundation, wrote: We propose to employ Professor Xu Chong as the project consultant. Professor Xu had made great contributions in the study of liquid metal steeping method developed in this laboratory. If we can secure him to work for this project, we believe, as in the past and present, his contributions will be of great value ...

A physics professor from University of Texas also asked Xu Chong to join his research group.

Others tried to talk him into staying in America to continue his research. They told him: The conditions for scientific research in China are much too backward.

Xu Chong declined all the job offers. Deep down, he knew" The working conditions for scientific studies in China are far behind those in the United States. However, backward as it may be, he'd be still working in his mother country. It is just for the very reason that we are behind that we should work twice as hard to catch up with developed countries. How could he indulge himself in the good material life in the United States and abandon his duty to China? He wanted to come back at the earliest possible moment, to found our own research institutes that are capable of carrying out high calibered research work, he wanted to devote himself to the further study of the pioneering ion doping technology in his own country. Xu Chong returned.

Xu Chong was entitled to a 1-month vacation after he came back. Yet, he considered the vacation as a waste of time. Thus, he immediately started to deliberate and plan to construct a research laboratory upon his return; he traveled from Taiyuan to the leading departments in Beijing many times for requesting instructions and briefing. He and his comrades from his laboratory jointly designed and built the facility, installed the research equipments; it took them from December, last year to June, this year to complete the first phase of the construction and equipping of their laboratory.

After staffing his research group, this new force was ready for operation. They had finished a finalized version of a scientific publication and built a small doping furnace for an American client.



Xu Chong (center) and engineering technicians inspect component parts with a microscope.



APPLIED SCIENCES

DEVELOPMENT OF SOL-GEL-SPHERE-PAC FUEL ELEMENT

Chengdu HE DONGLI GONGCHENG [NUCLEAR POWER ENGINEERING] in Chinese Vol 5,  
No 4, Aug 84 pp 47-56

[Article by Liu Naixin [0491 0035 2450]: "Development of Sol-Gel-Sphere-Pac Fuel Element"]

[Text] I. Overview

Research and development of vibratory compaction elements in nuclear reactor fuel elements began in the fifties. Since 1954 the  $UO_2$  ceramic pellet element has been successfully used in light water power reactors and after it became the present standard for light water power reactors and was extended to use as a fast reactor element, development of the vibratory compaction element stagnated. In the past 20 years, many countries have actively developed this type of element and for three reasons: 1) Industrial scale sol-gel technology can cheaply and safely provide the high density (approximately 99 percent TD, as below) ceramic microspheres of the grain size necessary for vibratory compaction, such as  $UO_2$ ,  $(U\cdot Pu)O_2$ ,  $(U\cdot Pu)C$ . Using this type of microsphere compaction, it is possible to obtain sol-gel microsphere vibratory compaction elements (called sphere-pac for short) of "effective density" corresponding to ceramic pellets can be obtained. 2) Production costs of sphere-pac elements are low and with deep burnup still has excellent radiation behavior and used in light water reaction power plants, can lower generating costs. 3) Sol-gel technology is easily controlled automatically and remotely and while greatly reducing radiation doses of operators and maintenance personnel, the daily increasing post-processor fuel produced by nuclear power stations can be recycled.

In the early sixties, the U.S. ORNL began research and development of  $(U\cdot Pu)O_2$  sphere-pac elements for fast reactor use.[1-6] In October 1977, according to the "Fuel Remanufacturing and Development" plans (FRAD) of the U.S. Department of Energy, ORNL fully demonstrated the commercial possibilities of using  $UO_2$  and  $(U\cdot Pu)O_2$  sphere-pac elements in light water power reactors and fast reactors.[7-12] The U.S. Department of Energy commissioned the Exxon Company to build an intermediate plant capable of producing 0.1 tons/day of (heavy metal) sphere-pac elements for the transition to commercial scale.[13] In 1972 Holland established the Interfuel Company whose main purpose was to expand  $UO_2$  sphere-pac elements through intermediate



plants to industrial scale and as quickly as possible become commercially used pressurized water reactor elements. In 1974 an intermediate plant with a production capacity of 6 tons/day (heavy metal) had been built.[17-19] Since 1967, the Swiss EIR has devoted itself to scientific work to develop (U·Pu)C sphere-pac elements as improved fast reactor elements.[20-27] In an improved fast reactor fuel plan formulated in the mid-seventies, England decided to develop (U·Pu)O<sub>2</sub> sphere-pac elements[28,29] and built two intermediate plants at Windscale.[30,31] Because the operational results of the two intermediate plants were very satisfying, England decided to build a plant for the manufacture of (U·Pu)O<sub>2</sub> sphere-pac elements at Dounreay. The West German Karlsruhe Nuclear Center set up the GA group[32,33] dedicated to research and demonstration work on (U·Pu)O<sub>2</sub> sphere-pac elements as pressurized water reactor elements. Other countries, such as Italy[34], the Soviet Union and Czechoslovakia[35,36] also actively developed sphere-pac elements. By 1981, countries had already obtained results showing that UO<sub>2</sub>, (U·Pu)O<sub>2</sub>, and (U·Pu)C sphere-pac elements are new ceramic fuel elements which can be used in light water power reactors and fast reactors, are far superior to ceramic pellet elements, and have commercial possibilities.

## II. Manufacture of Sphere-Pac Elements

The sphere-pac element is a very dense ceramic microsphere of two or three grain sizes which is prepared using sol-gel technology, by adopting "penetration method"[1] or "once method"[10] to pack the microsphere in an alloy (Zr-2, Zr-4, or 304LSS) container, and vibrated using a 0-3000 Hz vibrator. The vibrated element, like decontaminated sealing of ceramic pellets, is made into a sphere-pac element. The "effective density" of the sphere-pac elements obtained by using microsphere vibratory compaction of UO<sub>2</sub> or (U·Pu)O<sub>2</sub> of the three granular densities of 1000 microns, 100 microns, and <40 microns can reach the "effective density"--90-92 percent--of the ceramic elements used in light water reactors; the "effective density" of the sphere-pac elements obtained by using high density microsphere vibratory compaction of (U·Pu)O<sub>2</sub> and (U·Pu)C of the two grain sizes of 400-600 microns and 40-60 microns can also reach the "effective density"--80-85 percent--of the ceramic elements used in fast reactors. The thin uranium sphere-pac element was developed to reduce plutonium radiation injury and loss of plutonium. This process makes all microspheres containing plutonium into (U·Pu)O<sub>2</sub> microspheres of coarse granularity, the fine grain spheres used in permeation are UO<sub>2</sub> microspheres.[2,7]

The sol-gel technology used in the process of manufacturing sphere-pac elements has already been discussed in the literature [37-40] and after the sealing the operations are the same as for ceramic pellets. Here we will deal briefly with vibratory compaction technology.

Packing microspheres or granules into a casing for vibratory compaction into fuel rods is mainly done by two methods: "penetration method" and "once method." The "penetration method" first packs the coarse microspheres into the casing and compacts them by vibration; then the medium sized microspheres are added and compacted by vibration for penetration; finally, the fine microspheres are added and compacted by vibration for penetration. Each vibratory

compaction should reach the highest "effective density." The "once method" first mixes together evenly the microspheres of various degrees of granularity to be compacted by vibration in the percentages by weight of the microspheres of various degrees of granularity as provided in article [10] and then gradually adds them to the casing and compacts them by vibration. In both the "penetration method" and the "once method" the most important quality indicators are pac efficiency, pac time, and evenness of pac rod density.

(1) Efficiency of vibratory compaction. Efficiency of vibratory compaction is a percentage of spheres of one granularity in the canister after vibratory compaction relative to the theoretical efficiency of vibratory compaction. The "effective density" of the element is the product of density of the loaded microspheres and the efficiency of vibratory compaction. The main factors influencing the efficiency of vibratory compaction are the granularity (diameter) of the microspheres and the method of packing. J. E. Ayer[1] has induced an equation for the efficiency of vibratory compaction of a microsphere of a single grain size:

$$Pe = 0.635 - 0.216e^{-0.313\frac{D}{d}} \quad (1)$$

in which  $Pe$  is the efficiency of vibratory compaction as a percentage;  $D$  is the diameter of the casing in millimeters; and  $d$  is the diameter of the loaded spheres in millimeters. Equation (1) is also suitable for use with spheres of several grain sizes when using the "penetration method" of vibratory compaction. At such times, the overall efficiency of vibratory compaction is  $Po$  and can be expressed in the following formula:

$$Po = a - 0.216e^{-0.313\frac{D}{d_1}} + (1-a)a - 0.216e^{-0.313\frac{D}{d_2}} + [1-a-(1-a)a]a - 0.216e^{-0.313\frac{D}{d_3}} + \dots \quad (2)$$

in which  $a$  is 0.635;  $d_1, d_2, d_3, \dots$  are the diameters (in millimeters) of the spheres in coarse, medium, fine, ... grains. Obviously, the efficiency of vibratory compaction increases as the ratio of  $\frac{D}{d}$  and  $\frac{dn}{d_{n+1}}$  ( $n$  is a natural number) increases. When the ratio is greater than 7,  $e^{-0.313\frac{D}{d}}$  and  $e^{-0.313\frac{dn}{d_{n+1}}}$  can be ignored. Therefore, the theoretical efficiency of vibratory compaction of spheres of one grain size is 0.635, of spheres of two grain sizes, 0.867, and of spheres of three grain sizes, 0.951.

R. R. Suhomel used (U-Pu)O<sub>2</sub> microspheres of three grain sizes: coarse (1200 microns), medium (300 microns) and fine (30 microns) to study the relationship between the effective density and the proportion of grain size in the "once method." The results are given in Fig. 1.[10]. The results of the comparison of this method with the "penetration method" is given in Fig. 2.[7] From Fig. 1 and Fig. 2 one can clearly see that the highest effective density of the "once method" can reach about 85 percent TD, lower than the effective density of the "penetration method."

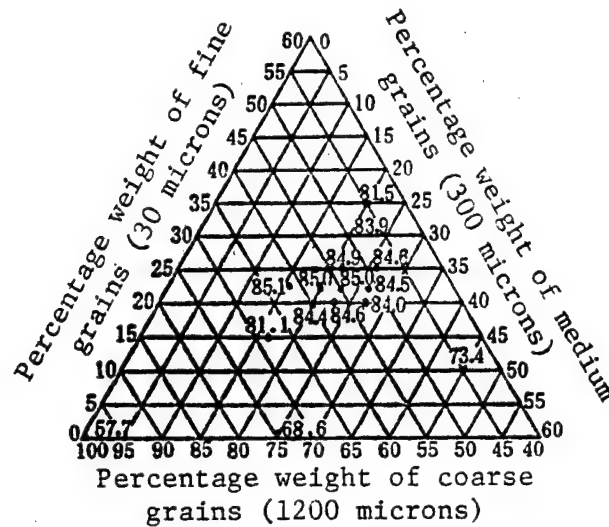


Fig. 1. Proportional relationship of coarse, medium, and fine granularity and effective density of "once method" (U·Pu)O<sub>2</sub> microspheres (fast reactor casing)

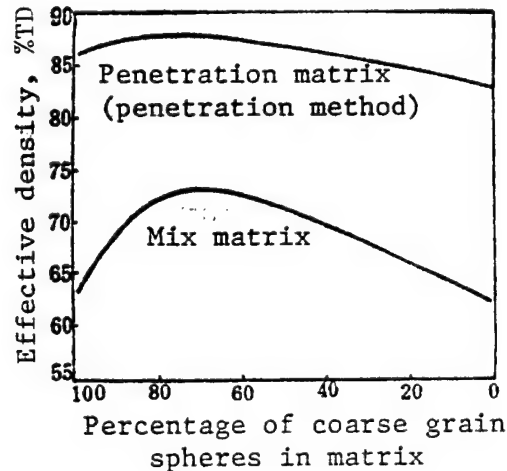


Fig. 2. Comparison of two vibration methods (casing diameter 0.380 inches)

(2) Vibratory compaction time. Vibratory compaction time is the shortest time in which the highest efficiency of vibratory compaction can be reached. J. E. Ayer, F. E. Soppet, and others [6, 41-43] have studied in detail some important factors, such as the influence of frequency of vibration, grain shape, grain granularity (diameter) ratio, fraction ( $V_f$ ) of volume of space in the matrix bed, and length of fuel rod on the vibratory compaction time. The results are presented in Figs 3, 4, 5, and 6. From these figures it can be seen clearly that the sphere is the most ideal packing material. The fraction of the volume of space in the matrix bed of two microspheres with diameters greater than 7 is 25 percent and using a vibration frequency of several tens of megaHertz, the vibration compaction time generally does not exceed 10 minutes. Experiments with vibratory compaction of 1:1 element rods shows that using the "penetration method" the vibration time of spheres

of two grain sizes is about 8 minutes,[31] and the time for spheres of three grain sizes is 10-30 minutes.[25] If the "primary method" is used, the vibratory compaction time is clearly reduced.[7,10]

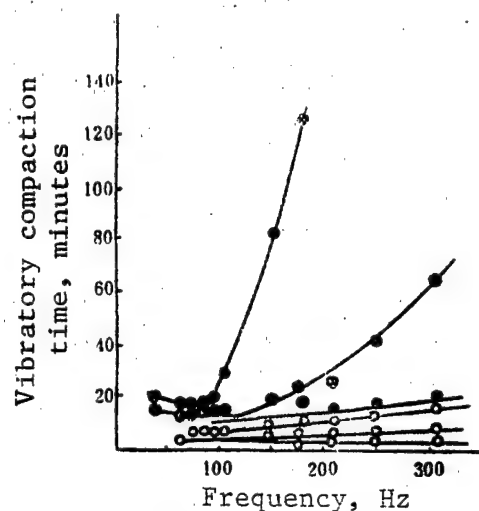


Fig. 3. At  $V_f$  time of 0.39, relation of sphere and angular granule vibration time and vibration frequency  
 o—sphere,  $d_1/d_2 = 7.8$   
 ●—angular granule,  $d_1/d_2 = 9.6$

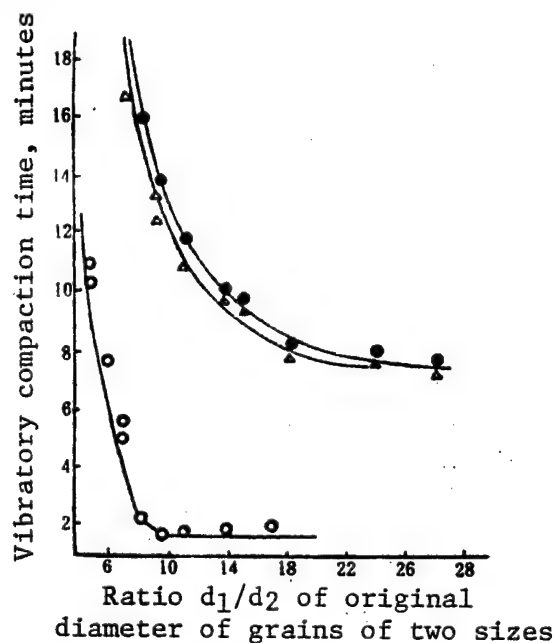


Fig. 4. Relationship of diameter ratio ( $d_1/d_2$ ) and vibration time of spheres and polished granules to angular granules in a 23 inch column at a 60-80 Herz, 7.5 gram vibration acceleration force  
 o—sphere,  $V_f = 0.43$   
 Δ—polished granules,  $V_f = 0.37$   
 ●—angular granules,  $V_f = 0.39$

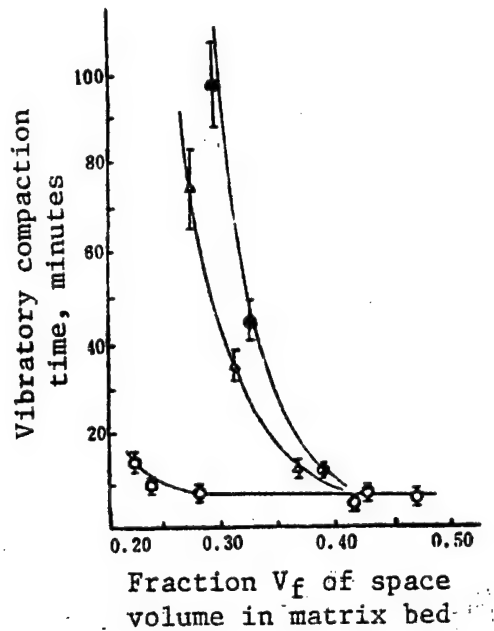


Fig. 5. Relationship of  $V_f$  and vibratory compaction time of spheres, polished granule, and angular granules in a 23 inch volume at 60-80 Herz and a 7 gram vibration acceleration force  
 o—spheres,  $d_1/d_2 = 6.0$   
 $\Delta$ —polished granules,  $d_1/d_2 = 10.0$   
 ●—angular granules,  $d_1/d_2 = 10.0$

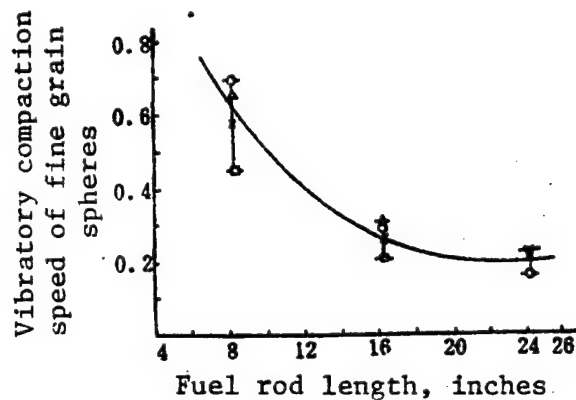


Fig. 6. Influence on fuel rod length on vibratory compaction speed of fine grain spheres\*

\*Diameters of fuel rods used in the experiment were:

- o 0.186 inches
- $\Delta$  0.246 inches
- $\square$  0.305 inches
- + 0.370 inches

(3) Uniformity of vibratory compacted rod density. This indicator is directly related to the uniformity of element rod power. P. F. Sens[14,15], H. W. H. Lahr[32,33], and R. W. Stratton[26] have studied the influence of microsphere density and proportion of microsphere granularity when using the "penetration method" on uniformity. The results show that it is necessary to use high density microspheres; and it is necessary to guarantee a proportion of microspheres of grain sizes of 1000 microns:100 microns:10-40 microns for pressurized water reactor elements and 400-600 microns:40-60 microns for fast reactor elements. Thus, effective density of elements after vibratory compaction can reach 90-92 percent T·D and 80-85 percent T·D, respectively, a variation in effective density of less than 2 percent, and a variation in axial density of 2 percent meet the requirements for pressurized water reactors and fast reactors. For materials containing plutonium[32,33], the uniformity of plutonium in (U·Pu)O<sub>2</sub> microspheres prepared using sol-gel technology is far superior to the powder ceramic pellet (U·Pu)O<sub>2</sub>.

### III. Comparison of Sphere-Pac Elements and Ceramic Pellet Elements

For sphere-pac elements to be used commercially, they must be clearly superior to the ceramic pellet elements already in commercial use in terms of technological process, radiation behavior, and production costs. Below is a detailed comparison of these three aspects of the two elements.

#### 1. Technological Process of Element Manufacture

The technological process of element manufacture is one of the basic indicators for evaluating the practicality of nuclear fuel elements. Simplicity, reliability, safety, and ease of long distance automated operation reflect important characteristics of nuclear technology and are also directly related to production costs. Fig. 7 is an outline of technological processes for manufacturing (U·Pu)O<sub>2</sub> ceramic elements for comparison. From Fig. 7 it can be seen that for similar initial liquid materials, manufacturing sphere-pac elements in comparison with manufacturing ceramic elements saves the six conversion processes of precipitation, filtering, calcination, reduction, manufacturing granules, and screening. Everyone knows that these six processes are the most highly radioactive and rather difficult to carry out with long distance automated operation. This demonstrates fully the simplicity and safety of the sphere-pac element manufacturing process. As far as operation is concerned, the object of the sol-gel technology operation for manufacturing microspheres at industrial scale is liquids and solids in microsphere form, and the degree of long distance automated operation is far higher than the ceramic pellet manufacturing technology which is primarily a powder operation, and is almost dust-free, involves less contamination of equipment, and less loss of heavy metals. These are all outstanding advantages as far as the direct environment post-processed fuel, lowering radiation dosage of working and maintenance personnel and labor intensity are concerned.

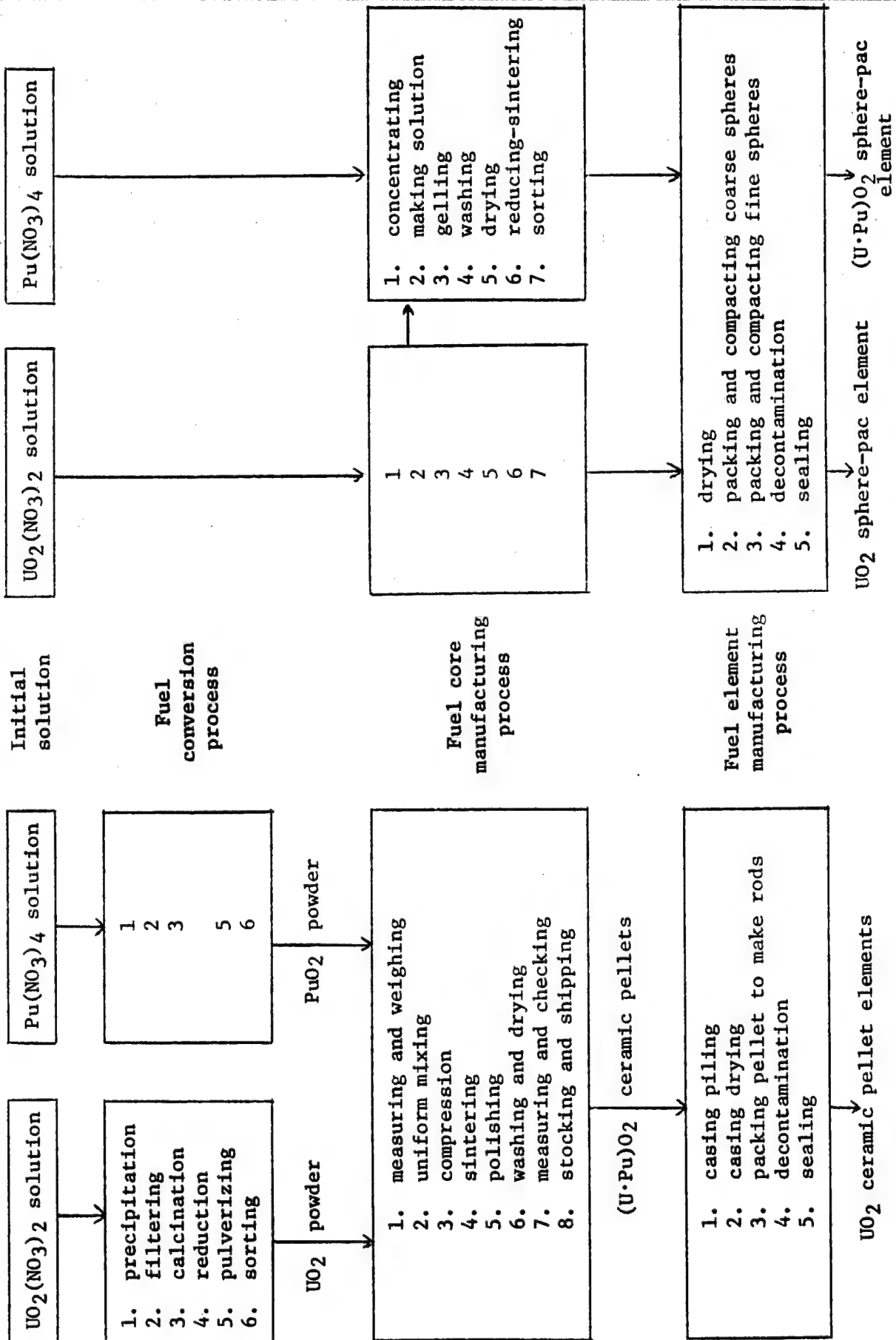


Fig. 7. Flow chart of (U·Pu)O<sub>2</sub> ceramic element manufacturing process [19,32-34]

## 2. Element Radiation Behavior

Element radiation behavior is an important property of elements. Commercialized ceramic pellet elements have the radiation behavior demanded by reactors. Sphere-pac elements have also secured radiation test results which are unusually attractive. Below we emphasize analysis of differences in radiation behavior.

(1) Heat transfer efficiency. Fuel element heat transfer efficiency is determined by the heat conduction of the fuel itself and the heat transfer efficiency of the fuel and its casing and it is an important radiation behavior. Heat conduction of sintered  $\text{UO}_2$  ceramic pellets has been studied and summarized by M. F. Lyons<sup>[45]</sup> and M. D. Freschley<sup>[46]</sup>. The primary results are: the integral heat conduction of  $\text{UO}_2$  pac fuel is  $\int_{0T}^{T_m} KdT = 63$  watts/cm, and  $\int_{550T}^{T_m} KdT = 49$  watts/cm;  $\text{UO}_2$  ceramic pellets correspond to 93 watts/cm, and 60 watts/cm. A. Calza-Bini<sup>[4]</sup> and others have studied the integral heat conduction of four kinds of elements in reactors and give the following formulae and the curves in Fig. 8:

$$\int_{T_0}^{T_1} K(T) dT = \frac{1}{C} \ln \frac{B+CT_1}{B+CT_0} + \frac{D}{4} (T_1^4 - T_0^4)$$

B, C and D test values in the formula are given in Table 1. These results show that heat conduction of the ceramic pellets themselves, should be higher than pac rods. However, the interval heat transfer efficiency between them is not the same. To satisfy reactor demands there should be an interval between the ceramic pellet and the casing. The width of this interval generally is taken as 0.17-0.20 microns for pressurized water reactors and 0.28-0.31 microns for water boiler reactors. At present it is felt that for the  $\text{UO}_2$  ceramic pellet element with an interval of 0.25 microns the most commonly used interval heat transfer coefficient is  $0.42 \text{ watts/cm}^2 \cdot ^\circ\text{C}$ <sup>[45]</sup>, and for  $(\text{U}\cdot\text{Pu})\text{O}_2$  ceramic pellet elements it is  $0.56\text{--}0.73 \text{ watts/cm}^2 \cdot ^\circ\text{C}$ <sup>[3,32,33]</sup>. There is no interval in sphere-pac elements and the heat transfer coefficient where the fuel and the casing touch is  $0.75\text{--}1.1 \text{ watts/cm}^2 \cdot ^\circ\text{C}$  ( $\text{UO}_2$ )<sup>[46]</sup> and  $0.84\text{--}1.93 \text{ watts/cm}^2 \cdot ^\circ\text{C}$   $(\text{U}\cdot\text{Pu})\text{O}_2$ <sup>[3,32,33]</sup>. Clearly, the interval heat transfer coefficient of sphere-pac elements is higher. To make an overall comparison of the heat transfer efficiency of these two elements, R. B. Fitts carried out random reactor operations tests on these two elements at the Oak Ridge Research Reactor (ORR). The main results of the tests<sup>[3]</sup> are given in Table 2. From Table 2 it can be seen that at times of low burnup although the core temperatures of both kinds of elements was the same, the average temperature inside the sphere-pac element casing was about 10 percent higher. This means that the heat transfer efficiency (what H. W. H. Lahr<sup>[32,33]</sup> calls "effective heat conduction") of the sphere-pac element is higher than that of the ceramic pellet element.



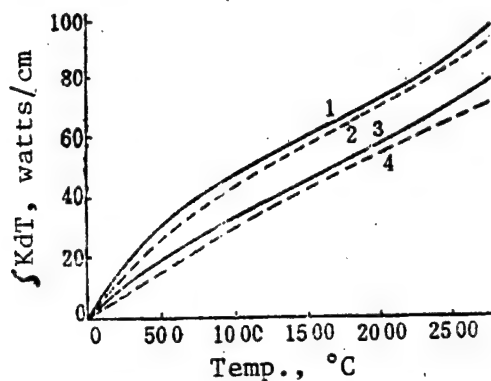


Fig. 8. Comparison of integral head conduction curve  
 1--UO<sub>2</sub> ceramic pellet  
 2--UO<sub>2</sub> grain vibratory compaction  
 3--(U-Pu)O<sub>2</sub> ceramic pellet  
 4--(U-Pu)O<sub>2</sub> sphere-pac

Table 1. Comparison of B, C, D Test Values

Element type	B	C	D
UO <sub>2</sub> ceramic pellet	2.75	0.02774	0.9 x 10 <sup>-12</sup>
(U-Pu)O <sub>2</sub> ceramic pellet	8.5	0.0207	0.6 x 10 <sup>-12</sup>
UO <sub>2</sub> pac element (initial start)	24.25	0.0091	0.18 x 10 <sup>-12</sup>
(U-Pu)O <sub>2</sub> sphere-pac element (initial start)	27.75	0.00797	0.1 x 10 <sup>-12</sup>

Table 2. Radial Temperature Distribution of (U-Pu)O<sub>2</sub> Ceramic Pellet Element

		Ceramic pellet element	Sphere-pac element
Maximum core temperature, °C		2000	2000
Irradiation time, hours		2180	2180
Irradiation time at maximum temperature, hours		120	35
Single rod power, kw/ft		14.5	16
Maximum temperature inside casing, °C	Average	625	700
	Hot point	665	745
Maximum temperature on fuel surface, °C	Average	860	750
	Hot point	900	800

(2) Mechanical function of fuel and casing. The mechanical function of fuel and the casing is another very important radiation behavior. Because at times of deep burnup the mechanical function can lead to casing strain and even casing split, it has a direct effect on the life of the element. The factor which gives rise to this mechanical function is the difference in heat expansion of the fuel and the casing and swelling in deep burnup, but mostly it takes place when the radiation initial period power is low.

In the initial radiation period, the expansion of the fuel rods takes place radially and axially. P. F. Sens<sup>[16]</sup> used UO<sub>2</sub> sphere-pac elements and ceramic pellet elements at the same "effective density" to study axial expansion of fuel rods at low power. The results are given in Fig. 9. Clearly, the axial expansion is more severe. The research work of H. W. H. Lahr<sup>[32,33]</sup> and M. D. Freschley<sup>[46]</sup> has also pointed out that in irradiation, there is some elasticity of the axial expansion of sphere-pac rods. Some preliminary conclusions have already been reached on the comparison of axial expansion in the two kinds of fuel rods by research work in the United States<sup>[47]</sup>, West Germany<sup>[32,33]</sup>, and Switzerland<sup>[32]</sup>. That is, in irradiation, sphere-pac rods always act as an integral supporting casing and action is uniform and slow. The cold area formed by larger pores surrounding the central high temperature area can store a great deal of the fission products produced in deep burnup and adjust to swelling. The ceramic pellet element, however, cannot maintain the uniform action of all the fuel rod and the casing thus a single-point contact may occur. In deep burnup, hot points from leading to partial stress on the casing and embrittlement and splitting. In view of the above analysis, the mechanical action of sphere-pac element fuel and casing is slow and uniform in both low burnup and deep burnup. This outstanding advantage has been proven by a great deal of research work<sup>[3,15,23,46]</sup>. In ceramic pellet elements, this mechanical action is very severe and sometimes can create casing hot point damage. Fig. 10<sup>[3]</sup> and Fig. 11<sup>[15]</sup> clearly show the clear differences between the two. The interface between the inside of the case and the fuel in the ceramic pellet element in Fig. 10B is not clear, there are three injuries to the inside of the casing. In the most severe place the fuel has penetrated the casing to a depth of 5 milimicrons and along a surface of about 50 milimicrons. From Fig. 10A and Fig. 11 one can see clearly that the boundary between casing and fuel in the sphere-pac element is very clear.

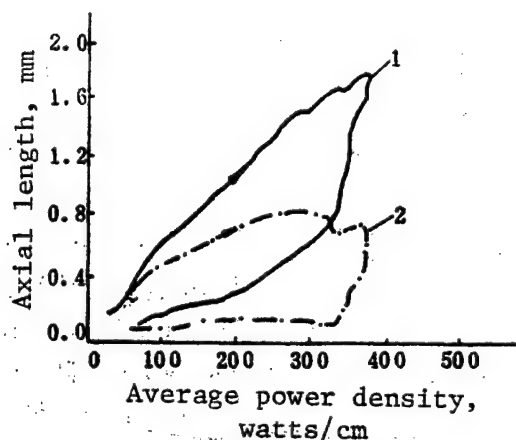


Fig. 9. Axial length of two kinds of fuel rods at time of lower power  
 1--Ceramic pellet rod  
 2--Sphere-pac rod

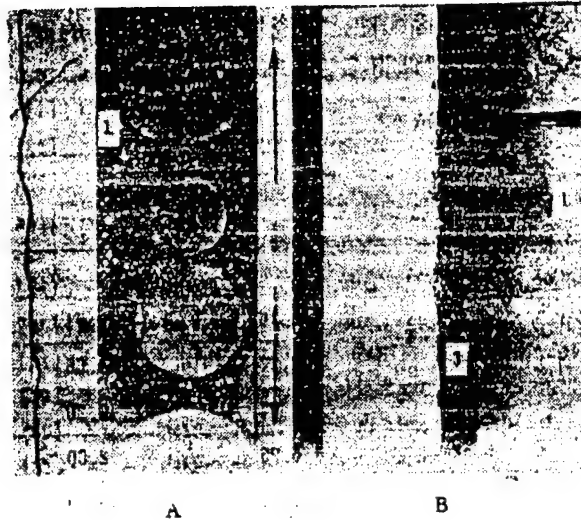


Fig. 10. Interaction of  $(U \cdot Pu)O_2$  fuel and approx. 0.5 percent FIMA, model 304 SS casing  
 A--Inside of  $(U \cdot Pu)O_2$  sphere-pac element casing at temperatures above  $650^\circ C$  for 430 hours  
 B--Inside of  $(U \cdot Pu)O_2$  ceramic pellet element case at temperatures above  $650^\circ C$  for 265 hours  
 1--fuel; 2--casing wall; 3--gap



Fig. 11. Enlargement (200x) of surface inside  $UO_2$  sphere-pac element casing\*  
 1--fuel; 2--casing wall  
 \*The black dot in the photograph is caused by the photography and not a reaction observed in the  $UO_2$  and the zirconium casing.

Radiation experiments under pressurized water reactor conditions conducted by the Dutch KEMA and Interfuel Company<sup>[15-18]</sup>, and the West German Karlsruhe Nuclear Center<sup>[32,33]</sup> using  $UO_2$  and  $(U \cdot Pu)O_2$  sphere-pac elements show that these two elements both completely meet the demands of use in pressurized water reactors. Their radiation behavior is at least not inferior to that of ceramic pellet elements, but the mechanical action of the fuel and casing in deep burnup is clearly improved and it can be used in deep burnup.

Radiation experiments on  $(U \cdot Pu)O_2$  and  $(U \cdot Pu)C$  sphere-pac elements under fast reactor conditions have been carried out in Switzerland<sup>[20-23]</sup>, the United

States[3,11,45], and England[48]. The results obtained show that they are suited to fast reactors. Their radiation behavior is at least equal to that of ceramic pellet elements and their outstanding superiority is in that the mechanical action of the casing and fuel under deep burnup is slow and uniform.

### 3. Production Costs

Production costs of nuclear fuel elements are directly related to their commercial prospects. The Dutch Interfuel Company[19], West German Karlsruhe Nuclear Center and U.S. ORNL[11] have made production cost comparisons for pressurized water reactor power stations using  $UO_2$  or  $(U\cdot Pu)O_2$  sphere-pac elements and ceramic pellet elements. The results of a comparison at 100 tons/year (heavy metal) are given in Table 4 [sic]. These results did not take into consideration the economic benefits derived from such advantages as long distance automated operation and ease of maintenance in the sphere-pac element manufacturing process. From Table 4 and synthesizing the results of the analyses by other countries, one can see that the production costs using sphere-pac elements in pressurized water reactors is 12-30 percent lower than using ceramic pellet elements. The U.S. ORNL[2,5,6,12] and Italy's CNEN[34] have both compared use of  $(U\cdot Pu)O_2$  sphere-pac elements in fast reactors with  $(U\cdot Pu)O_2$  ceramic pellet elements and have made detailed production cost estimates. From Table 5 it can be seen that the economic nature of using  $(U\cdot Pu)O_2$  sphere-pac elements in fast reactors is superior to using ceramic pellet elements.

Table 4. Comparison of Production Costs of Two Elements for Pressurized Water Reactors

Item	Sphere-pac element*	Ceramic pellet element**
Total capital investment (relative)	0.756	1.00
Total operating expenses (relative)	0.983	1.00
Total monthly expenses (relative)	0.770	1.00

\*Source of materials is post-processed nitrate solution

\*\*Classic ADU processing

The above production costs are considered only from the perspective of element manufacturing process. If the fact that the mechanical action of fuel and casing of sphere-pac elements under deep burnup is much lighter than that of ceramic pellet elements and thus can be used in deeper deep burnup operation than can ceramic pellet elements, then the production costs of sphere-pac elements are much lower than those of ceramic pellet elements.

Table 5. Estimate of Production Costs for Elements for Fast Reactor Use\*

Item	Production costs \$/kg (heavy metal)				Sphere-pac element**
	Element shape	Ceramic element	Ditto	Ditto	
	Manu- facturing process	Mechanical mixing process	Total precipitation process	Sol-gel process	
Equipment invest- ment		11.23	12.91	11.74	9.51
Operations		31.58	35.37	32.27	24.68
Plutonium loss		19.47	17.77	17.77	10.20
Fragments		8.20	6.52	5.93	2.60
Total		70.48	72.57	67.71	46.90
Production cost difference		23.49	25.58	20.72	0

\*Nuclear pure  $UF_6$  and  $Pu(NO_3)_4$  as the startup material, production capacity of 0.5 tons/day (heavy metal)

\*\*Fine uranium sphere-pac element

#### IV. Conclusion

Sphere-pac elements manufactured using sol-gel technology and sphere-pac technology are new ceramic elements for use in pressurized water reactors ( $UO_2$ ,  $(U \cdot Pu)O_2$ ) and fast reactors ( $(U \cdot Pu)O_2$ ,  $(U \cdot Pu)C$ ) which have commercial prospects. Compared with currently commercialized ceramic pellet elements, they have the following advantages: production technology is simple and safe, and especially suited to long distance automated operation of post-processing fuels; production costs are lower by 10-30 percent; radiation behavior satisfies the demands of pressurized water reactors and fast reactors. Mechanical action of fuel and casing is slow and uniform and suited to deep burnup operations. In low burnup the element's heat transfer efficiency is high and in deep burnup the element's adaptability to swelling is high. For this reason, in the past 20 years it has become a new type of ceramic element actively developed by many countries.

#### REFERENCES

1. J. E. Ayer, CONF-700502, p 310. Gatlinburg, USA (1970).
2. J. D. Sease et al., CONF-700502, p 323. Gatlinburg, USA (1970).
3. R. B. Fitts and F. L. Miller, NUCLEAR TECHNOLOGY, 21(1), 26 (1974).
4. A. C. Bini et al., NUCLEAR TECHNOLOGY, 21(2), 208 (1974).
5. F. E. Harrington et al., ORNL-TM-2813 (1970).

6. J. D. Sease, ORNL-4360 (1970).
7. R. R. Suchomel, CONF-780535-1, p 21, Richland, USA (1978).
8. D. W. Brite, TRANSACTIONS OF THE AMERICAN NUCLEAR SOCIETY, 32, 244 (1979).
9. A. D. Ryon et al., TRANSACTIONS OF THE AMERICAN NUCLEAR SOCIETY, 32, 274 (1979).
10. R. R. Suchomel et al., TRANSACTIONS OF THE AMERICAN NUCLEAR SOCIETY, 32, 276 (1979).
11. R. L. Beatty et al., ORNL-5469 (1979).
12. W. J. Lackey et al., ORNL-5466 (1978).
13. R. E. Feit et al., DOE/ET/34026-1 (USA) (1980).
14. P. F. Sens et al., TRANSACTIONS OF THE AMERICAN NUCLEAR SOCIETY, 20, 593 (1975).
15. F. W. Hambury et al., PEACEFUL USES OF ATOMIC ENERGY, Vol 8, p 263, Geneva (1971).
16. P. F. Sens et al., TRANSACTIONS OF THE AMERICAN NUCLEAR SOCIETY, 20, 238 (1975).
17. A. V. D. Linde et al., ECN-38 (Netherlands) (1978).
18. A. V. D. Linde et al., ECN-66 (Netherlands) (1979).
19. W. L. Lyon et al., TRANSACTIONS OF THE AMERICAN NUCLEAR SOCIETY, 38, 201 (1981).
20. K. Bischoff et al., EIR-Bericht-236 (Swiss) (1973).
21. R. W. Stratton and K. Bischoff, TRANSACTIONS OF THE AMERICAN NUCLEAR SOCIETY, 20, 298 (1975).
22. R. W. Stratton and K. Bischoff, CONF, Advanced LMFBR Fuels, p 348, Tucson, Arizona (USA) (1977).
23. A. Delbrassine and L. Smith, NUCLEAR TECHNOLOGY, 49(1), 129 (1980).
24. K. Bischoff et al., INFCE/DEP/WG-5/38 (1978).
25. R. W. Stratton et al., INFCE/DEP/WG-5/39 (1978).
26. R. W. Stratton et al., INFCE/DEP/WG-5/40 (1978).
27. R. W. Stratton et al., TRANSACTIONS OF THE AMERICAN NUCLEAR SOCIETY, 32, 231 (1979).

28. J. F. W. Bishop et al., CONF. Advanced LMFBR Fuels, p 15, Tucson, Arizona (USA) (1977).
29. J. F. W. Bishop et al., IAEA-CN-36/64 (1977).
30. R. L. Nelson et al., TRANSACTIONS OF THE AMERICAN NUCLEAR SOCIETY, 32, 227 (1979).
31. R. L. Nelson et al., NUCLEAR TECHNOLOGY, 53(2), 196 (1981).
32. H. W. H. Lahr, NUCLEAR TECHNOLOGY, 31(2), 183 (1976).
33. H. W. H. Lahr, CONF. Advanced LMFBR Fuels, p 153, Tucson, Arizona (USA) (1977).
34. G. Colomb et al., CONF-700502, p 264, Gatlinburg (USA) (1970).
35. Ganush Lonusnerski, JADERNA ENERGIE, 22(3), 104 (1976).
36. V. M. Makarov et al., IAEA-161, p 71, Vienna (1974).
37. IAEA PROCEEDINGS OF A PANEL ON SOL-GEL PROCESSES FOR CERAMIC NUCLEAR FUELS, Vienna (1968).
38. CONF-799502 PROCEEDINGS OF A SYMPOSIUM ON SOL-GEL PROCESSES AND REACTOR FUEL CYCLE, Gatlinburg (USA) (1970).
39. IAEA THE PANEL ON SOL-GEL PROCESSES FOR FUEL FABRICATION, Vienna (May 1973).
40. Liu Naixin [0491 0035 2450], GUOWAI HE JIZHU [NUCLEAR TECHNOLOGY ABROAD], 4.13 (1980).
41. J. E. Ayer et al., JOURNAL OF THE AMERICAN CERAMIC SOCIETY, 48(4), 180 (1965).
42. J. E. Ayer et al., JOURNAL OF THE AMERICAN CERAMIC SOCIETY, 49(4), 207 (1977).
43. J. E. Ayer et al., JOURNAL OF THE AMERICAN CERAMIC SOCIETY, 52(8), 417 (1969).
44. R. W. Stratton, CONF, Advanced LMFBR Fuels, p 74, Tucson, Arizona (USA) (1977).
45. M. F. Lyons, NUCLEAR ENGINEERING DESIGN, 21 (1-3), 167 (1972).
46. M. D. Freschley, NUCLEAR ENGINEERING DESIGN, 21 (1-3), 264 (1972).
47. S. O. Battelle, BNWL-1442 (1970).
48. K. M. Swanson et al., CONF, Advanced LMFBR Fuels, p 95, Tucson, Arizona (USA) (1970).

APPLIED SCIENCES

DISTANCE-INERTIAL GUIDANCE OF LAUNCH VEHICLE DESCRIBED

Beijing ZIDONGHUA XUEBAO [ACTA AUTOMATICA SINICA] in Chinese No 4, Oct 84  
pp 361-364

[Article by Guo Xiaokuan [6753 1321 1401], Yue Peiyu [1471 0012 3768], An  
Weilian [1344 4850 1670]]

[Text] I. Coordinate System and Transformation

Let us define the affine inertial coordinate system  $O-X_1X_2X_3$ , where the origin  $O$  coincides with the origin of the launch-centered inertial coordinate system  $O-XYZ$ , and the axes  $OX$  are defined by the angles  $\alpha_i, \beta_i$  ( $i=1,2,3$ ) respectively. The three accelerometers of the inertial guidance system are installed along the  $OX_1, OX_2, OX_3$  axes on the inertial platform. The accelerations  $\dot{W}_i$  sensed by the accelerometers are the orthogonal projections of the apparent acceleration of the rocket along the affine base directions. As shown in Fig. 1, the relationship between the orthogonal projections of  $\dot{W}$  along the affine bases  $\dot{W}_1, \dot{W}_2, \dot{W}_3$  and the orthogonal projections along the orthogonal bases  $\dot{W}_x, \dot{W}_y, \dot{W}_z$  is

$$(\dot{W}_1 \dot{W}_2 \dot{W}_3)^T = A(\dot{W}_x \dot{W}_y \dot{W}_z)^T. \quad (1)$$

where

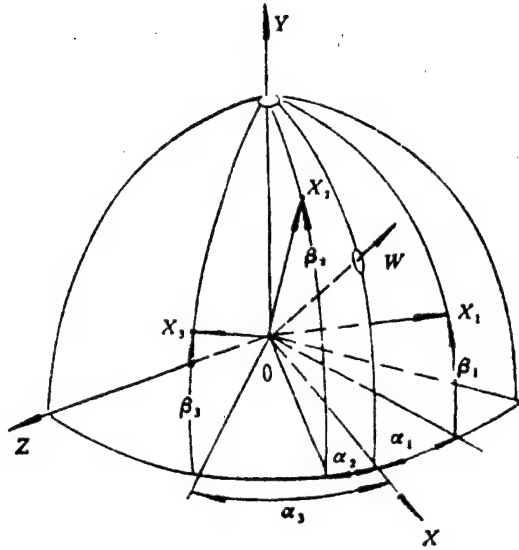
$$A = \begin{pmatrix} a_{11} & a_{12} & a_{13} \\ a_{21} & a_{22} & a_{23} \\ a_{31} & a_{32} & a_{33} \end{pmatrix}. \quad (2)$$

$$a_{11} = \cos \alpha_1 \cos \beta_1, \quad a_{12} = \sin \beta_1, \quad a_{13} = \sin \alpha_1 \cos \beta_1. \quad (3)$$

Since  $O-XYZ$  and  $O-X_1X_2X_3$  are both inertial coordinate systems, the above transformation also applies to the velocity and position vectors of the rocket motion.



Fig. 1



## II. Error Model of the Inertial Guidance System

The error model of the inertial guidance system can be characterized by the formula for calculating the measurement errors of accelerometers.

$$\begin{pmatrix} \Delta \dot{W}_1 \\ \Delta \dot{W}_2 \\ \Delta \dot{W}_3 \end{pmatrix} = \begin{pmatrix} \Delta \dot{W}_{10} \\ \Delta \dot{W}_{20} \\ \Delta \dot{W}_{30} \end{pmatrix} + \begin{pmatrix} \dot{W}_1 & 0 \\ 0 & \dot{W}_3 \end{pmatrix} \begin{pmatrix} k_{w1} \\ k_{w3} \end{pmatrix} + (\varphi_{ij}) \begin{pmatrix} \alpha_{x0} \\ \alpha_{y0} \\ \alpha_{z0} \end{pmatrix} + (\varphi_{iii}) \begin{pmatrix} k_{x0} \\ k_{y0} \\ k_{z0} \end{pmatrix} \quad (4)$$

$$+ (\varphi_{wij}) \begin{pmatrix} k_{x1} \\ k_{y1} \\ k_{z1} \end{pmatrix} + \begin{pmatrix} \dot{W}_{12} & 0 \\ 0 & \dot{W}_{32} \end{pmatrix} \begin{pmatrix} \beta_{11} \\ \beta_{31} \end{pmatrix} + \begin{pmatrix} \dot{W}_{11} & 0 \\ 0 & \dot{W}_{31} \end{pmatrix} \begin{pmatrix} \beta_{12} \\ \beta_{32} \end{pmatrix}.$$

where  $\Delta \dot{W}_{i0}$  are the bias errors of the individual accelerometers;  $k_{wi}$  are the error coefficients of the scale factors of the accelerometers;  $\alpha_x, \alpha_z$  are errors in the platform leveling system;  $\alpha_y$  is the error in the aiming system;  $k_{x0}, k_{y0}, k_{z0}$  are the platform drift rates which do not depend on overload;  $k_{x1}, k_{y1}, k_{z1}$  are the platform drift rates which are proportional to overload; and  $t$  is the flight time of the launch vehicle;

$$(\varphi_{ij}) = A \begin{pmatrix} 0 & -\dot{W}_x & \dot{W}_y \\ \dot{W}_x & 0 & -\dot{W}_z \\ -\dot{W}_y & \dot{W}_z & 0 \end{pmatrix}, \quad (\varphi_{iii}) = t(\varphi_{ij}), \quad (\varphi_{wij}) = (\varphi_{ij}) \begin{pmatrix} \dot{W}_x & 0 \\ \dot{W}_y & \dot{W}_z \\ 0 & \dot{W}_x \end{pmatrix}. \quad (5)$$

Based on how the accelerometers are installed, an orthogonal system  $O-X_1 X_{11} X_{12}$  is determined.  $\beta_{11}$  is the angular installation error of the  $i$ th accelerometer about the  $X_{12}$  axis;  $\beta_{12}$  is the angular installation error of the  $i$ th accelerometer about the  $X_{11}$  axis;  $\dot{W}_{11}$  is the apparent acceleration of the launch vehicle in the  $X_{11}$  direction;  $\dot{W}_{12}$  is the apparent acceleration in the  $X_{12}$  direction.

If the inertial guidance system is used only during the boost phase, then the main issue is to estimate the total velocity and position errors of the guidance system caused by various error sources. The various errors in the platform system can be characterized by errors of the equivalent time-varying scale factors. By performing an analysis of the error characteristics of a practical inertial guidance system, one can express the error model as follows:

$$\begin{pmatrix} \Delta \dot{W}_1 \\ \Delta \dot{W}_2 \\ \Delta \dot{W}_3 \end{pmatrix} = \begin{pmatrix} \dot{W}_1 & 0 \\ & \dot{W}_2 \\ 0 & \dot{W}_3 \end{pmatrix} \begin{pmatrix} k_1 \\ k_2 \\ k_3 \end{pmatrix}. \quad (6)$$

where the error coefficients of the equivalent scale factors  $k_i$  are time varying; in some cases they can be modeled by a second-order time function:

$$k_i(t) = k_{i0} + k_{i1}t + k_{i2}t^2. \quad (7)$$

Substituting equation (7) into (6) gives

$$\begin{pmatrix} \Delta \dot{W}_1 \\ \Delta \dot{W}_2 \\ \Delta \dot{W}_3 \end{pmatrix} = \begin{pmatrix} \dot{W}_1 & 0 \\ & \dot{W}_2 \\ 0 & \dot{W}_3 \end{pmatrix} \begin{pmatrix} k_{10} \\ k_{20} \\ k_{30} \end{pmatrix} + \begin{pmatrix} \dot{W}_1 t & 0 \\ & \dot{W}_2 t \\ 0 & \dot{W}_3 t \end{pmatrix} \begin{pmatrix} k_{11} \\ k_{21} \\ k_{31} \end{pmatrix} + \begin{pmatrix} \dot{W}_1 t^2 & 0 \\ & \dot{W}_2 t^2 \\ 0 & \dot{W}_3 t^2 \end{pmatrix} \begin{pmatrix} k_{12} \\ k_{22} \\ k_{32} \end{pmatrix}. \quad (8)$$

The fact that the coefficient matrix of the error model described by equation (8) is a diagonal matrix will greatly simplify the real-time on-board computations. In practice, the error model of the inertial guidance system is determined using system identification theory and experimental analysis of actual inertial guidance systems.

### III. Distance-Inertial Guidance

For a deterministic inertial guidance system and a deterministic flight, the errors generated are also deterministic. By taking highly accurate distance measurements from exterior ballistics, and using an error model represented by equation (8) or some other equation, these deterministic error coefficients can be estimated. They can in turn be used to estimate and correct for the velocity and position errors of the inertial guidance system, thus increasing the accuracy of the guidance system.

The measurement equation for the distance-inertial guidance system is of the form:

$$Y(t) = C(t)K + V(t), \quad (9)$$

$$Y(t) = (y_i(t)) = X_I(t) - X_R(t). \quad (10)$$

where  $X_I$  is the range vector used by the inertial guidance system for ballistic trajectory calculation;  $X_R$  is the corresponding range vector given by the distance measurement system;  $K=(k_j)$  is the error coefficient matrix;  $C=(c_{ij})$  is the measurement matrix, where the element  $c_{ij}$  reflects the degree of sensitivity of the measured value  $y_i$  with respect to the error coefficient  $k_j$

$$c_{ij} = \frac{\partial y_i}{\partial k_j}. \quad (11)$$

Once the error model is defined, the measurement matrix can be readily determined.

The measurement noise  $V$  includes uncertainties in the ranging signals of exterior ballistics. It is assumed to be zero mean and uncorrelated with the error coefficients  $K$ .

With  $n$  measurements, the error coefficients  $K$  can be estimated from the recursive formulas:

$$\hat{K}_n = \hat{K}_{n-1} + H_n(Y_n - C_n \hat{K}_{n-1}), \quad (12)$$

$$H_n = P_{n-1} C_n^T (\Sigma_n + C_n P_{n-1} C_n^T)^{-1}, \quad (13)$$

$$P_n = (I - H_n C_n) P_{n-1}. \quad (14)$$

where  $\hat{K}_n$  is the estimated value of  $K$  at  $t=t_n$ ;  $H_n$  is the gain matrix;  $P_n$  is the covariance matrix of the estimation errors; and  $\Sigma_n$  is the covariance matrix of the measurement noise  $V$ .

The initial values of  $P_n$  and  $K_n$  are the pre-test statistical estimates of the error coefficients, which are generally determined from pre-flight calibration tests.

Having determined the error coefficients  $\hat{K}$  from equations (12), (13), (14), one can then estimate the state variable  $\hat{Z}_n$  of the inertial guidance system.

$$\hat{Z}_n = Z_I + \Delta \hat{Z}_n, \quad (15)$$

$$\Delta \hat{Z}_n = D_n \hat{K}_n. \quad (16)$$

where the state variable of the inertial guidance system output is  $Z_I = (v_{x1}, v_{x2}, v_{x3}, x_1, x_2, x_3)^T$ ;  $\hat{Z}_n$  is the estimated value of  $Z_I$  at  $t=t_n$ ;  $\Delta \hat{Z}_n$  is the estimated bias error of  $Z_I$  at  $t=t_n$ ;  $D_n=(d_{ij})$  is a matrix of trajectory functions, the element  $d_{ij}$  is the sensitivity function of the  $i$ th component of the state variable of the guidance system with respect to the error coefficient  $k_j$ , and is determined from the error model and actual trajectory parameters.

The basic principle of a distance-inertial guidance system is summarized in the block diagram shown in Fig. 2.

1. thrust vector control
2. motion of the center of mass of the launch vehicle
3. correction calculation
4. optimum estimation of error coefficient
5. distance measuring instrument
6. engine cut-off control
7. lateral normal control
8. identification calculation
9. calculation of measurement matrix
10. inertial platform
11. inertial navigation calculation
12. on-board computer

Simulation and flight test results show that during the boost phase, the accuracy of a distance-inertial guidance system is considerably higher than a pure inertial guidance system with the same inertial components. This type of composite guidance system is also more accurate than other types of composite guidance systems for less cost. Since the system requires only simple ranging equipment near the launch site and only to be used during the boost phase of the launch vehicle, not only launch preparation is relatively easy, but the likelihood of outside interference is very small. Furthermore, since the pure inertial guidance section and the distance-inertial navigation section are independent of each other, the correction given by the composite navigation is applied after the identification calculation; therefore, introduction of the distance information does not affect the autonomy or the reliability of the inertial guidance system.

## References

1. Qian Xuesen, Song Jian, "Theory of Engineering Control," Science Publishers, 1981
2. Guo Xiaokuan, Yue Peiyu, "Disturbance Predictive Guidance of Launch Vehicles, Acta Automatics Sinica, 5 (1979), No 3
3. P. Aikehuofu, "System Identification," Science Publishers, 1980

3012

CSO: 4008/213

27 March 1985

## APPLIED SCIENCES

## SYSTEMS RESEARCH ON 'CHINA IN YEAR 2000'

Beijing XITONG GONGCHENG LILUN YU SHIJIAN [SYSTEMS ENGINEERING--THEORY AND PRACTICE] in Chinese No 2, 1984 pp 15-23

[Article by Wang Huijiang [3769 1979 3518] and Li Boxi [2621 3124 3305]:  
"Systems Research on China by the Year 2000"]

[Text] "China by the Year 2000" is one of the national key research projects and we participated in this work. The objective of the research, "China by the Year 2000," is to provide a scientific basis for our country, the Party Central and the State Council in policymaking in order to realize the strategic goals of the 12th Party Congress. It also provides a scientific basis for various regions, trades and business in drafting development plans. Furthermore, the Chinese people are encouraged to endeavor to carry out the magnificent plan of the Communist Party by publicizing the grand blueprint for China by the year 2000.

Because the subject of study is a huge complex system on the national level, in addition to the necessary professional knowledge, systems research methods are required to carry out this work. In the following, we will separately discuss the subject of the study, the methodology and the organization design. These three problems are interrelated, as shown in Figure 1.

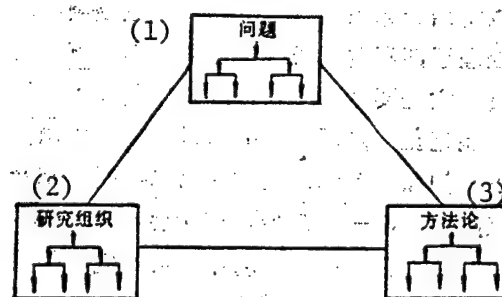


Figure 1. Triangular Diagram in Studying Complex Problems

## Key:

1. Problem
2. Organization study
3. Methodology

# 1. Contents and Scope of the Study on "China by the Year 2000"

The contents of the study on "China by the Year 2000" include projects on the five major sources of income of the Chinese national economy (industry, agriculture, transportation, construction and business), finance and foreign trade, population and related areas such as employment, culture and education, health and hygiene, etc., consumer demand and its structure, social stability, social fashion and spiritual civilization, natural resources, ecosystems, science and technology, domestic regions, and international environment. We want to understand the present status and problems in the areas mentioned above and the situation and consequences in these areas if they are allowed to develop naturally by the year 2000. We should also study how to select a controlled growth path to allow a coordinated growth in the economy, as well as our society and science and technology, so that the overall strategic goal formulated by the 12th Party Congress can be achieved more effectively. To this end, we must draft an overall development strategy and policy as well as strategies for various levels and specific policies. The contents and scope of the research discussed above can be schematically expressed as shown in Figure 2.

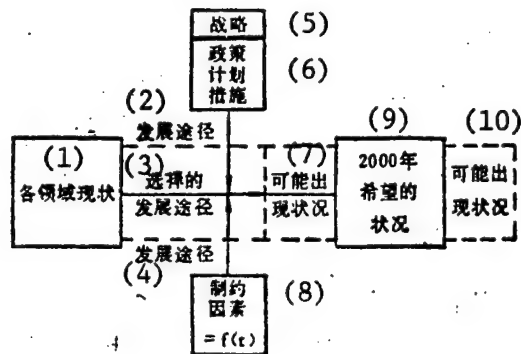


Figure 2. Contents and Scope of the "China by the Year 2000" Research

Key:

- |                                  |                                   |
|----------------------------------|-----------------------------------|
| 1. Status of various territories | 6. Policy, planning and measures  |
| 2. Development path              | 7. Possible situations            |
| 3. Chosen development path       | 8. Constraints = $f(t)$           |
| 4. Development path              | 9. Desired situation by year 2000 |
| 5. Strategy                      | 10. Possible situation            |

"China by the Year 2000" includes a wide range of areas. The problems in these areas are interrelated and mutually affecting. For instance, the prediction of the changing international political and economic environment will affect the development in various aspects in China as well as the policies and measures to be adopted. In the process, some constraints vary with growth and the changing environment. For example, in the first 5-year period, land and water resources were not limiting factors in the area of industrial and economic construction. However, land and water have become

serious limiting factors in certain regions today in site selection for industrial construction. Hence, we must constantly address ourselves to some overall and regional limiting factors and their variations in future development. Furthermore, we have to adopt corresponding development policies and countermeasures.

## 2. Development Strategy

We believe that the study of Chinese development strategy is to study the overall pattern for the comprehensive coordinated development of the economy, the society and S&T. This study is relatively complicated. The study of strategy is considered as an art abroad. To a certain extent, it reflects that this discipline has not yet reached a scientific stage.

Regarding the guiding ideology for the research and drafting of development strategy in China, Comrade Ma Hing [7456 3163] pointed out in the discussion meeting on the development strategy that we should (1) combine the generalized truth of Marxism with the Chinese reality, (2) conduct comprehensive research by integrating the economic, social and S&T development strategies, (3) correctly treat the relation between developing rate and actual benefit, (4) correctly consider the relation between near- and long-term benefits, (5) pay simultaneous attention to socialist material civilization and spiritual civilization, and (6) take the changes in the international environment into account.

The basis for drafting an accurate development strategy is to thoroughly understand the situation and characteristics of China to consequently formulate the correct development strategy and policy. For instance, Comrade Mao Zedong analyzed the four major characteristics of the Chinese Revolutionary War in the second revolutionary era that China was a semi-colonial country with imbalanced political and economic development. Furthermore, it went through the revolution between 1924 and 1927 which made the enemy strong and the Red Army weak. In addition, the leadership of the Communist Party and land reform were also included. A series of correct strategic and tactic measures were drawn up which led to the victory of the Chinese revolution.

Strategies and policies can be classified as general strategies and general policies, auxiliary strategies and policies derived from general strategies and policies, secondary (sub) strategies and policies and emergency strategies.

Several policy and strategy making viewpoints used abroad can be used as a reference: strategies and policies must assist the implementation of objectives and plans, they should have continuity, they should be flexible and they should be placed under control.

## 3. Policy and Policy Science

In order to accomplish projected objectives in social, economic and S&T areas, general and specific policies must be drawn up under the guideline of the general strategy.



We have the following understandings on policy and policy science:

- (1) The function of a policy is to influence the behavior of people under various situations. Usually, they have the following functions: to guide people to take certain actions, to adjust the behavior of people to fit a certain model, and to stop or prohibit the spreading of certain actions. A certain policy may simultaneously have all three functions. However, a certain aspect may be emphasized when formulating the policy.
- (2) Policies should stay above the comparison of different plans. When a certain plan is selected, the effectiveness of the policy must be accessed.
- (3) The consequence of a policy must be predicted. A policy very often has some unpredictable consequences. If the consequence of a policy is uncertain, then more opinions should be digested in the policymaking process to expose various aspects of the uncertainty. Argument meetings may be a possible format. Small scale test points may be another feasible format.

The so-called policy science abroad has five aspects: policy strategy (including the guideline, scope and assumption of a specific policy), policy analysis (including models used to draw up policies such as rational model, economic ration model, infinitesimal increment model, policymaking program model and mutation model, as well as cost analysis and feasibility analysis), improvement of policymaking system, policy evaluation and advancing policy science.

A policy is drawn up with respect to a certain object. The policy science abroad presents a model for the policymaking system as shown in Figure 3.

The mathematical model of the policymaking system is expressed by the following formula:

$$g_i(X_1, X_2, \dots, X_n) \geq b_i \quad i = 1, 2, \dots, m$$

where,  $X_1, X_2, \dots, X_n$  are the variables of the policymaker, and  $b_i$  is the expectation level. The function  $g_i$  is controlled by the different policy group.

The left side of the equation is equivalent to the measures while the right side represents the objective. The aim is to obtain the solution of the series of measure-objective relations. Different policymakers have different mathematical formulas.

## II

Because of the breadth and complexity of the contents of the study of "China by the Year 2000," in addition to the knowledge in a special field, fundamental methods in frontier science are more in demand. Hence, our study also includes the theoretical problems in systems engineering and its applications.

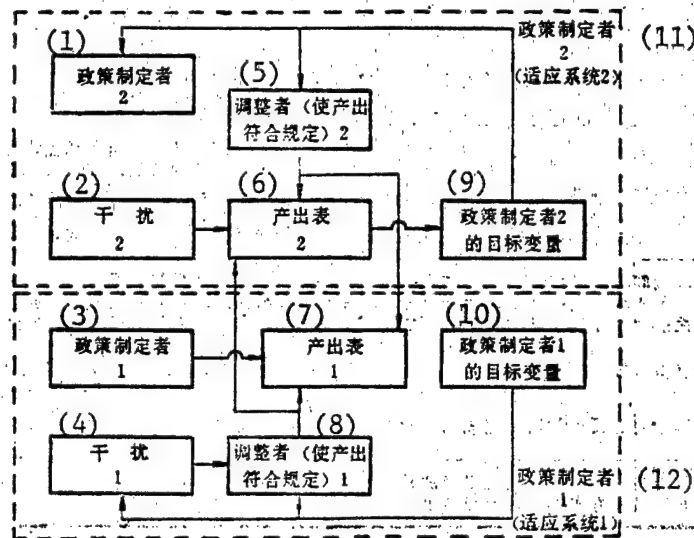


Figure 3. The Policymaking System

Key:

1. Policymaker 2
2. Interference 2
3. Policymaker 1
4. Interference 1
5. Adjuster 2 (to make output meet specifications)
6. Output list 2
7. Output list 1
8. Adjuster 1 (to make output meet specifications)
9. Target variation of policymaker 2
10. Target variation of policymaker 1
11. Policymaker 2 (adaptation system 2)
12. Policymaker 1 (adaptation system 1)

### 1. Generalized Systems Theory

The generalized systems theory can serve as the theoretical basis for systems engineering. In the "Generalized Systems" published in 1956, Peter Longfellow presented the following objectives of this new discipline:

- A. To create a trend to integrate different disciplines such as natural and social sciences.
- B. To reflect this integration in the generalized theory of systems.
- C. To become an important means in establishing the correct theory for sciences in the non-materialistic domain.
- D. To form a unified theory through the "longitudinal" development of various scientific disciplines so that the theory will bring the goal of unifying science closer.
- E. To lead to integration which is urgently needed in science education.

Table 1 shows an example in which general systems theory was used to investigate the complicated subject "China by the Year 2000."

Table 1

No.	Argument by generalized systems theory	Attempted use in "China by the Year 2000"
1	A system is formed by inter-related subsystems and its characteristics should be considered as a whole.	The subject matter was divided into departmental and regional subsystems to be studied and analyzed in a comprehensive manner.
2	The system has a layered structure.	It is a good point to study the structure of "China by the Year 2000." A department was further divided into material producing and nonproducing subsystems. A production system is further divided into subsystems such as agriculture, energy, transportation, metallurgy, and chemicals. Agriculture and energy are further divided into lower levels.
3	A system can be classified as an open or a one depending on whether there is exchange of energy, information and materials. The "openness" of a system is usually a relatively open system.	China is a part of the world. We can exchange energy, information and materials with the rest of the world. In studying "China by the Year 2000," we must study the effect of the international environment on various development stages.
4	A social system has many objectives.	On the basis of clarifying problems, the objectives of the system are studied and the comprehensive targets are evaluated.
5	Different investment and activity in a social system can accomplish the same economic goal.	Under the guidance of the six strategic points, various feasible ways for the socialist China were explored in order to recommend a satisfactory route.
6	An open system can be considered as a transition model of the environment in a dynamic equilibrium. It accepts the investment and produces results in a certain way.	Various qualitative and quantitative models.

## 2. Methodology of the Working Process

Figure 4 shows the working process. This diagram has a general significance in the methodology.

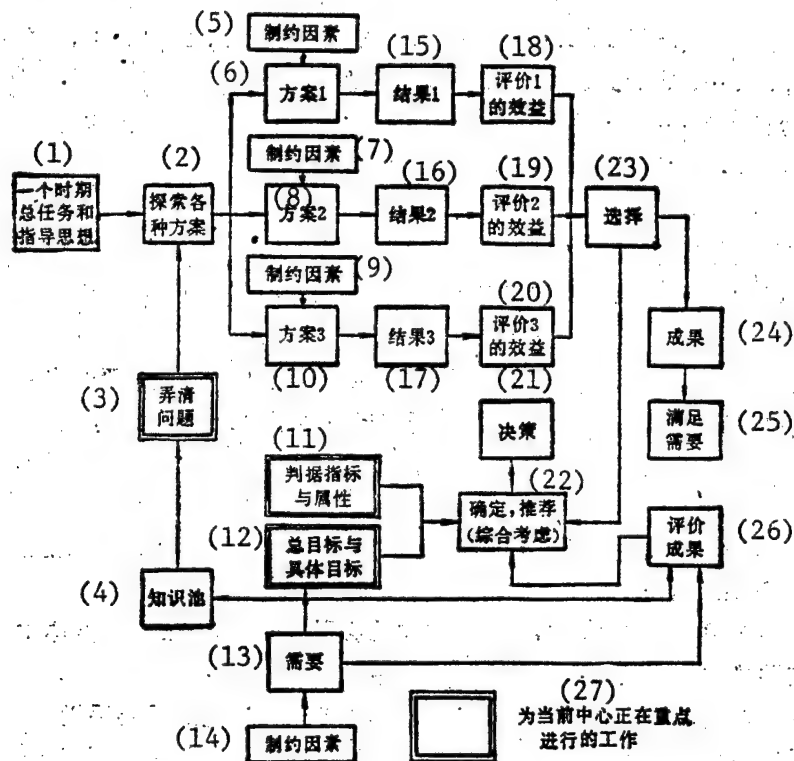


Figure 4. The Working Process Diagram

Key:

- |  |  |
|--|--|
| 1. Major task and leading ideology in an era | 15. Result 1   |
| 2. Exploration of various plans              | 16. Result 2   |
| 3. Clarification of problems                 | 17. Result 3   |
| 4. Knowledge pool                            | 18. Evaluation of result 1   |
| 5. Limiting factors                          | 19. Evaluation of result 2   |
| 6. Plan 1                                    | 20. Evaluation of result 3   |
| 7. Limiting factors                          | 21. Policymaking   |
| 8. Plan 2                                    | 22. Determination and recommendation (comprehensive consideration) |
| 9. Limiting factors                          | 23. Selection  |
| 10. Plan 3                                   | 24. Accomplishments  |
| 11. Evaluation criteria                      | 25. Requirements satisfied   |
| 12. Overall goal and specific objectives     | 26. Evaluation of accomplishments                                  |
| 13. Requirements                             | 27. Current key focus  |
| 14. Limiting factors                         |  |

### 3. Problem Identification and Goal Determination

Problem identification is the beginning of any "systems engineering" project. The series of work done by the Technical Economics Center before and during the discussion meeting on development strategy in October was aimed at identifying the problems. Through this meeting, most of the major problems have been identified. In the future, a series of discussion meetings will be held to clarify the problems in various areas and discuss the preliminary plans for solving the problems.

### 4. Regarding Quantitative Analysis

In systems engineering, various quantitative analysis models are widely used to provide data for policymaking. In the year 2000 global study in the study, various models, such as the "M-P World Model," the "agricultural international relationship model" as well as the "Latin America Global Model" and "United National Global Model" developed by MIT, were used.

A lot of quantitative analysis work has been done in China by the systems engineering community. We believe that an economic analysis should reflect the laws of economics. When we apply various models, we must understand its theoretical basis. On the other hand, quantitative models must be used realistically. If the accuracy of the original data is only 80 percent, then the accuracy of the calculated results cannot be better than 80 percent no matter how huge and complicated the model is. One of the difficulties in modeling is that very little convincing accomplishments are obtained despite the amount of work. If we start from a relatively simple model to obtain convincing results which can be verified and then continue to perfect the original model, it may be more effective.

## III

In systems engineering, not only the subject matters are studied but also the organization and the process to perform a certain task are investigated.

### 1. Organization in Systems Engineering

Figure 5 shows an organization commonly used in systems engineering.

Each organization is situated in an environment. It takes materials, energy and information from the environment and delivers its output to the environment. The organization in systems engineering is composed of five factors:

A. Objectives and Requirements. An organization is established in order to achieve a specific goal to satisfy a certain need of the society. The aim to set up an organization to study "China by the Year 2000" is to initiate various research activities in order to provide recommendations for the leadership in policymaking. The structure and activity of the organization are centered around this goal.

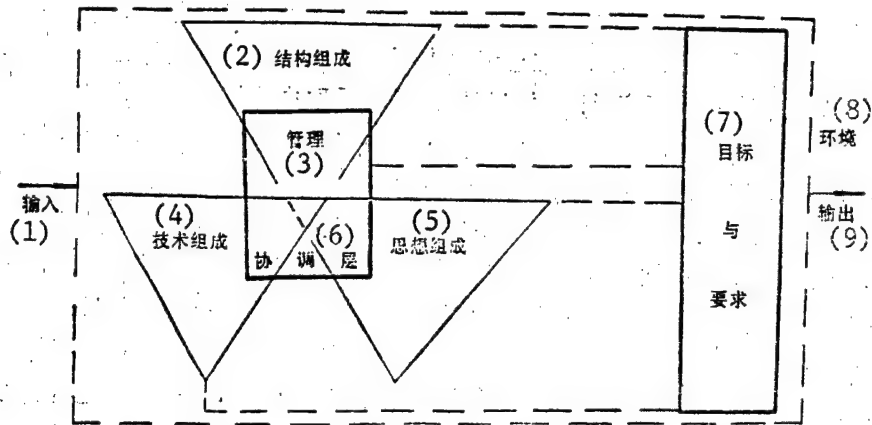


Figure 5. Organization in Systems Engineering

Key:

- |                            |                                |
|----------------------------|--------------------------------|
| 1. Input                   | 6. Coordination level          |
| 2. Structural composition  | 7. Objectives and requirements |
| 3. Management              | 8. Environment                 |
| 4. Technical composition   | 9. Output                      |
| 5. Ideological composition |                                |

B. The technical composition is the knowledge required to accomplish the objective. Within the subject matter, not only the specialty knowledge but also general knowledge are required in order to understand the past and to plan the future. We need natural sciences as well as social sciences. We need qualitative as well as quantitative consideration, and local as well as overall considerations. For a production organization, the technical composition is product design and technology. In order to finish an article of high quality, we should also have a set of scientific working processes to ensure the result. This includes preparing the outline, defining the scope, direction and depth of the study, performing the computation, evaluating the original data, and determining the terms to calculate quantitatively. The technology of our technical organization is "software." We receive information in our organization, and finally output information (reports). Our technical composition is centered around the characteristics of the "software technology."

C. Ideological Composition. This research organization consists of members from a wide cross-section of disciplines--researchers, teachers in higher learning institutions, administrators and practitioners. Each member has a different post, background and working habit. Some have acquired a lot of practical experience, accumulated some empirical data and possessed the capability of judgment. Some have devoted most of their time to theoretical research. Those who studied a certain discipline in depth have different understanding with regard to a specific problem from those who worked on certain projects for a long time. This kind of ideological difference is required in systems engineering. However, we must also recognize the conflict of this special feature so that it can be dealt with.

D. Structural Composition. This often implies sharing responsibility and coordination. The organization charts in other countries clearly identify the responsibilities and overlapping areas. In the structural composition, usually it should include duties, tasks, regulations, processes (including communication). In our organization, the technical economic center is responsible for coordinating the work as well as for linking various processes. Other items are handled by various departments according to the actual situation. In order to ensure the product quality, we wish the responsible unit to have rules governing the working process. We should establish a product inspection system so that the management level will not be overburdened.

E. Management and Coordination Level. In the "China by the Year 2000" organization, there is a leadership group. Its major duties are: to strategically define the organization and work plan of this subject matter, to control the progress, to coordinate among major tasks, to set quality requirements for the final product, to notice the characteristics of various components in the organization and to take measures to unify them under the primary principle, and to adopt timely measures to solve all the problems according to progress.

## 2. Secondary Research Organization "China by the Year 2000" and Preliminary Considerations for the Process

### A. Secondary Research Organization

We preliminarily decided to adopt a substructural form as the one shown in Figure 6 based on the characteristics of this work. A departmental research organization has more planning experience. It is capable of grasping historical data and the research accomplishments are more practical. Although we are somewhat limited by the "line" system and our working habit, however, the project can be completed in a serious atmosphere. The regional research structure is based on a combination of "block" and "line" structures. They mutually complement each other in order to bring out the special situations of the region to avoid any bias in the conclusion. An interdisciplinary society has more "freedom" in conducting research. There are a few traditional "limitations." However, to some extent it does not have certain advantages of a departmental research institute.

The information flow connecting these three kinds of organizations is in the form of itemized reports and summaries.

### B. Symposium—a Kind of Structure

The main result of "China by the Year 2000" is a final report which will be prepared by preserving the essential and true information gathered through various information generation and exchange mechanisms.

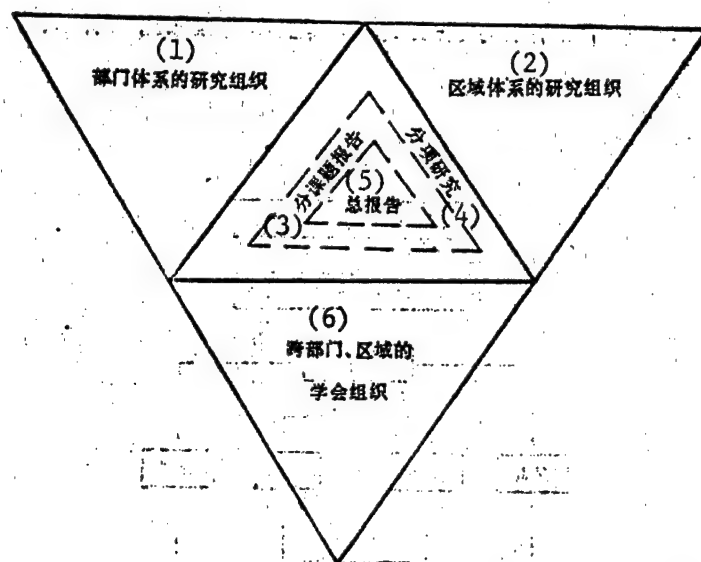


Figure 6. The Research Structure in "China by the Year 2000"

Key:

1. Departmental research organizations
2. Regional research organizations
3. Topic report
4. Itemized report
5. Summary report
6. Interdepartment, interdisciplinary academic societies

In dealing with a very complicated assignment, when the individual knowledge is not deep enough, we must rely on temporary organizations such as symposiums. As the discussion becomes deeper and the problems get clarified, it is necessary to continuously change the subject matter and the members involved. Another series of symposiums must be held in order to solve these problems.

Several characteristics and principles must be noted for this type of organization:

- (1) Inhomogeneity of Oral Expression. In a short meeting, the time for each participant to speak is not uniform. Some people like to talk while others don't like to say much. The presiding person should take measures accordingly.
- (2) Sufficient Preparation. All the attendants should be provided with the details ahead of time. The subject to discuss and anticipated results should be provided.
- (3) Discussing Problems and Arguments Developed Spontaneously To Research a Stage Agreement. The organizer must estimate the time required for each stage based on the nature of the problems and devise an appropriate plan.



(4) Characteristic of Acceptance. There is a specific process for people to accept, comprehend and memorize a new concept. We should take measures to promote this process.

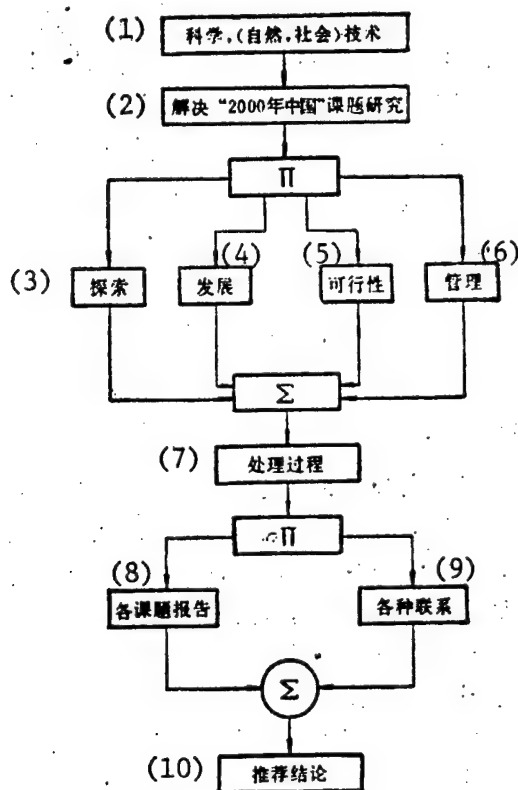
(5) Avoiding Complications. Because of the profession and interests, people tend to concentrate on certain aspects of a subject matter instead of a certain aspect of several subject matters. Hence, we should grasp the program according to this principle in the discussion.

(6) Quantitative and Qualitative Correlation. It is easy to reach conclusions by performing qualitative discussion and exploration quantitatively. We should avoid discussing quantitative calculations in a meeting without any preparation.

### C. Process of Concept Formation

We should not depend on a single concept and method to solve a complicated problem. Instead, we need a series of concepts and methods. This is the systems engineering approach to solving problems.

The work on "China in the Year 2000" should begin with encouraging people to supply ideas so that these ideas can be summarized stage by stage. This is the process of summation  $\rightleftharpoons$  analysis and deduction  $\rightleftharpoons$  initiation. It can be mathematically expressed as a  $\Pi$ - $\Sigma$  process as shown in Figure 7.



#### Key:

1. Science (natural and social) and technology
2. Research on "China in the Year 2000"
3. Exploration
4. Development
5. Feasibility
6. Management
7. Treatment process
8. Various topic reports
9. Various links
10. Recommending conclusions

Figure 7. The Process for "China in the Year 2000"

In the above introduction, there are a large number of systems engineering subjects in "China in the Year 2000," including the study on goals and policies, the relation between the target and the rate distribution, targets and indicators, relation between economic, social and environmental benefits, evaluation of economic benefit, relation between macroeconomic and micro-economic benefits, study of the population problem, comprehensive study on people's life, analysis of the structure and effectiveness of science and technology, study of energy and transportation problems, study of education and professionals, study of comprehensive social factors, study of the ecosystem, study of regional economics and study of international situation.

How to draw up a coordinated development plan for economic, social and S&T growth, how to consider the overall population resources and economic problems, how to control the population to within 1.2 billion, and how to quadruple the GNP under premise of continuously improving economic benefit are also subject matters to be studied in systems engineering.

We believe that the research and application of systems engineering in China can be pushed to a new stage through some key research organizations (see Figure 8).

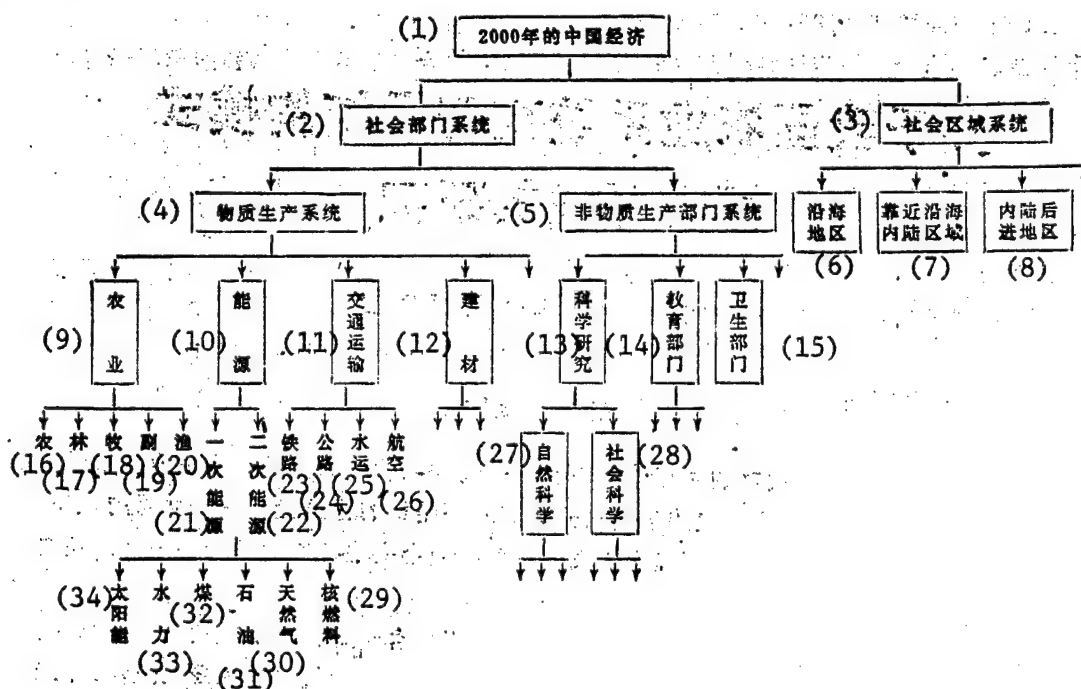


Figure 8. Design of the Research Structure

Key:

- |                                 |                                    |
|---------------------------------|------------------------------------|
| 1. Chinese economy in year 2000 | 6. Coastal area                    |
| 2. Social department system     | 7. Inland area near the coast line |
| 3. Regional social system       | 8. Far inland area                 |
| 4. Manufacturing system         | 9. Agriculture                     |
| 5. Nonproduction system         | 10. Energy                         |

11. Transportation
12. Construction material
13. Scientific research
14. Education
15. Hygiene
16. Agriculture
17. Forestry
18. Animal husbandry
19. Part-time trade
20. Fishing
21. Primary energy source
22. Secondary energy source

23. Railroad
24. Highway
25. Shipping on water
26. Aviation
27. Natural science
28. Social science
29. Nuclear fuel
30. Natural gas
31. Petroleum
32. Coal
33. Hydropower
34. Solar energy

12553

CSO: 4008/384

## POTENTIAL AT ATOMIC BOUNDARIES IN THE TF (OR TFD) MODEL AND EQUATIONS OF STATES

Beijing WULI XUEBAO [ACTA PHYSICA SINICA] in Chinese, Vol 33, No 2, Feb 84 pp 176-192

[Article by Cheng Kaijia [4453 7030 3946], Fan Qike [2868 0796 4430], Gao Zhanpeng [7559 0594 7720]]

[Text] I. Introduction

A method of applying Fermi statistics to treat atomic problems was proposed by Thomas<sup>[1]</sup>; while the method is not as accurate as the Hartree-Fock self-consistent method, it is simple to use and provides a clear picture of physical insight. Many authors have applied the theory of statistics to calculate the equations of state of matter; the most comprehensive calculations are given by Latter<sup>[2]</sup>. The calculated results are shown to be in good agreement with observed values for elements with high atomic numbers or in the high pressure range; but in the low pressure range, they are higher than the observed values by an order of magnitude. Dirac<sup>[3]</sup> applied a correction to the TF theory to account for the exchange energy; it is called the TFD model. Metropolis and Reitz<sup>[4]</sup> have used the TFD model to generate numerical solutions for 24 different elements. While the results show that the TFD method yields lower pressure, the calculated results are still much higher than the measured values in the low pressure range. Subsequently, other authors<sup>[5-8]</sup> proposed corrections to account for the quantum effect and the correlation effect, but the basic problem of disagreement with observations at the low pressure range still remains. In this article, it is pointed out that in calculating the pressure at atomic boundaries using the virial theorem, the potential at the boundary should not vanish.

One of the authors of this article pointed out in 1958<sup>[9]</sup> that in applying TF statistics, the  $Z$  electrons inside the atom are all included in the statistical calculation to determine the charge density at each point within the atom. When the potential energy is determined from the charge density, one should note that it refers to the energy of a particular electron in a potential field produced by the nucleus and other electrons; in other words, it is the energy produced by the interaction between this electron and the nucleus (with  $Z$  positive charges) and  $(Z-1)$  other electrons. This article presents a detailed analysis which shows that the potential energy imposed on an electron at the boundary  $r_0$  of an atom approaches

$$W(r_0) = -\frac{e^2}{r_0} n(r_0). \quad (1)$$

(The detailed analysis is given in the next section). This value corresponds to the self-energy of the electron, where  $n(r_0)$  is the density of electron distribution.

We know that the electron distribution  $n(r)$  is determined by the Poisson equation

$$\nabla^2 V(r) = 4\pi e \cdot n(r) \quad (2)$$

with boundary conditions

$$\begin{aligned} rV(r) &= eZ \quad r \rightarrow 0, \\ \frac{\partial n(r)}{\partial r} &= 0 \quad r = r_0 \end{aligned} \quad (3)$$

This is undoubtedly correct because the Wigner-Seitz spherical symmetric potential  $V(r)$  strictly obeys the Poisson equation. The second boundary condition of equation (3) can also be written as  $V'(r)=0$ , but it does not imply  $V(r_0)=0$ . Therefore, the condition of zero potential at the boundary which leads to results inconsistent with actual observations should not be imposed.

Herman and Skillman<sup>[10]</sup> pointed out in the book "Atomic Structure Calculations" that when the electron is very far from the nucleus, the potential energy of this electron is not zero, but should be  $-e^2/r$ . They believe that when  $r$  is large, the exchange energy formula using the free electron approximation

$$W_{ex} = -6 \left[ \frac{3}{8\pi} \rho(r) \right]^{1/3} \quad (4)$$

no longer applies. Therefore, the self-exchange portion of the total exchange energy cannot completely cancel the self coulomb energy of the electrons.

The Hartree-Fock-Slater equation can be written in the form:

$$\left[ -\frac{d^2}{dr^2} + \frac{\lambda(\lambda+1)}{r^2} + W(r) \right] P_{n1}(r) = E_{n1} P_{n1}(r), \quad (5)$$

where  $W(r)$  is the sum of the coulomb potential of the nucleus, the total coulomb potential of the electrons, and the exchange potential, i.e.,

$$W(r) = -\frac{2Z}{r} + \frac{2}{r} \int_0^r \sigma(t) dt + 2 \int_r^\infty \sigma(t) dt - 6 \left[ \frac{3}{8\pi} \rho(r) \right]^{1/3}. \quad (6)$$

$Z$  is the atomic number,  $\rho(r) = (4\pi r^2)^{-1} \sigma(r)$  is the spherical average charge density of the total electrons. Equation (4)-(6) are all in atomic units. It can be seen from equation (6) that when  $r$  is sufficiently large, the first two terms cancel, the third term is zero, only the last term remains; the last term depends only on  $\rho(r)$ , when  $r$  is large,  $\rho(r) \rightarrow 0$ , hence  $W(r) \rightarrow 0$ . But this argument is incorrect. Herman and Skillman believe that at this point

the electron is acted upon by a positive field, and its potential energy is  $-e^2/r$ . This is in fact the potential energy at the atomic boundary suggested by this article. We believe that the potential energy at the atomic boundary should be  $-e^2/r_0$  not only when  $r$  is large, but at any value of  $r$ ; only when  $r$  is small, the value of  $-e^2/r_0$  is negligible compared to the total energy. For sufficiently large values of  $r$ , the correction to  $W(r)$  proposed by Herman and Skillman agrees well with actual observations; even today this correction is being used in some atomic structure calculations. Its main deficiency however is that at  $r=r_1$ ,  $W'(r)$  is discontinuous, where  $r_1$  refers to the value of  $r$  at which  $W(r)=-e^2(Z-N+1)/r$ ,  $N$  is the number of electrons in the atom or ion. This deficiency has been removed in the present analysis.

The TF theory requires that the electron density at the boundary  $n(r)$  must be continuous, i.e., it must be periodic:

$$\left. \frac{\partial \psi^2(r)}{\partial r} \right|_{r=r_0} = \left. \frac{\partial \psi^2(-r)}{\partial r} \right|_{r=-r_0}, \quad (7)$$

but it cannot satisfy the requirement imposed by a periodic field on the wave function

$$\left. \frac{\partial}{\partial r} \psi(r) \right|_{r=r_0} = \left. \frac{\partial}{\partial r} \psi(-r) \right|_{r=-r_0} \quad \& \quad \psi(r_0) = \psi(-r_0). \quad (8)$$

Clearly, if equation (8) holds, then equation (7) must hold; but the reverse is not always true. This illustrates why the TF theory cannot describe the action of a periodic field on an electron at atomic boundaries. In this article, a pseudo-potential term is introduced at the boundary, whose form is

$$W_{ps}(r_0) = \frac{Ae^2}{r_0} n(r_0), \quad (9)$$

where  $A$  is a constant to be determined; the method of determination will be discussed in section 3. Based on the above considerations, the total potential energy of an electron at the boundary  $r_0$  should be

$$E_{pot} = -\frac{(1-A)}{r_0} n(r_0) e^2. \quad (10)$$

Therefore, when we apply the virial theorem (averaging with respect to a single electron) to determine the pressure at the boundary, it should be

$$P = \frac{2}{3} \frac{E_{kin}}{v} - \frac{(1-A)}{3} \frac{e^2}{r_0} n(r_0), \quad (11)$$

where  $E_{kin}$  is the kinetic energy of the electron,  $v=4\pi r_0^3/3$  is the volume of the atomic cell,  $n(r_0)$  is the electron density at the boundary. Thus, considering the effect of electron exchange, the expression for the pressure becomes

$$P = P_{TFD} - \frac{(1-A)}{3} \frac{e^2}{r_0} n(r_0). \quad (12)$$

The above expression has been used to calculate the cold pressure equations of states for 10 metallic elements; the results agree with measured values to within 10 percent.

## II. Determination of the Potential at Atomic Boundaries

### 1. The Case Where the Electron Wave Function Satisfies the Hartree-Fock Condition

Suppose an atom contains  $Z$  electrons, then according to Pauli's exclusion principle, the anti-symmetric wave function due to the  $Z$  electrons is

$$\Phi = \frac{1}{\sqrt{Z!}} \begin{vmatrix} \varphi_1(r_1) & \varphi_1(r_2) & \cdots & \varphi_1(r_Z) \\ \varphi_2(r_1) & \varphi_2(r_2) & \cdots & \varphi_2(r_Z) \\ \vdots & \vdots & \ddots & \vdots \\ \varphi_Z(r_1) & \varphi_Z(r_2) & \cdots & \varphi_Z(r_Z) \end{vmatrix}, \quad (13)$$

The electron  $L$  at the boundary is acted upon by  $(Z-1)$  other electrons within the atom and the nucleus  $Ze^+$ , i.e.,

$$W_L = \sum_j' \frac{e^2}{r_{Lj}} - \frac{Ze^2}{r_L}, \quad (14)$$

The potential distribution of the electrons inside the atom and the electron  $L$  at the boundary is

$$\Delta W_{Lj} = \sum_j^{Z-1} \frac{e^2}{r_{Lj}} \Phi^* \Phi dr_1 dr_2 \cdots dr_Z, \quad (15)$$

The total potential of the electron  $L$ :

The second term in equation (14) is quite simple; let us examine the first term

$$\begin{aligned} U_L &= \iint \cdots \int \sum_j' \frac{e^2}{r_{Lj}} \Phi^* \Phi dr_1 dr_2 \cdots dr_Z \\ &= \sum_j^{Z-1} \iint \cdots \int \frac{e^2}{r_{Lj}} \Phi^* \Phi dr_1 dr_2 \cdots dr_Z, \end{aligned} \quad (16)$$

where the symbol  $\sum_j'$  denotes summation excluding  $L$ . By expanding the wave function  $\Phi^*$  and  $\Phi$  about the second-order minor of the  $j$ th row and the  $L$ th column, a  $(Z-2)!$  term expansion is obtained, which consists of the minor and other cofactors (independent of the coordinates of the  $j$ th electron and the  $L$ th electron). Thus, after integration the summation becomes

$$\begin{aligned}
U_{Lj} &= \frac{(Z-2)!}{Z!} \int_{r_{Lj}} \frac{e^2}{r_{Lj}} \sum_{i < k=2}^Z \left| \frac{\varphi_i^*(r_j) \varphi_i^*(r_L)}{\varphi_k^*(r_j) \varphi_k^*(r_L)} \right| \cdot \left| \frac{\varphi_i(r_j) \varphi_i(r_L)}{\varphi_k(r_j) \varphi_k(r_L)} \right| dr_j, \\
&= \frac{2}{Z(Z-1)} \int_{r_{Lj}} \frac{e^2}{r_{Lj}} \sum_{i < k=2}^Z [|\varphi_i(r_j)|^2 \cdot |\varphi_k(r_L)|^2 \\
&\quad - \varphi_i^*(r_j) \varphi_i(r_L) \varphi_k^*(r_L) \varphi_k(r_j)] dr_j,
\end{aligned} \tag{17}$$

By adding and subtracting the following term

$$\frac{1}{Z(Z-1)} \frac{e^2}{r_{Lj}} \sum_{i=1}^Z |\varphi_i(r_j)|^2 \cdot |\varphi_i(r_L)|^2,$$

equation (17) becomes

$$\begin{aligned}
U_{Lj} &= \frac{1}{Z(Z-1)} \int_{r_{Lj}} \frac{e^2}{r_{Lj}} \left\{ \left[ \sum_{i=1}^Z |\varphi_i(r_j)|^2 \right] \cdot \left[ \sum_{i=1}^Z |\varphi_i(r_L)|^2 \right] \right. \\
&\quad \left. - \left| \sum_{i=1}^Z \varphi_i^*(r_j) \varphi_i(r_L) \right|^2 \right\} dr_j,
\end{aligned} \tag{18}$$

Equation (18) represents the action of the boundary electron L on any electron within the sphere; since the electron L can be any one of the (Z-1) electrons, there are a total of Z(Z-1) terms of  $U_{Lj}$ . Therefore, substituting equation (18) into (16) gives the potential energy of any electron at the boundary

$$\begin{aligned}
U_L &= \int_{r_{Lj}} \frac{e^2}{r_{Lj}} \left\{ \left[ \sum_{i=1}^Z |\varphi_i(r_j)|^2 \right] \cdot \left[ \sum_{i=1}^Z |\varphi_i(r_L)|^2 \right] \right. \\
&\quad \left. - \left| \sum_{i=1}^Z \varphi_i^*(r_j) \varphi_i(r_L) \right|^2 \right\} dr_j.
\end{aligned} \tag{19}$$

Define

$$n(r) = \sum_{i=1}^Z |\psi_i(r)|^2, \quad \psi_i(r) = \varphi_i(r) \eta_i(\sigma), \tag{20}$$

where  $\eta_i$  is the spin wave function,  $\sigma$  is the spin function which satisfy

$$\int \eta^*(\sigma) \eta(\sigma) d\sigma = 1,$$

then

$$U_L = \int_{r_{Lj}} \frac{e^2}{r_{Lj}} n(r_j) n(r_L) dr_j - \int_{r_{Lj}} \frac{e^2}{r_{Lj}} \left| \sum_{i=1}^Z \psi_i^*(r_j) \psi_i(r_L) \right|^2 dr_j. \tag{21}$$

The first term on the right side of equation (21) is

$$\begin{aligned}
\int_{r_{Lj}} \frac{e^2}{r_{Lj}} n(r_j) n(r_L) dr_j &= n(r_L) \int_{r_{Lj}} \frac{e^2}{r_{Lj}} n(r_j) dr_j \\
&= n(r_L) \cdot e \cdot \int_{r_{Lj}} \frac{dQ_j}{r_{Lj}} = \frac{Z e^2}{r_L} n(r_L),
\end{aligned}$$



where  $dQ_j = n(r_j) e dr_j$ ,  $dQ_j/r_{Lj}$  is the contribution of the charge  $dQ_j$  at the point  $L$ . If  $n(r_j)$  is spherically symmetric, which is a basic assumption of the TF statistical model, then from the Gauss theorem, the contribution of the total charge within the sphere at the point  $L$  is equal to the potential at a radius  $r_L$  with the total charge concentrated at the center of the sphere:  $Q/r_L = Ze/r_L$ .

Now we shall discuss the question of spherical symmetry and the characteristics of the wave function  $\psi_i(r)$  of the electrons within the sphere.

$$\begin{aligned} n(r) &= \sum_i \phi_i^*(r) \phi_i(r), \\ \phi_i(r) &= \sum_{m,l} \beta_{m,l} Y_{lm}(\theta, \varphi) f_{nl}(r) \eta_i(\sigma), \end{aligned} \quad (22)$$

where  $f_{nl}(r)$  satisfies

$$(rf_{nl}(r))'' + \frac{8\pi^2 m}{h^2} \left( E_{nl} - \frac{\hbar^2 l(l+1)}{r^2} - W(r) \right) (rf_{nl}(r)) = 0,$$

$$\int |Y_{lm}(\theta, \varphi)|^2 d\Omega = 1 \quad \text{normalization of solid angle}$$

$$\int_0^\infty f_{nl}^2(r) r^2 dr = 1 \quad \text{normalization with respect to } r$$

$$\int \eta_i^*(\sigma) \eta_i(\sigma) d\sigma = 1 \quad \text{normalization with respect to spin function}$$

$$\sum_l \beta_{m,l}^* \beta_{m,l'} = \delta_{mm'}.$$

Thus, equation (22) becomes

$$\begin{aligned} \sum_i \phi_i^*(r) \phi_i(r) &= \sum_i \beta_{m,l}^* Y_{lm}^*(\theta\varphi) f_{nl}^*(r) \beta_{m,l'} Y_{lm'}(\theta\varphi) f_{nl}(r) \\ &= \sum_{m,l} |Y_{lm}|^2 f_{nl}^2(r) = \sum_{l,n} \frac{2l+1}{4\pi} f_{nl}^2(r). \end{aligned}$$

$n(r)$  is assumed to be spherically symmetric; if for each  $l \neq 0$ ,  $\psi_l$  becomes a filled shell, then there may be two filled shells, even though there is no constraint on the electron spin direction. However, the basic assumption of spherical symmetry is a topic that requires further study.

If we substitute equation (22) for the integration factor of the 2nd term of  $W_L$ ,  $\sum_i \psi_i^*(r_j) \psi_i(r_L)$ , we get

$$\begin{aligned} \sum_i \phi_i^*(r_j) \cdot \phi_i(r_L) &= \sum_{nl} f_{nl}^*(r_j) f_{nl}(r_L) \cdot \left( \sum_m Y_{ml}^*(\theta_j \varphi_j) Y_{ml}(\theta_L \varphi_L) \right) \\ &= \sum_{nl} \frac{2l+1}{4\pi} \cdot P_l(\theta_{jL}) \cdot f_{nl}^*(r_j) f_{nl}(r_L). \end{aligned}$$

which for  $\lambda \neq 0$  has the state of a filled shell. Therefore,  $f_{n1}(r)$  has a large contribution only when  $r < r_L$ ; with the exception of  $\lambda = 0$ , particularly in the outermost valence electron shell,  $f_{n0}(r)$  is very large at  $r \sim r_L$ . Thus, in the above expression, the contribution of the  $\lambda \neq 0$  term is significant only when  $r_j$  is small. The integration factor can be regarded as a uniform distribution plus terms of the second, fourth, etc. polar moments (the functions  $P^1(\theta_{12})$ ) of the inner small region. Therefore, as a zeroth order approximation where the effects of polar moments are omitted, the above integration can still be carried out using the Gauss theorem by first finding the total charge

$$\int \left| \sum_i \psi_i(r_j) \psi_i(r_L) \right|^2 dr_j,$$

and making use of the orthogonality and normalization conditions of the wave function to obtain

$$\begin{aligned} & \sum_i \int |\psi_i(r_j)|^2 \cdot |\psi_i(r_L)|^2 dr_j \\ &= \sum_i |\psi_i(r_L)|^2 \cdot 1 = n(r_L). \end{aligned} \quad (23)$$

The second term of equation (21) can be derived by again using the Gauss theorem and equation (23)

$$-\int \frac{e^2}{r_{Lj}} \left| \sum_i \psi_i^*(r_j) \psi_i(r_L) \right|^2 dr_j = -\frac{e^2}{r_L} n(r_L). \quad (24)$$

Therefore,

$$U_L = \frac{Ze^2}{r_L} n(r_L) - \frac{e^2}{r_L} n(r_L).$$

The second term of  $W_L$  which represents the potential on the spherical surface (i.e., the total energy of the  $L$  electron due to the action of the nucleus) is  $-Ze^2 n(r_L)/r_L$ . Therefore, the total potential energy of the electrons on the spherical surface is

$$\begin{aligned} W &= \frac{Ze^2}{r_L} n(r_L) - \frac{e^2}{r_L} n(r_L) - \frac{Ze^2}{r_L} n(r_L) \\ &= -\frac{e^2}{r_L} n(r_L). \end{aligned} \quad (25)$$

## 2. The Case Where the Electron Wave Function Satisfies the Hartree Condition

In this case, the wave function is the product of the diagonal terms of equation (13). By using a completely analogous procedure, one can derive an expression for the potential energy of any electron at the boundary due to the action of  $(Z-1)$  other electrons inside the sphere.

$$U_L = \int \frac{e^2}{r_{Lj}} \left\{ \sum_{i < k}^Z |\varphi_i(r_j)|^2 \cdot |\varphi_k(r_L)|^2 \right\} dr_j. \quad (26)$$

By adding and subtracting the term

$$\frac{e^2}{r_{Lj}} \sum_{i=1}^Z |\varphi_i(r_j)|^2 \cdot |\varphi_i(r_L)|^2,$$

to the integrand, one obtains

$$U_L = \int \frac{e^2}{r_L} \left\{ \left[ \sum_{i=1}^Z |\varphi_i(\mathbf{r}_i)|^2 \right] \cdot \left[ \sum_{i=1}^Z |\varphi_i(\mathbf{r}_L)|^2 \right] - \sum_{i=1}^Z |\varphi_i(\mathbf{r}_i)|^2 \cdot |\varphi_i(\mathbf{r}_L)|^2 \right\} d\mathbf{r}_i. \quad (27)$$

From equation (27) and equations (20-24), one can derive the same result as given in equation (25).

It is clear from this result that the potential of an electron at the boundary is not equal to zero, and is independent of the exchange energy.

It should be pointed out that equation (25) represents the potential energy produced by the interaction between an electron at the boundary and (Z-1) other electrons; it is independent of the electron exchange energy density used to determine the TFD pressure as described in section 3. The exchange energy density is

$$E_{ex} = -\frac{3}{4} e^2 \left( \frac{3}{4} \right)^{1/3} n(r)^{4/3}. \quad (28)$$

It refers to the effect of cross integration in the "proximity" of an electron, and is derived under the free-electron approximation; it represents the average exchange energy density at a particular point, not the total exchange energy of the atom and electrons. Of course, many authors have questioned the validity of this expression, but this issue is beyond the scope of this article. Strictly speaking, the exchange energy we referred to should be the effective exchange potential of a particular state on the Fermi surface; it is not related to equation (25) and can only be a part of the cross integration (the part which is neglected in this derivation).

In practice, equation (28) and equation (25) are used to calculate

$$P_{ex} = \left| \frac{1}{3} E_{ex} \right| < \left| \frac{1}{3} W_L \right| = P_i. \quad (29)$$

This shows that equation (28) does not include equation (25), i.e., the pressure produced by the electron process and the pressure produced by electron self-energy result from two different mechanisms (see Table 8).

### III. Numerical Method and Results

#### 1. Numerical Solution of the Thomas-Fermi-Dirac Equation

On the basis of the TFD statistical theory, one can derive an expression for the electron density under the condition of absolute zero temperature.

$$n(r) = \frac{8\pi}{3h^3} \left\{ \frac{2me^2}{h} + \left[ \frac{4m^2e^4}{h^2} + 2me(V(r) - E_0) \right]^{1/2} \right\}^3, \quad (30)$$

where  $m$  and  $e$  are respectively the electron mass and the absolute value of the electron charge,  $V(r)$  is the potential inside the Wigner-Seitz sphere

which is dependent on the nucleus distance,  $-eE_0$  is the maximum total energy of the electron,  $h$  is the Planck's constant.

Let

$$\mu = a_0 \left( \frac{9\pi^2}{128Z} \right)^{\frac{1}{3}} = 0.88534 a_0 Z^{-\frac{1}{3}}, \quad (31)$$

$$r = \mu x, \quad (32)$$

$$\varepsilon = \left( \frac{3}{32\pi^2} \right)^{\frac{1}{3}} Z^{-\frac{1}{3}} = 0.2117832 Z^{-\frac{1}{3}}, \quad (33)$$

$$V(r) = E_0 + \frac{2me^3}{h^2} = \frac{Ze}{\mu x} \phi(x), \quad (34)$$

From equations (30)-(34), one obtains,

$$n(r) = \frac{Z}{4\pi\mu^3} \left[ \left( \frac{\phi(x)}{x} \right)^{\frac{1}{3}} + \varepsilon \right]^3, \quad (35)$$

where  $Z$  is the atomic number,  $a_0$  is the radius of the first Bohr orbit of a hydrogen atom,  $x$  is the atomic radius measured in units of  $\mu$ .

Assume that the distribution of  $V(r)$  is spherically symmetric, by substituting  $n(r)$  and  $V(r)$  into the Poisson equation

$$\nabla^2 V(r) = 4\pi e \cdot n(r), \quad (36)$$

one can derive the TFD equation for a non-isolated central atom under the condition of absolute zero temperature.

$$\psi''(x) = x \left[ \left( \frac{\phi(x)}{x} \right)^{\frac{1}{3}} + \varepsilon \right]^3, \quad \psi(0) = 1, \quad \psi'(x_0) = \phi(x_0)/x_0, \quad (37)$$

where  $x_0$  is the radius of the atomic boundary measured in units of  $\mu$ .

Equation (37) is a second order non-linear differential equation. If the integration step size is chosen improperly, the numerical integration will become unstable; small changes in  $\psi'(x_0)$  will have a large impact on  $\psi(x_0)$  and  $x_0$ . As a result, the condition  $\psi'(x_0) = \psi(x_0)/x_0$  will be violated, and computational accuracy will be adversely affected. Metropolis et al [4,11] have obtained TFD numerical solutions for a number of elements by solving equation (37) but these solutions have limited accuracy and narrow compression range. The data provided by these solutions are inadequate for calculating the equations of states of elements over the entire compression range. For this reason, a new numerical method of solving the TFD equation is developed in this article; it is based on the same method used by Latter [2] in solving the TF equation.

By introducing the transformations:

$$\begin{aligned} w = r/r_0 = x/x_0, \quad eV(r) + \alpha + \frac{2me^3}{h^2} &= \frac{\alpha\varphi(w)}{w}, \\ \alpha = -eE_0, \quad \lambda = \left( \frac{r_0}{\mu} \right)^{\frac{1}{3}} \left( \frac{r_0\alpha}{Ze^2} \right)^{\frac{1}{3}}, \quad \mu &= \left( \frac{9\pi^2}{128Z} \right)^{\frac{1}{3}} a_0, \end{aligned} \quad (38)$$

one can obtain the following equation in terms of the new variable

$$\varphi''(\omega) - a\omega \left[ \left( \frac{\varphi(\omega)}{\omega} \right)^{\frac{1}{2}} + \varphi^{\frac{1}{2}}(0) a^{\frac{1}{2}} \varepsilon \right],$$

$$\varphi'(1) - \varphi(1) = 1, \quad \varphi(0) = \frac{Ze^2}{\alpha r_0} \quad (39)$$

and

$$\psi(x) = \frac{\varphi(\omega)}{\varphi(0)}, \quad \psi(x_0) = \frac{1}{\varphi(0)}, \quad x_0 = a^{2/3} \varphi^{1/3}(0). \quad (40)$$

It can be shown that in the vicinity of  $\omega = 1$ ,  $\varphi(\omega)$  can be expanded in a power series of the following form:

$$\varphi(\omega) = \omega + a \sum_{k=0}^{\infty} A_k \left[ \frac{(1-\omega)^{k+1}}{(k+1)(k+2)} - \frac{(1-\omega)^{k+3}}{(k+2)(k+3)} \right]. \quad (41)$$

By substituting equation (41) into (39) and comparing coefficients of like powers of  $\omega$  on both sides of the equation, one can obtain the coefficients  $A_k$  of the power series expansion. To calculate the equations of states, it is only necessary to take the first four terms of the power series. In this article, the coefficients of the first four terms have been calculated to be:

$$A_0 = (1+b)^3, \quad A_1 = 0,$$

$$A_2 = \frac{3}{4} a(1+b)^3, \quad A_3 = \frac{1}{2} a(1+b)^3,$$

where  $b = \varphi^{\frac{2}{3}}(0) a^{\frac{1}{3}} \varepsilon$ .

Once the coefficients  $A_k$  have been determined, a numerical solution of equation (39) can be readily carried out. Since equation (39) does not contain terms of first derivatives of  $\varphi(\omega)$ , we chose Stormer's method to carry out the numerical computation. The initial values required for the numerical integration can be obtained from equation (41). The numerical integration starts from  $\omega = 1$  and terminates at  $\omega = 0$ ; the integration step size  $h$  is 0.005.

For each  $Z$ , once the parameter  $\alpha$  is given, a numerical solution of equation (39) can be obtained to yield  $\varphi(\omega)$  in the closed region  $0 \leq \omega \leq 1$ .

Since a transformed variable is used, the two boundary conditions of the transformed TFD equation becomes:

$$\varphi'(\omega) - \varphi(\omega) = 1 \quad \omega = 1,$$

$$\varphi(\omega) = \frac{Ze^2}{\alpha r_0} \quad \omega = 0.$$

These two conditions are easily satisfied in the integration process. Since the numerical integration is carried out within a closed region, it can be seen from equation (41) that at the origin  $\omega = 1$ ,  $\varphi(\omega) = 1$ . However, at the end point  $\omega = 0$ ,  $\varphi(0)$  cannot be obtained from the formula  $\varphi(0) = Ze^2 / \alpha r_0$  because  $\alpha$  and  $r_0$  are unknown; hence  $\varphi(0)$  must be determined iteratively. If  $\varphi(0)$

satisfies the required accuracy of the iterative solution (the required accuracy is chosen to be  $10^{-8}$ ), then  $\varphi(0)$  is the final solution to be sought. Once  $\varphi(0)$  is determined, equation (40) can be used to calculate  $\psi(x)$ ,  $\psi(x_0)$  and  $x_0$ , and the power function  $\alpha$  can be obtained from the secondary boundary condition of the TFD equation  $\varphi(0) = Ze^2/\alpha r_0$ ; then,  $V(r)$  and the electron density at the boundary  $n(r_0)$  can be readily determined. It is clear that the numerical method proposed in this article for solving the TFD equation circumvents the difficulties often encountered in numerical solutions and at the same time yields improved accuracy.

## 2. Calculation of the Equation of State

Based on the theory proposed in section 1 and section 2 of this article, the cold pressure expression can be written as

$$P = P_{TFD} + P_s + P_{ps}, \quad (42)$$

where  $P_{TFD}$  is the TFD pressure when the effect of electron exchange is taken into consideration;  $P_s$  is the pressure contribution when non-zero electron potential at the atomic boundary is taken into consideration; and  $P_{ps}$  is the contribution due to the pseudo-potential. These three terms are respectively given by the following expressions:

$$P_{TFD} = \frac{Z^2 e^2}{10\pi\mu^4} \left[ \left( \frac{\psi(x_0)}{x_0} \right)^{\frac{1}{2}} + s \right]^5 \left\{ 1 - \frac{\frac{5}{4}s}{\left( \frac{\psi(x_0)}{x_0} \right)^{1/2} + s} \right\}, \quad (43)$$

$$P_s = -\frac{n(r_0)e^2}{3r_0}, \quad (44)$$

$$P_{ps} = \frac{An(r_0)e^2}{3r_0}. \quad (45)$$

$\psi(x_0)$ ,  $x_0$ , and  $n(r_0)$  are obtained from the numerical solution of the TFD equation.

The unknown constant  $A$  in the pseudo-potential is determined by the following procedure:

Let 
$$P_{TFDS} = P_{TFD} + P_s,$$

then 
$$P = P_{TFDS} + \frac{An(r_0)e^2}{3r_0}.$$

if  $P = P_{meas}$  is the converted cold pressure at a particular point based on the Hugoniot value, then

$$A = \frac{3r_0(P_{meas} - P_{TFDS})}{n(r_0)e^2}. \quad (46)$$

$P_{TFDS}$  can be obtained from theoretical calculation.

It can be seen from equation (46) that by selecting an appropriate compression ratio  $\eta$  ( $\eta = v_0/v$ ), and measuring the corresponding pressure  $P_{meas}$ , the constant A can be readily determined. Once A is determined, the required cold pressure equation of state for a particular element can be calculated using equation (42).

### 3. Results

Based on the theory presented above, the cold-pressure equations of states have been calculated for 10 different elements: U, Pb, Au, Ag, Cu, Fe, K, Al, Na and Li.

The curves for the pressure P and the compression ratio  $\eta$  of these elements are presented in Figure 1-Figure 10; the triangles in the figures are the cold pressure measurements based on Hugoniot conversions. The experimental data for aluminum are taken from Ref. [12], the experimental data for iron are taken from Ref. [13], and the experimental data for other elements are all taken from Ref. [14]. The P- $\eta$  curves in the figures are obtained from the theoretical calculations of this article; TFDS denotes the calculated pressure in the TFD statistical model when the condition of non-zero potential at the atomic boundary is taken into consideration; TFDS-P is the calculated pressure when the pseudo-potential is taken into consideration. The numerical solution of the TFD equation and the P- $\eta$  data for the elements Li, Na, Al, Fe, Ag, U are presented in Table 1-Table 6; one can see that the compression ratios range between 1 and 10, and the pressure varies from  $10^4$  bar to  $10^8$  bar. Table 7 gives the parameters used in calculating the equations of states.

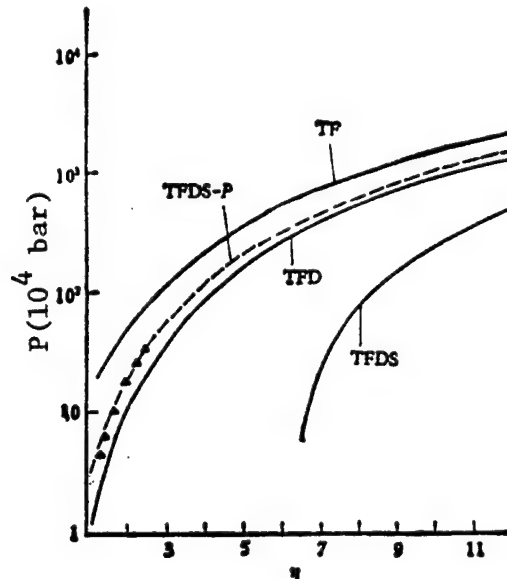


Figure 1. Relationship Between Pressure P and Compression Ratio  $\eta$  for Li

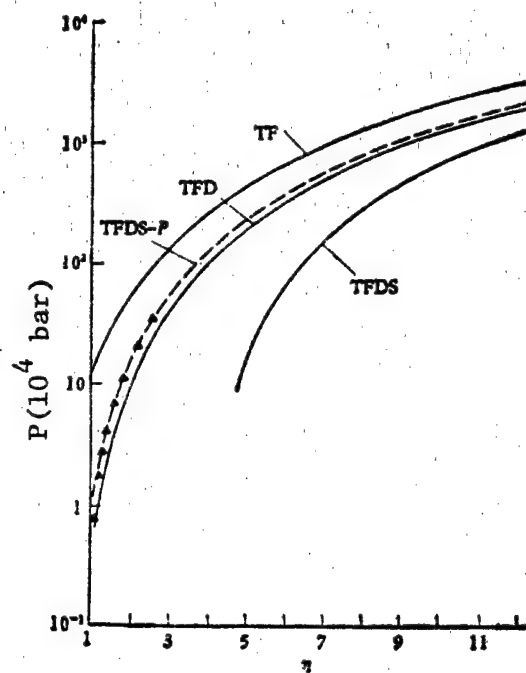


Figure 2. Relationship Between Pressure  $P$  and Compression Ratio  $\eta$  for Na

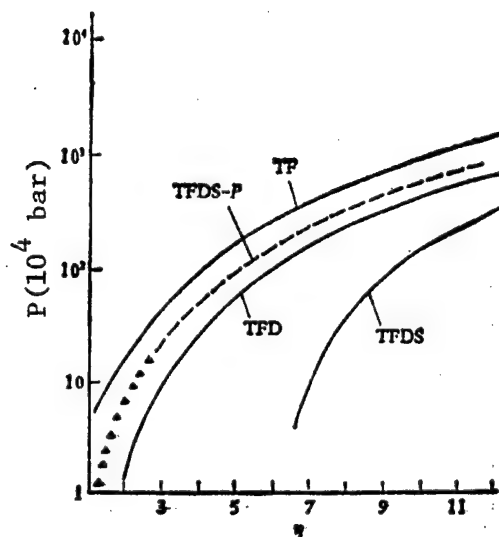


Figure 3. Relationship Between Pressure  $P$  and Compression Ratio  $\eta$  for K



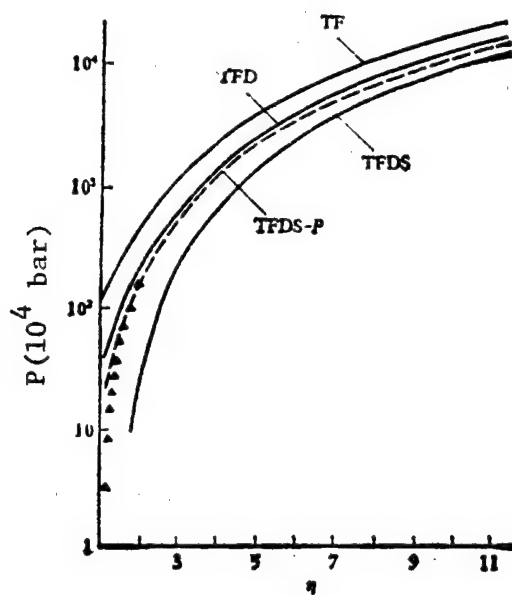


Figure 4. Relationship Between Pressure  $P$  and Compression Ratio  $\eta$  for Al

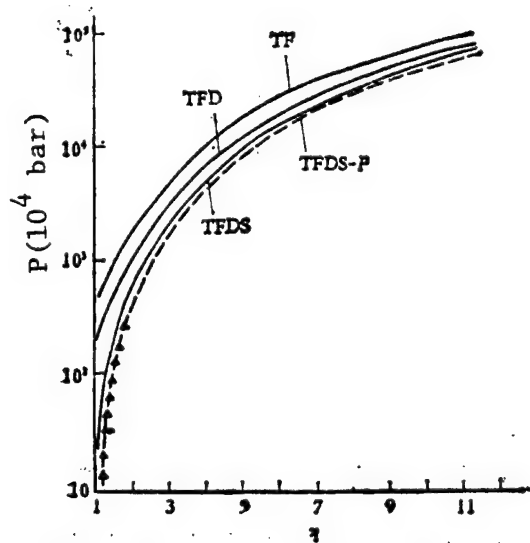


Figure 5. Relationship Between Pressure  $P$  and Compression Ratio  $\eta$  for Fe

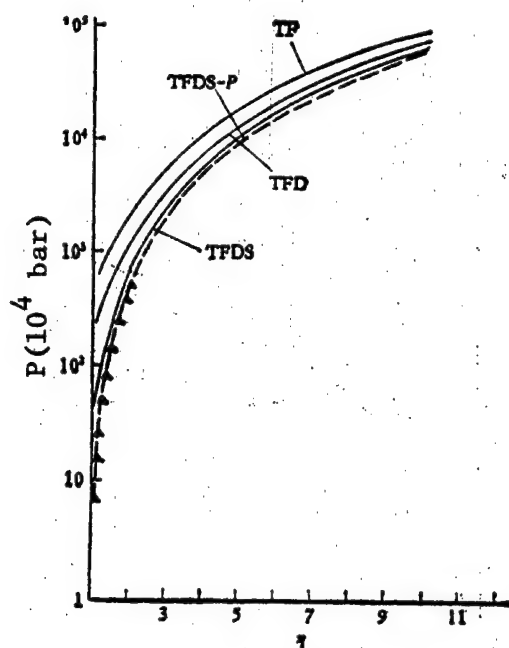


Figure 6. Relationship Between Pressure  $P$  and Compression Ratio  $\eta$  for Cu

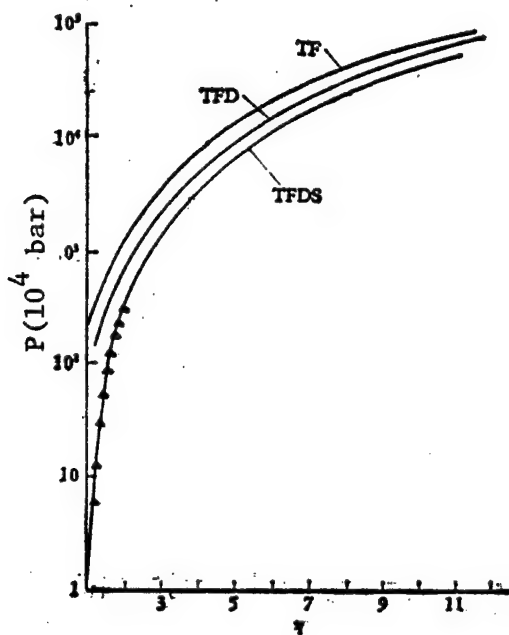


Figure 7. Relationship Between Pressure  $P$  and Compression Ratio  $\eta$  for Ag

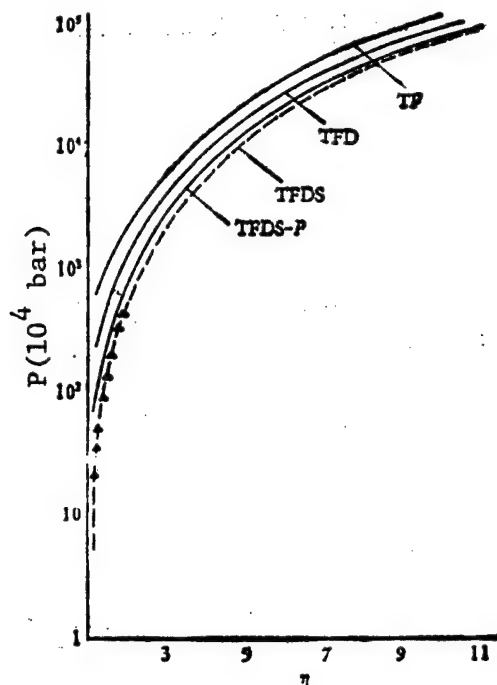


Figure 8. Relationship Between Pressure  $P$  and Compression Ratio  $\eta$  for Au

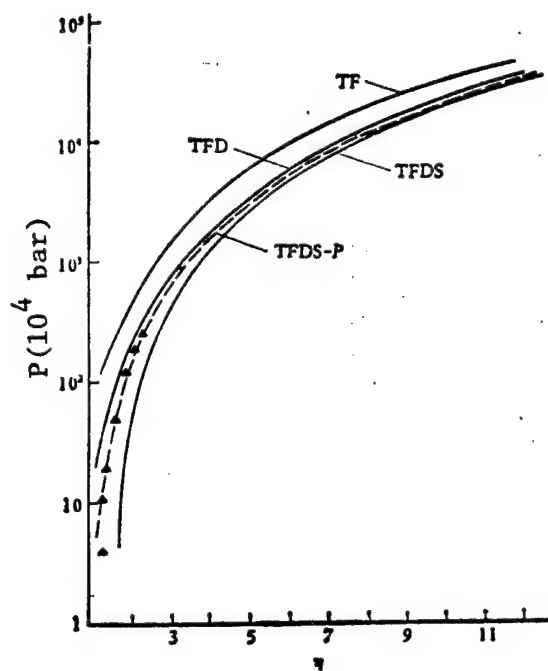


Figure 9. Relationship Between Pressure  $P$  and Compression Ratio  $\eta$  for Pb

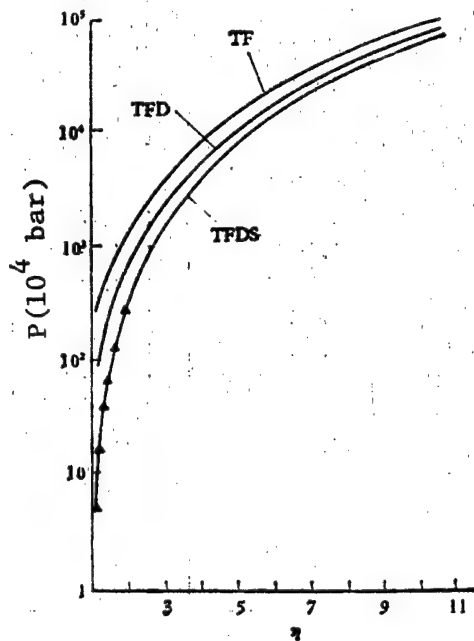


Figure 10. Relationship Between Pressure  $P$  and Compression Ratio  $\eta$  for U

Table 1.  $P$ - $\eta$  Data and Numerical Solution of TFD Equation for Li

$x_0$	$\psi(x_0)$	$\eta$	$P_{TFD}$ ( $10^4$ bar)	$P_{TFDS}$ ( $10^4$ bar)	$P_{TFDS-P}$ ( $10^4$ bar)
2.47060(0)	3.23871(-1)	1.00436(1)	9.25161(2)	2.58997(2)	1.04760(3) <sup>1)</sup>
2.63309	2.79780	8.29666(0)	5.97358	1.07153	6.87456(2)
2.75534	2.50692	7.24060	4.34343	4.13650(1)	5.06572
2.91943	2.16311	6.08760	2.86611	-8.88230(0)	3.40922
3.10874	1.82254	5.04138	1.79984	-3.58156(1)	2.19647
3.51445	1.25065	3.48922	6.89436(1)	-4.60202	9.00729(1)
3.70620	1.03912	2.97519	4.43010	-4.25458	6.02634
4.21483	6.11626(-2)	2.02284	1.37665	-2.91950	4.79383
4.42240	4.81155	1.75117	8.44871(0)	-2.42015	1.44498
4.59620	3.87615	1.55991	5.54068	-2.05095	1.04068
4.88386	2.59900	1.30020	2.62990	-1.53905	5.99611(0)
5.00735	2.14221	1.20636	1.85442	-1.35429	4.68442
5.15314	1.66623	1.10684	1.18194	-1.16015	3.53160

Note 1) The number in the parenthesis denotes the power of 10; for example,  $1.04760(3)=1.04760 \times 10^3$ . The data in the following tables are in the same format as in Table 1.

Table 2. P- $\eta$  Data and Numerical Solution of TFD Equation for Na

$x_0$	$\psi(x_0)$	$\eta$	$P_{TFD}$ ( $10^4$ bar)	$P_{TFDS}$ ( $10^4$ bar)	$P_{TFDS-P}$ ( $10^4$ bar)
4.62670(0)	1.28682(-1)	1.01479(1)	1.35889(3)	6.78659(2)	1.42472(3)
4.96015	1.07381	8.23587(0)	8.01468(2)	3.29126	8.47189(2)
5.82336	6.70935(-2)	5.08949	2.21658	2.29274(1)	2.40894
6.93370	3.54993	3.01508	4.69783(1)	-2.67768	5.41179(1)
7.91886	1.87331	2.02398	1.19743	-2.10461	1.51706
8.11064	1.63108	1.88377	9.09729(0)	-1.92950	1.18456
8.37276	1.33570	1.71233	6.18838	-1.69530	8.42848(0)
8.53375	1.17302	1.61724	4.84783	-1.55790	6.82511
8.68558	1.03168	1.53390	3.82443	-1.43416	5.58286
8.96615	7.99103(-3)	1.39436	2.40990	-1.22220	3.82626
9.17191	6.50303	1.30261	1.67101	-1.08109	2.87924
9.40943	4.99539	1.20643	1.04723	-9.33036(0)	2.05168
9.66949	3.58372	1.11169	5.72420(-1)	-7.88125	1.39073

Table 3. P- $\eta$  Data and Numerical Solution of TFD Equation for Al

$x_0$	$\psi(x_0)$	$\eta$	$P_{TFD}$ ( $10^4$ bar)	$P_{TFDS}$ ( $10^4$ bar)	$P_{TFDS-P}$ ( $10^4$ bar)
3.64191(0)	2.32326(-1)	1.03298(1)	1.36978(4)	1.02867(4)	1.30186(4)
3.87707	2.04232	8.56191(0)	8.91024(3)	6.40922(3)	8.41228(3)
4.62872	1.37299	5.03152	2.51627	1.49863	2.31364
5.44308	9.04882(-2)	3.09421	7.35275(2)	3.01484(2)	6.48906(2)
6.28285	5.88375	2.01192	2.28581	3.05732(1)	1.89157
6.48742	5.28870	1.82754	1.73805	8.34451(0)	1.40862
6.64033	4.87994	1.70418	1.41910	-3.13377	1.13031
6.76800	4.56029	1.60954	1.19946	-1.01949(1)	9.40350(1)
6.93156	4.17756	1.49826	9.68272(1)	-1.66592	7.42317
7.15950	3.69017	1.35967	7.19864	-2.21062	5.32525
7.35323	3.31419	1.25501	5.60222	-2.44485	4.00005
7.68000	2.75083	1.10154	3.67428	-2.54089	2.43685
7.76712	2.61429	1.06488	3.28330	-2.52437	2.12699

Table 4.  $P$ - $\eta$  Data and Numerical Solution of TFD Equation for Fe

$x_0$	$\psi(x_0)$	$\eta$	$P_{TFD}$ ( $10^4$ bar)	$P_{TFDS}$ ( $10^4$ bar)	$P_{TFDS-P}$ ( $10^4$ bar)
4.15815(0)	2.06167(-1)	9.90571(0)	6.37915(4)	5.45948(4)	5.25649(4)
4.72342	1.59513	6.75797	2.63533	2.15139	2.04457
4.99004	1.41965	5.73155	1.78367	1.41831	1.33766
5.64677	1.07523	3.95535	7.23535(3)	5.31569(3)	4.89198(3)
6.14569	8.76273(-2)	3.06819	3.81990	2.59574	2.32554
7.01152	6.19222	2.06609	1.35819	7.60441(2)	6.28508(2)
7.94372	4.27650	1.42073	4.83057(2)	1.86212	1.20692
8.11628	3.99219	1.33203	4.01711	1.39176	8.12292(1)
8.35697	3.62550	1.22022	3.11529	8.96444(1)	4.06701
8.45361	3.48737	1.17885	2.81550	7.39567	2.81367
8.62118	3.25935	1.11144	2.36506	5.13139	1.04383
8.76606	3.07332	1.05723	2.03628	3.56389	-1.43963(0)
8.89560	2.91520	1.01171	1.78256	2.41474	-9.86753

Table 5.  $P$ - $\eta$  Data and Numerical Solution of TFD Equation for Ag

$x_0$	$\psi(x_0)$	$\eta$	$P_{TFD}$ ( $10^4$ bar)	$P_{TFDS}$ ( $10^4$ bar)	$P_{TFDS-P}$ ( $10^4$ bar)
6.04969(0)	1.06238(-1)	8.41494(0)	3.59458(4)	3.04332(4)	same as $P_{TFDS}$ , as $P_{ps}=0$ .
7.01253	7.57211(-2)	5.40290	1.18939	9.38770(3)	
8.45026	4.69043	3.08774	2.73017(3)	1.83413	
9.06218	3.84598	2.50352	1.53211	9.29261(2)	
9.55026	3.28595	2.13897	9.82262(2)	5.36388	
1.00289(1)	2.81638	1.84709	6.42807	3.07421	
1.03008	2.57972	1.70465	5.07551	2.20984	
1.05140	2.40769	1.60302	4.22604	1.68761	
1.07783	2.20963	1.48799	3.37573	1.18616	
1.12638	1.88484	1.30364	2.24741	5.67728(1)	
1.15489	1.71512	1.20945	1.77525	3.32439	
1.17043	1.62853	1.16191	1.56241	2.32889	
1.18506	1.55061	1.11942	1.38611	1.54261	

Table 6.  $P-\eta$  Data and Numerical Solution of TFD Equation for U

$x_0$	$\phi(x_0)$	$\eta$	$P_{TFD}$ ( $10^4$ bar)	$P_{TFDS}$ ( $10^4$ bar)	$P_{TFDS-P}$ ( $10^4$ bar)
7.61064(0)	7.24157(-2)	1.01323(1)	6.90556(4)	6.10359(4)	same as $P_{TFDS}$ , as $P_{ps}=0$ .
7.99558	6.46822	8.73826(0)	4.74329	4.13013	
9.26453	4.52722	5.61701	1.49924	1.22801	
1.11944(1)	2.71373	3.18406	3.15919(3)	2.23998(3)	
1.29445	1.73244	2.05927	8.86774(2)	4.98095(2)	
1.34166	1.53568	1.84945	6.60170	3.27278	
1.39536	1.33834	1.64402	4.44959	1.98823	
1.45219	1.15599	1.45947	3.24908	1.12596	
1.53679	9.26848(-3)	1.23263	1.75576	4.07435(1)	
1.58419	8.17198	1.12344	1.29440	1.82912	
1.60606	7.70557	1.07816	1.12540	1.07422	
1.62695	7.28195	1.03716	9.85052(1)	4.83382(0)	
1.64698	6.89477	9.99792(-1)	8.67229	1.77389(-1)	

Table 7. Parameters Used in Calculating the Equations of States

Param. Element	Z	M	$\rho_0$ [g/cm <sup>3</sup> ]	A	Remarks
Li	3	6.941	0.53	1.1838	M=atomic weight, A=unknown constant in pseudo-potential
Na	11	22.990	0.97	1.0968	
Al	13	26.982	2.71	0.8009	
K	19	39.098	0.86	1.5696	
Fe	26	55.847	7.86	-0.22072	
Cu	29	63.546	8.93	-0.26334	
Ag	47	107.868	10.49	0.	
Au	79	196.967	19.29	-0.26289	
Pb	82	207.200	11.34	0.58633	
U	92	238.029	18.90	0.	

Table 8. Comparison of  $P_{ex}$  and  $P_s$  for Fe

$\eta$	1.011	1.22	1.42	2.07	3.07	5.73	9.91
$ P_{ex} $ ( $10^4$ bar)	107.6	157.5	216.4	465.8	1016	3308	8882
$ P_s $ ( $10^4$ bar)	154.1	221.8	296.8	597.7	1224	3653	9196

#### IV. Discussion

The calculated results show that by taking into consideration the non-zero potential at the atomic boundary and the effect of the pseudo-potential, the theoretically calculated pressure is in good agreement with observations in the low pressure range; the error is generally less than 10 percent (except for alkaline metals Li, Na, K; their properties below 50,000 bar require further study). Above 10 million bar, the solution presented here is very close to the conventional TFD solution; it is somewhat lower for elements with large  $Z$ , and somewhat higher for elements with small  $Z$ . By using the theoretical model given in this article, it is possible to calculate the complete  $P$ - $\eta$  data of a given element over the pressure range from  $10^4$  bar to  $10^8$  bar, thus removing the difficulties previously encountered in theoretical calculations during the transition phase from low pressure region to high pressure region.

For large  $Z$  elements, the electron density is symmetrically distributed, and treating the atom as a single cell is a good approximation to the actual crystal structure. Therefore, the theoretical results are generally in good agreement with measurements, and the correction due to pseudo-potential is quite small; for example, for U and Ag, the unknown parameter  $A$  in the pseudo-potential is equal to zero.

For medium- $Z$  elements such as Fe, Cu, etc., there are some discrepancies between theoretical and measured values (see Figure 5 and Figure 6), but with the pseudo-potential correction, the errors are reduced to within 10 percent. This illustrates the fact that, for medium- $Z$  elements, both the electrons and the crystal structure have an effect on the pressure.

For low- $Z$  elements ( $Z < 25$ ) such as Al, the discrepancies between theoretical and measured values are quite large; this is particularly true in the case of Li and Na. But with the pseudo-potential correction, the calculated results agree with measurements to within 10 percent. This shows that in the case of low- $Z$  elements, treating the atom as a single cell using the TFD statistical model is no longer a good representation of the crystal structure itself. Under these conditions, the effects of crystal structure and valence electrons are quite pronounced, hence the effect of pseudo-potential on the pressure must be considered. The results show that for elements with small bulk modulus and large inter-atom distance, the agreement between theoretical and measured values is in general very poor. This implies that the quantum effect of the structure has a definite impact. Furthermore, the valence electron of a low- $Z$  element has a larger orbital radius than the ion, causing the electron cloud to overlap at the boundary of a free atom during the process of crystal formation. This will increase the repulsive potential between atoms, which tend to cancel the potential energy at the boundary. Therefore, for low- $Z$  elements, the previous TFD results which do not consider any effect at the atomic boundary are interestingly very close to the measured results. In summary, while low- $Z$  elements have rather poor symmetry, the evidence of structural effects is quite clear, and consideration of the effect of pseudo-potential reflects the actual physical phenomenon.



It should be pointed out that we only used one measured point to determine the pseudo-potential constant A. But the results so obtained are uniformly in agreement with measured values over the entire range. This illustrates that the theoretical values before the pseudo-potential correction are correct; on the other hand, incorporating a simple pseudo-potential constant in the previous TFD calculations will not produce results consistent with measured values. Of course, it is possible to achieve good agreement for an individual element, but it is not possible to achieve good agreement with all the experimental data for all the elements because there are clear differences in the low pressure range between the previous TFD results and the present theoretical results. Therefore, the method of determining the pseudo-potential constant A is theoretically justified.

Incorporating other corrections in the TF statistics such as correlation correction quantum correction, and correction of Zink shell structure will yield different degrees of improvement to the electron density  $n(r)$ . However, the largest improvement to the equation of state still occurs at the cell boundary. If the effects of symmetry and crystal structure on the boundary can be accurately predicted, then the results will be further improved. The results can also be improved if the energy level at the boundary or an improved form of pseudo-potential can be obtained using the energy band theory.

It is worth pointing out that while we have imposed a non-zero electron potential at the boundary, the electron density  $n(r)$  and the potential energy  $V(r)$  strictly obey Poisson's equation, and the first derivative of the potential energy still vanishes at the boundary, i.e.,

$$V'(r)_{r=r_0} = 0.$$

Therefore, the TFD equation and its boundary conditions are affected, and the numerical solution is the same as that in the case where  $V(r_0) = 0$ .

The author would like to express his thanks to Comrade Chiao Dengjiang for discussions during the course of this work.

#### References

- [1] L. H. Thomas, PROC. CAMB. PHIL. SOC., 23 (1927), 542.
- [2] R. Latter, J. CHEM. PHYS., 24 (1956), 281.
- [3] P. A. M. Dirac, PROC. CAMB. PHIL. SOC., 26 (1930), 376.
- [4] N. Metropolis and J. R. Reitz, J. CHEM. PHYS., 19 (1951), 555.
- [5] D. A. Kirzhnits, ZhETF [JOURNAL OF EXPERIMENTAL AND THEORETICAL PHYSICS], 35 (1958), 1545.
- [6] N. N. Kalimkin, ZhETF, 38 (1960), 1534.

- [7] J. W. Zink, PHYS. REV. A, 176 (1968), 279.
- [8] E. E. Salpeter and H. S. Zapalsky, PHYS. REV., 158 (1967), 876.
- [9] Cheng Kaijai, ACTA PHYSICA SINICA, 14 (1958), 106.
- [10] F. Herman and S. Skillman, "Atomic Structure Calculations," Prentice-Hall, Inc., New Jersey, (1963).
- [11] R. P. Feynman, N. Metropolis and E. Teller, PHYS. REV., 75 (1949), 1561.
- [12] L. V. Al'mshuler, ZhETF, 38 (1960), 791.
- [13] L. V. Al'mshuler, ZhETF, 34 (1958), 874.
- [14] M. Van Thiel et al., UCRL-50108, (1966).

3012

CSO: 4008/231

APPLIED SCIENCES

WAVEFORM CONTROL AND APPLICATION OF DETONATION WAVE IN EXPLOSIVES

Beijing LIXUE YU SHIJIAN [MECHANICS AND PRACTICE] in Chinese No 5, 1984 pp 7-12

[Article by Chen Weibo [7115 4850 3134] of Institute of Mechanics Chinese Academy of Sciences: "Waveform Control and Application of Detonation Wave in Explosives"]

[Text] Control of the detonation waveform and improvement of the utilization of the explosives are the main research subjects studied by many investigators. They are also required in engineering. The detonation wave has certain "optical" characteristics. It can be reflected or diffracted when encountering obstacles during propagation.

Some scientists applied this phenomenon to control various waveforms. Examples include the precise control of the waveform of the detonation wave for focusing and detonating an atomic bomb, to obtain high pressure and high temperature by the contracting cylindrical wave for synthesizing new materials, and the change of the detonation waveform by inserting an object of special shape in the regular ammunition for improving the efficiency of the ammunition. Missiles and spacecraft have been extensively using explosives to switch circuits, to open and shut valves, and to separate and eject objects.

The plane detonation wave has been widely applied in dynamic high pressure equipment in China. It has been used for moving metal plates to investigate the characteristics of the material under the impact of high dynamic pressure. Similar equipment has also been successfully applied in converting graphite to diamonds. The plane lens of the explosives are also the necessary tools for investigating the equations of state of explosives.

In summary, the control of detonation waves is very important in both engineering and scientific research.

I. Methods of Waveform Control

There are many ways to control the waveform. The following three are most common. The first method is electrical detonation which involves the passing of a strong electric current through a thin metal wire. The metal wire is rapidly vaporized and expanded into the surrounding medium which creates a shock wave and high temperature plasma and detonates the explosive. According

to the literature, detonating wire of several feet in length has been developed.<sup>1</sup>

A piece of metal film can be corroded into a porous mesh structure with about 200 nodes per square inch. The metal mesh sprayed with dissolved PETN explosive can provide several square meters of shock load after detonation. This method of detonation can be used to drive metal plates.

The use of light to detonate explosives is the second method of waveform control.<sup>2</sup> Solid laser device can produce a pulse wave which is passed through the Q switch and is converted to a pulse of high power and short duration. The detonation of explosives usually requires a strong pulse. The PETN explosive is most sensitive to the laser beam. The minimal detonating energy is 1 joule. The detonation speed obtained from laser blasting is very close to the theoretical speed. So far only a small area plane wave can be obtained.

Eggert<sup>6</sup> first indicated that certain sensitive explosives can be detonated by a light flash. He and his colleagues have tested at least 16 solid mixtures detonated by light. The surface of the thin explosive is heated rapidly to its detonation temperature by the energy released from the flash. The light sensitive explosive can be made and sprayed on a flat or curved surface which can produce various waveforms when detonated by a flash.

Nevill investigated a light sensitive explosive. Simultaneous detonation could be obtained on a 9-inch long light sensitive explosive by light of specific wave length.

Since the above two methods are technically more complicated and the applications are limited, no details will be discussed. We would like to emphasize the third technique which employs a single detonator to obtain linear, plane and cylindrical contracting waveforms.

With single point detonation, the shock wave can usually be controlled to reach a certain curve or curved surface by inserting a special shape object near the detonating point which can delay the propagation rate or increase the traveling path of the wave. It can also be controlled by using low speed explosive which reduces the traveling velocity of the wave. This method can obtain various waveforms such as plane wave, curved wave, square wave and star-like wave, etc. Busco<sup>3</sup> gave a simple introduction to the optical characteristics of the detonation wave in the Fifth International Conference of Detonation.

## II. Linear Wave

The linear wave is the simplest of all detonation waves. The following three types are the most popular ones in applications.

### Type A Linear Wave

This is an approximately linear waveform of a wave expanded from the apex after detonation. It can be obtained by puncturing the flat explosive with numerous circular holes according to equilateral triangle design (Figure 1).

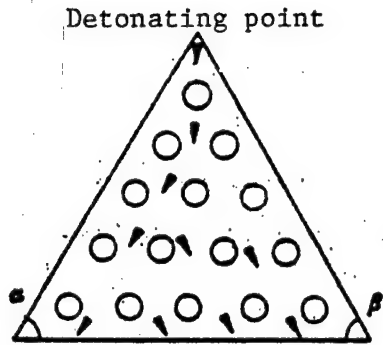


Figure 1. Type A Linear Wave

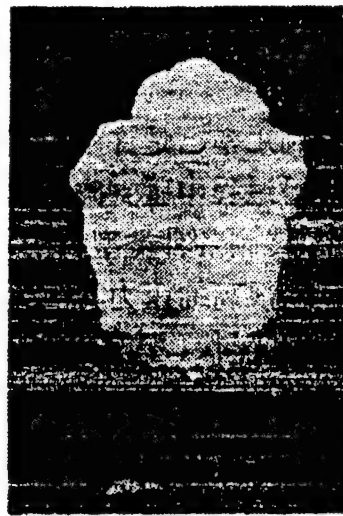


Figure 2. High-speed Photograph of Type A Linear Wave

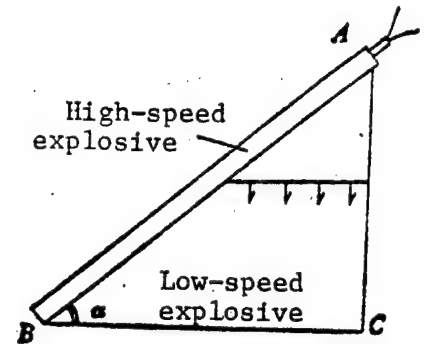


Figure 3. Type B Linear Wave

Since the detonation speeds at various areas on the flat explosive are the same, angles  $\alpha$  and  $\beta$  are the same. The detonation waves are considered to reach the base line of the triangle simultaneously. The waveform approximates more closely to a linear one with more holes on the flat explosive. Figure 2 is the picture obtained using high-speed photography. However, the number of holes cannot be too many and the holes cannot be too small, otherwise detonation will be directly induced between two holes.

Conditions of the experiment: Plastic flat explosive, 10 mm in thickness 16 mm diameter holes, distance between centers of holes 23 mm, the frequency of the high-speed photograph 500 KHz/sec.

#### Type B Linear Wave

It is formed by combining two different detonation velocities. The fast explosive should be the plastic flat explosive with a detonation velocity of 6,500 M/sec. The slow explosive should have a detonation velocity of 2,600 M/sec. A combination of the fast and slow explosives produces a linear wave (Figure 3).

The detonation starts at point A. The wave from the fast explosive proceeds from A to B and the wave from the slow explosive proceeds from A to C. In order to have both waves reach B and C from A simultaneously, the combination angle  $\alpha$  of the two types of explosive can be calculated from the following equation:

$$\alpha = \sin^{-1} \left( \frac{D_s}{D_f} \right)$$

where  $D_s$  is the velocity of the slow explosive

$D_f$  is the velocity of the fast explosive

The time required to proceed through an arbitrary path ADE should be the same as the duration from A to B or A to C. The image obtained from a high-speed camera is shown in Figure 4.

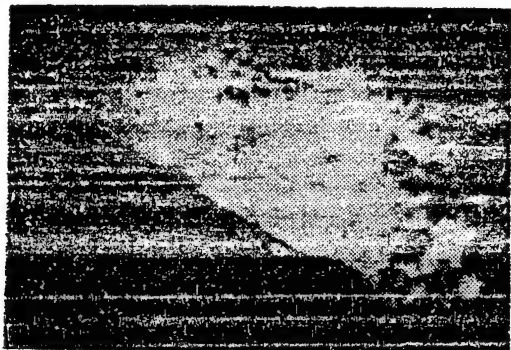


Figure 4. High-speed Photograph of B Type Linear Wave

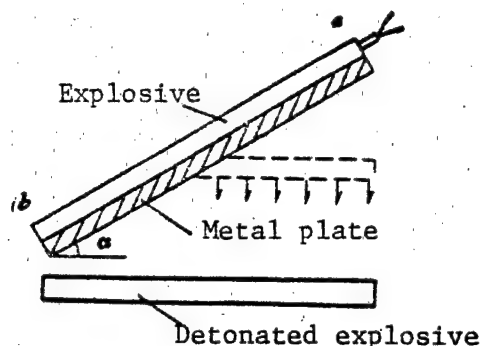


Figure 5. C Type Linear Wave

#### Type C Linear Waveform

This is a simple linear waveform obtained by installing a thin explosive on a narrow metal strip. There is an angle  $\alpha$  between the metal strip and the explosive to be impacted as shown in Figure 5.

The detonation of the explosive starts from upper right corner and proceeds from a to b. With steady detonation and proper selection of the angle  $\alpha$ , the explosive at the bottom will be detonated simultaneously by shock. The size of the angle  $\alpha$  can be determined using the following equation;

$$t_{g\alpha} = \frac{V}{D}$$

where  $V$  is the impact speed of the flying plate (M/sec);  $D$  is detonation velocity (M/sec) of the explosive on the driving plate.

The impact speed of the flying plate can be calculated using the equation:

$$V = D \left( 1 + \frac{\theta - 1}{\eta \cdot \theta} - \frac{h_0 \theta}{Dt} \right)$$

where  $\theta = [1 + 2\eta(1 - h_0/Dt)]^{1/2}$ ,  $\eta = \frac{16}{27} \frac{m}{M}$ ,  $D$  is the detonation speed of the explosive (cm/ $\mu$ sec),  $h_0$  is the thickness of the explosive (cm),  $m$  is the mass of the explosive (g),  $M$  is the mass of the flying plate (g),  $t$  is the duration ( $\mu$ sec).

With fixed explosive and the plate material, it is readily concluded from the above equation that the relative impact speed,  $V/D$  is a function of time  $t$  and the mass ratio  $m/M$ .

For example, with the explosive RDX/TNT (60/40);  $\rho_0$ : 1.68 g/cm<sup>3</sup>,  $D$ : 0.795 cm/ $\mu$ sec, thickness: 1 cm, steel flying plate:  $\rho$  7.8 gm/cm<sup>3</sup>, thickness 0.1 cm,  $M$ : 3.12 gm. The mass ratio  $\eta = 0.798$ . Calculating from the above equation,  $V_{\max} = 0.1862$  cm/ $\mu$ sec,  $\alpha_{\max} = 13^\circ 11'$ .

### III. Plane Waveform (Plane Wave Lens)

Plane wave lens has been widely applied in investigation of the shock wave explosives and the propagation of detonation waves. It can also be used for driving metal plates in high dynamic pressure techniques.

The size of the plane wave lens can be as small as 1 inch or as large as several dozen inches in diameter. The common sizes used in experiments are 4 inches and 8 inches. There are various types of the plane wave lens. We will focus our discussion on the "mouse trap type" and the composite explosive plane wave lens.

#### 1. The "Mouse Trap" Type Plane Wave Lens

The "mouse trap" plane wave lens is similar to the mouse trap in structure. The detonation transforms from point to linear and finally to plane form. Figure 6 is a sketch of the plane wave. It has the feature of simple in structure. However, the accuracy is poor. The flatness of the central portion is better than that at the periphery. The calculation of the angle  $\beta$  of the "mouse trap" plane wave is similar to that of the angle  $\alpha$  of the C type linear wave. With proper selection of the angle, the whole metal plate is regarded to impact on the explosive simultaneously at the end of detonation, which generates a plane wave.

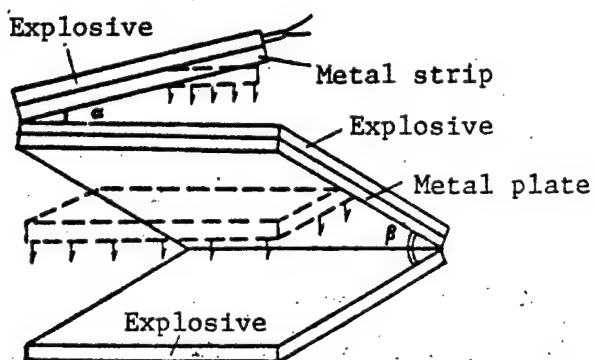


Figure 6. The Mouse Trap Plane Wave

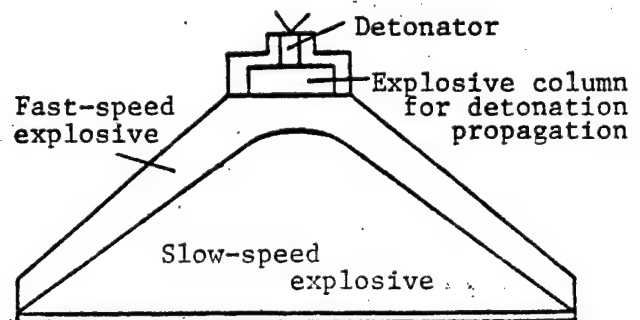


Figure 7. The Structure of a Composite Explosive Charge

#### 2. Composite Charge Plane Wave

The composite charge plane wave is generated by combining both the fast-speed and the slow-speed explosives. The fast-speed explosive is a mixture of TNT and RDX and the slow-speed explosive is a mixture of TNT and barium nitrate. Figure 7 shows the structure of the composite charge of explosives.

The formation of a plane wave is determined by the selection of the boundary curve of two explosives. The assumptions of the calculation include that the detonation velocity is constant for the same type of explosive, the propagation of the detonation wave follows the principles of geometric optics and

that the detonation wave proceeds with new velocity after crossing the boundary. Since there are many references on the mathematics, parametric distribution and experimental techniques, no detail will be discussed in this paper.

Development work on the composite charge plane wave lens has been carried out all over the world. Progresses have been made on the improvement of the quality of the explosives as well as the structure of the explosive charge. The low pressure plane wave lens is discussed in the following. Detonating directly by a detonator is the main feature of this type of wave lens. The boundary is linear. The technology has been significantly simplified.

The explosive for this type of plane wave is composed of PBX-9404 and foam explosive of nitro-guanidine. The detonation velocity of PBX-9404 is 8.8 mm/ $\mu$ sec. The density of the nitro-guanidine foam explosive is 0.3-0.4 gm/cm<sup>3</sup>. The detonation velocity is 3.15 mm/ $\mu$ sec. The amplitudes of the shock wave on aluminum and brass are 35 and 50 Kilo-bar, respectively. The flatness can be as low as  $\pm 0.01 - \pm 0.02$   $\mu$ sec. The structure of this type of plane wave is shown in Figure 8.

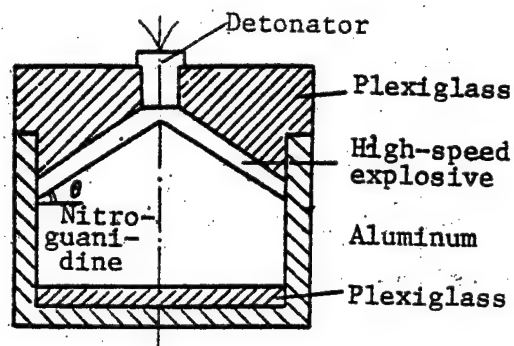


Figure 8. Low-pressure Plane Wave

The angle  $\theta$  is readily calculated from the detonation velocities of both explosives,  $\theta = 20-21^\circ$ . The setup is very simple. The slow-speed explosive is initially packed into the package in consecutive steps. The maximum thickness of each step is less than 1.5 cm. It is then compacted to the required density using a cone-shape hammer and scraped into the required shape using a plexiglass templet. The PBX-9404 explosive is finally installed on the top. The progress of the waveform investigated using a high-speed camera is shown in Figure 9.

The experimental result indicates that the use of PBX-9404 explosive to detonate the nitro-guanidine foam explosive has an affected region. A region of high detonation velocity is formed within the slow-speed explosive. This area was measured to be about 2.5 cm. The affected area is smaller with cast slow-speed explosive; usually only a few millimeters.

Benedick<sup>4</sup> carried out detailed studies on this type of installation. The fact that the plane waveform could be obtained with composite explosive charge was



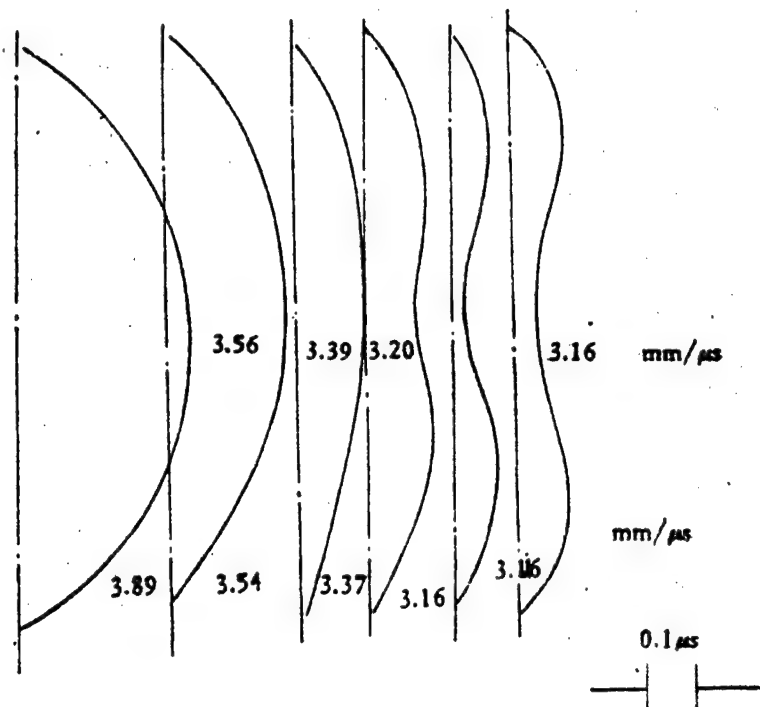


Figure 9. Progress of Waveform

demonstrated by the laws of propagation of detonation. The distribution of these two types of explosive was investigated to insure the planeness of the waveform.

The author measured the arrival times of the detonation wave at various locations in the foam explosive 7.125 cm in diameter with a density of  $0.4 \text{ gm/cm}^3$  and a fixed charge length  $L$ . The detonation velocity was calculated which changed with  $L$  as shown in Figure 10.

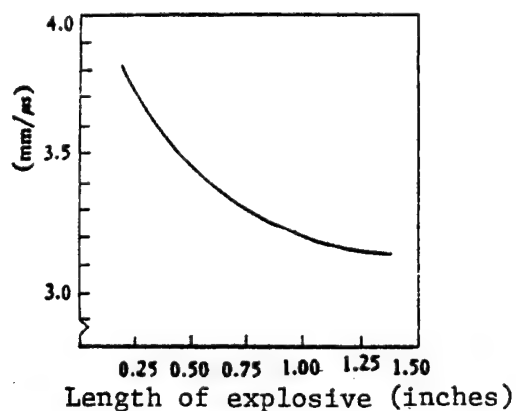


Figure 10. Detonation Velocity vs. Charge Length

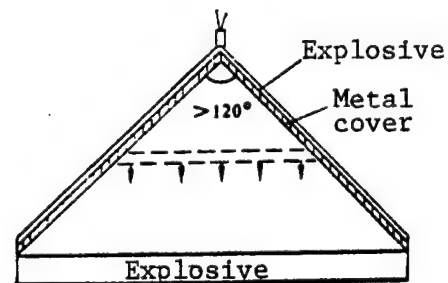


Figure 11. Flying Disk Lens With Metal Cover Having Large Conical Angle

The test results indicated that the detonation velocities at various locations approached the same value when L was increased to 1 inch. This equipment could be used to obtain a waveform of high planeness and low pressure. A small plane wave lens can be made with only 150 gm of explosive.

### 3. Flying Disk Lens

The flying disk lens is a metal cover with large conical angle as shown in Figure 11.

It detonates at the vertex of the cone. The explosive strains the cone during detonation and causes the cone to inverse inwardly. The explosive disc at the base will blast simultaneously when the detonation reaches the base and impacts the explosive.

P.L. Stanton developed a very simple plane wave lens at Sandia Laboratories in the United States called the Stanton Flying Disk Lens; it is shown in Figure 12.

The cone is a machined part while the explosive plate is loaded by hand. The detonation starts at the vertex and leads to the explosive plate through a linear explosive. W.B. Benedick calculated the destruction process of the cone under pressure using a computer. Scientists in our country have also carried out some calculations.

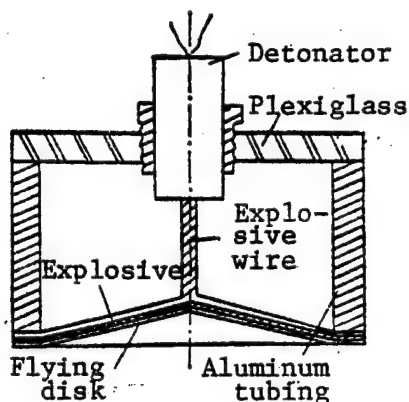


Figure 12. Stanton Flying Disk Lens

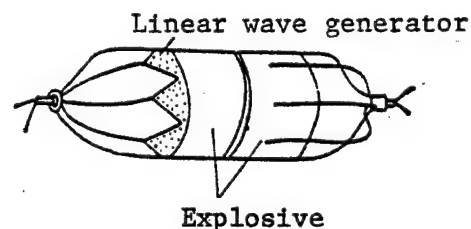


Figure 13. Cylindrically Contracting Wave

### IV. Cylindrically Contracting Wave

Cylindrically contracting wave can produce very high pressure. It is an ideal technology from both the engineering and research viewpoint. It can be used to weld thick wall tubes and to synthesize new materials.<sup>5</sup>

There are many techniques to obtain a cylindrically contracting wave. The simplest method to form a cylindrically contracting wave is through point detonation and linear detonation. As shown in Figure 13, after detonating

the detonator at the left end, the detonation propagates through the same distance to individual vertices of the linear waves and finally forms a detonation ring. This detonation ring proceeds along the generatrices of the cylindrical column to create a cylindrically contracting wave. Occasionally, an accurate cylindrically contracting wave is not required in engineering. An approximate cylindrically contracting wave can be formed by transmitting the detonation from a single point to the surface of the column through the explosive wires of equal length as shown in the left part of Figure 13.

Only an approximate cylindrically contracting wave is obtained by the above two methods. In order to obtain the ideal cylindrically contracting wave, a combination of fast-speed and slow-speed explosives has recently been employed. A sketch of the set-up is shown in Figure 14.

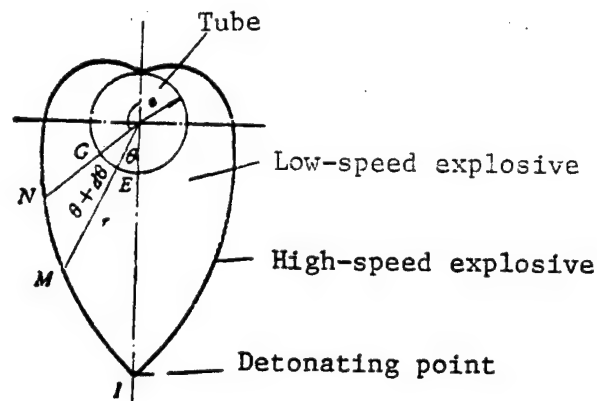


Figure 14. Logarithmoid Cylindrically Contracting Wave

A tube with a radius is coated with a low-speed explosive and then enclosed in the high-speed explosive. It is detonated at I using a linear wave. The high-speed explosive is detonated along the periphery, while the low-speed explosive is detonated by the adjoining high-speed explosive. With fixed explosives, the detonation velocities can be obtained. The shape of the interface is very important for the detonation waves to arrive at the tube simultaneously. Since detonation wave propagates according to the principles in geometric optics, the detonation wave propagates at low speed after passing through the interface of the low-speed explosive. The geometric shape of the interface can be readily determined by the following calculation. Selecting arbitrarily two points, M and N, within the high-speed explosive with the corresponding angles,  $\theta$  and  $\theta + d\theta$ , since the shock waves arrive at the surface of the tube simultaneously, the duration of the detonation wave transmits from point I through the path IME should be the same as that through the path IMNG. Eliminating the common term, IM, the following equations can be obtained:

$$\frac{r-a}{D_i} = \frac{r d\theta}{D_F} + \frac{r-dr-a}{D_i}$$

$$\frac{1}{D_i} \frac{dr}{d\theta} = \frac{-1}{D_F} \cdot r$$

$$\int \frac{dr}{r} = \frac{-D_i}{D_F} \cdot \int_0^\pi d\theta$$

By integration,

$$\ln r = \frac{-D_i}{D_F} (\pi - \theta) - c$$

$$r = a \exp \left[ -\frac{D_i}{D_F} (\pi - \theta) \right], \quad 0 \leq \theta \leq \pi$$

The interfacial curve of the two explosives can be calculated from the above equations.

Control of the detonation waveform is required in engineering projects and experiments. A systematic investigation of the rules and methods of controlling the waveform not only can provide new tools for production and research, but also these methods of data analysis and solutions can be used for certain common engineering problems.

The high-speed photographs were provided by Gu Daoliang, Wang Xiaorong and He Xilian, etc. Their assistance is gratefully appreciated.

#### REFERENCES

1. Davis, W.C., Proceedings of the 12th Annual Symposium, 2-3, March 1972, 5-14, Albuquerque, New Mexico.
2. Benedick, W.B., Proceedings of the 12th Annual Symposium, 2-3, March 1972, 47-56, Albuquerque, New Mexico.
3. Busco, M., Proceedings of the Fifth Symposium on Detonations, U.S. Naval Ordnance Laboratory, 1970, pp 513-522.
4. Benedick, W.B., REV. SCI. INSTR., 36, 9, 1965, pp 1309-1315.
5. Guenther, A.H. Proceedings of Second Conference on Exploding Wires, November 1961 pp 14-16.
6. Butler, R.I. and Duggin, B.W. Proceedings SESA Fall Meeting, 1969.

12553

CSO: 4008/103

APPLIED SCIENCES

BRIEFS

RECOMBINANT VACCINE VIRUS--Researchers at the Biochemistry Research Institute of the Chinese Academy of Sciences in Shanghai through the application of genetic engineering methods have successfully constructed a recombinant vaccine virus which incorporates an anti-hepatitis B surface antigen gene. The research results of this genetic research are up to advanced international levels and have opened up a new way to prevent hepatitis B in China. [Excerpts] [Beijing RENMIN RIBAO in Chinese 26 Jan 85 p 1]

CSO: 5400/4127

LIFE SCIENCES

APPLICATION OF YAG LASER TO OTORHINOLARYNGOLOGY

Shanghai YINGYONG JIGUANG /APPLIED LASER/ in Chinese Vol 4, No 4, Aug 84  
pp 189-188

/Article by Ru Yizhong and Meng Zhaohe: "Preliminary Report on Application of YAG Laser to Otorhinolaryngology"/

/Text/ Since October 1982, with the cooperation of the Laser Research Laboratory, Shanghai Second Medical College, we have applied Nd:YAG laser to the treatment of 137 cases of ear, nose and throat disorders, a followup study lasted more than a year, of these cases showed satisfactory results. This paper is our preliminary report.

Laser System and Method

The Nd:YAG laser optical fiber emits at a wavelength of 1.06 m; the laser source has a power of 55W; optical fibers of core diameters 500 and 650 m were used; an input coupling efficiency of more than 80 percent was achieved; the fiber output power was 40W; the working current is adjusted to around 35mA; the system was also equipped with an automatic control and a manual control, built in timer and counter; there were five power selectors: 20W, 25W, 30W, 35W and 40W; a Cu-Ni optical fiber tube was also available.

Method: Most of the throat disorders were membranous pharyngitis; the more serious cases with larger inflammatory areas, patients usually received local anesthesia with lidocaine, those with throat allergy complications were given neural anesthesia as well; the inflammatory area was then irradiated with a laryngeal mirror as used in the indirect laryngoscopy and the procedures were similar to that of excision of polyps from vocal cords with an indirect laryngeal mirror; the irradiation of the inflammatory areas were carried out one by one through a metallic hollow tube. For the nasal cases, after the mucosa had been stringed, the irradiation was conducted starting from the rear of the inferior concha and working its way up to the front.

The absorption of YAG laser is better with red, blue and black objects, thus for irradiating hemangioma, a longer working distance, approximately 2 cm, was used; during the irradiation, it was observed that the tumor shrank gradually and a congealed, white membrane appeared on the wound. Better results were obtained with shorter working distances for irradiating vocal polyps and

nodules, usually around 0.3 cm, in order to accelerate the vaporization of polyps. The vaporization processes were often accompanied by a clapping sound, a sign of fast vaporization.

### Clinical Results

Classification of Healing Results: 1. Cases Healed: The patient felt all the symptoms were gone and the previously affected organs started functioning normally; examination showed the disorder signs disappeared.

2. Cases Improved: The conditions were improving, affected organs functioning better, examination showed the symptoms and signs alleviating.

3. Cases showed no effect: The patient complained of no improvement.

As shown in Table 1, 74.4 percent of the cases were healed and a total of 93.4 percent of them showed positive results after the laser treatment. Most of the cured cases (96) required only 1 irradiation; for cases treated with insufficient irradiating power or those in which larger areas were involved, 2 to 3 exposures were needed to heal; after the laser surgery, patients were usually checked 4 times at intervals of 24 hours, 1 week, 2 week and 1 month to review the results. Generally, after the exposure to laser, no serious side reactions were observed, mild fever and dryness were common complaints and there was no visible swelling. Sometimes the mucosa were covered with a congealed membrane and exudent; it usually took 2 to 4 weeks for the wound to heal, the length of time varied with the magnitude of the irradiating power; other signs including external ear and skin pustules, which bursted with a discharge of small amounts of hydrorrhea; it ordinarily, took 4 days for the sore to scab, 2 to 4 weeks for the scab to come off and no visible scar left after healed.

Table 1. The Results of YAG Laser Treatment of Ear, Nose and Throat Disorders

Disorder	Number of Cases	Cases Healed	Cases Improved	Cases Showed No Effect
Hemangioma in Ear, Nose and Throat	31	31	7	
Disorders in Vocal Cord (Papilloma, Polyps and Nodules)	45	36	7	2
Nasal Hemorrhage	17	12	4	1
Hypertrophic Rhinitis	20	16	4	1
Allergic Rhinitis	18	4	10	4
Hyperplastic Rhinitis	2	1	1	
Epiglottiditis and Ranula	4	2		2
Total	137	102	26	9
Percentages	100%	74.4%	19%	6.6%

## Typical Cases

Case 1. Wu X X, female, age 68; examination revealed a purplish red, earthworm-shaped projection on the left and aft pharyngeal tube walls, the cavernous hemangioma, 4.2 x 1.8 cm in dimension, extended from the upper part of nasopharynx, lower end of the eustachian tube to the upper tonsil; this case had been subjected to solidifying treatment 9 times and did not show any improvement. She was treated with YAG Laser in February 1983: with her epiglottis restrained, the affected area was irradiated, with the aid of a nasopharyngoscope, from top to bottom for 18 seconds. The resulted crust over the sore came off 2 weeks after later and the wound recovered well. We have followed this case for more than a year; no relapse has been observed.

Case 2. Pan X X, male, age 47. The patient had suffered hoarseness for 2 years and a complication of thrombocytopenic purpura; he gave a platelet number of 3,4000; examination disclosed red bean-shaped polyps covering a large area of the left vocal cord, near the fore junction. He was treated with YAG laser and no bleeding was observed during the surgery; a followup check indicated residual polyps remained, the patient was given a second exposure 1 week later. The wound healed in a month, leaving a smooth vocal cord, which has functioned normally since then and no relapse was reported.

Conclusions: Because of its high penetrating power, YAG laser can pass through mucosa doing little damage and reach the infected area; postsurgery reactions, as a result, were generally mild; serious hydrops of laryngopharyngeal mucosa were rare, in addition, this kind of treatment will not cause any postsurgery discomfort in swallowing and breathing. We believe the YAG laser irradiation is one of the best treatments for laryngopharyngeal hemangioma. It is a relatively simple operation, than the conventional symptomatic measures, to execute, preferred by patients and can be carried out in the outpatient department; it also offers high healing rates; examples of cases reoccurring are rare and patients benefited by rapid recoveries. The YAG laser treatment can also be used for treating disorders in superior concha and nasopharynx.

12817

CSO: 4008/55



Acoustics

AUTHORS: ZHANG Fucheng [1728 4395 2052]  
GUO Xiaowu [6753 1321 2976]  
ZHAO Hengyuan [6392 1854 0337]

ORG: All of Institute of Applied Acoustics, Shaanxi Normal University

TITLE: "Focusing Principle and Calculation of Quasi-parallel-sided Sound Lens"

SOURCE: Beijing YINGYONG SHENGXUE [APPLIED ACOUSTICS] in Chinese Vol 3 No 4, Oct 84 pp 21-26

ABSTRACT: The sound lens has been widely used in the areas of sonar, no-wear detection, medical diagnosis, and applications requiring concentration of sound energy. Hence it is very important to understand how to design and manufacture a sound lens with high discriminability and low loss of sound energy.

The paper presents the focusing principle of the quasi-parallel-sided sound lens during the incidence of a point sound source and parallel sound beams under the premise of the law of sound reflection stating that sound beams arriving at the focus should be in the same phase. By using an example of the incidence of parallel sound beams, the formulas derived are used to design and make inclined plane and arc surface quasi-parallel-sided sound lenses. Thus, the focusing characteristics are observed and the correlated curves and graphs are plotted. Based on observations, the focusing characteristics of the sound lens are in satisfactory agreement.

Two tables show data on an inclined plane and an arc surface quasi-parallel-sided sound lens. Five figures show the cross section and the focusing of quasi-parallel-sided sound lenses, focusing of a quasi-parallel-sided sound lens with incidence of a parallel sound beam at one side of a stepped and an unstepped plane of the sound lens, and the sound field distribution curves as detected inside a focal plane with the incidence of parallel sound beams. Six photos show a quasi-parallel-sided sound lens and the focusing zone sound field during incidence of parallel sound beams, as well as water jetting from the sound lens. Eighteen equations give formulas and calculations.

10424  
CSO: 4009/49

Acoustics

AUTHORS: LI Qihu [2621 0796 5706]

ORG: Acoustics Institute, Chinese Academy of Sciences

TITLE: "Detection Performance of Digital Multibeam System"

SOURCE: Beijing YINGYONG SHENGXUE [APPLIED ACOUSTICS] in Chinese Vol 3 No 4, Oct 84 pp 12-16, 20

ABSTRACT: The paper discusses the detection characteristics of digital multilayer multibeam system in the time domain. It is pointed out first that the detection characteristics of an amplitude limiting system of 1-bit quantization will be considerably degraded. The paper proceeds to analyze the effect on the single-beam detection characteristic of the number of bits in different layers. The concept of estimating the system overall gain of the detection characteristics in a digital multibeam system is proposed. The concept states the function of system homogeneity when detecting weak signals. Based on theory, explanations are given for the selection criteria of analog-digital conversion of a digital multibeam system, postpositioning storage time, and output activity.

In order to insure that the digital multilayer multibeam system still has nearly the characteristics of a simulation system subjected to high interference, the number of bits quantized by the A/D system should be five or more. The system overall gain is related to homogeneity between beams. Particularly as to the detection of weak signals, only when the system homogeneity attains certain index, is the longer postpositioning storage time then effective.

There are many factors bearing on the output homogeneity of the several beams, such as anisotropy of oceanic noise, and inconsistency between different channels of the system. These are problems calling for further exploration.

Seven figures show the digital multilayer multibeam system, two ways of dividing layers, the relative gain of amplitude limiting correlation, the detected gain of the amplitude limiting system when interference is present, effect on detection characteristics of the number of layers, a detection curve when the postpositioning storage is in the absolute value detection mode, and the effect on system overall gain of beam homogeneity.

The paper was received for publication on 5 May 1983.

10424

CSO: 4009/49

## Acoustics

AUTHORS: WEI Moan [7614 1075 4152]  
QIAN Menglu [6929 1125 7498]

ORG: Both of Acoustics Laboratory, Tongji University

TITLE: "Photoacoustic Effect and Its Applications"

SOURCE: Beijing YINGYONG SHENGXUE [APPLIED ACOUSTICS] in Chinese Vol 3 No 4,  
Oct 84 pp 5-11

ABSTRACT: As early as in 1980 and 1881, the photoacoustic effect of matter was discovered. Since the rapid development of laser technology, transducers and electronic detection techniques, a new discipline, photoacoustics, has gradually taken form. In early 1970's, the photoacoustic effect was utilized to make simple (but sensitive) photoacoustic detection device for monitoring atmospheric pollution, thus promoting research into the gas photoacoustic technique. The photoacoustic effect involves the modulation of light energy into heat energy, and then into acoustic energy. The photoacoustic spectrum technique is also a combination of optical spectrum technique and heat measuring method.

The paper briefly introduces photoacoustic detection characteristics, as well as the principle and applications of the photoacoustic effect in gases and solids. To nontransparent and highly scattering materials, as well as such materials as aerosol, powder and gel, it is often more advantageous to adopt the photoacoustic technique over other detection methods. In recent years, with the emergence of such new sensitive detection methods as the pulse photoacoustic spectrum technique and the photothermal deflecting optical spectrum, the application range of the photoacoustic technique has grown larger. We may expect that photoacoustics will continue to advance with the continuous development of laser techniques, transducers, and weak signal detection techniques.

Ten figures show a gas photoacoustic detection system, a photoacoustic spectrum of benzene and Lamb's depression for methyl alcohol as displayed by a  $\text{CO}_2$  laser, a correlation curve of pure  $\text{CH}_4$ , resonance curves for  $^{12}\text{CO}_2$  and  $^{13}\text{CO}_2$ , a photoacoustic resonator of a microphone detection system, a transducer-specimen assembly of detection system of a piezoelectric transducer, a weak-absorption set-up for photoacoustic detection of solids, an optico-acoustical spectrum for the epidermis of guinea-pigs, and determination of photoelectric quantum efficiency  $Q$  of thin dye films. Two tables give the  $P_T$  values of the oscillatory relaxation of  $\text{CH}_4$  determined by several methods, and a comparison of results of weak absorption determination.

The paper was received for publication on 26 June 1984.

10424  
CSO: 4009/49

Acoustics

AUTHOR: HUANG Guanglun [7806 1684 0243]  
ORG: Sichuan Piezoelectricity and Acoustico-optical Research Institute  
TITLE: "Compensation of Skew Passband of a SAW Filter Using Predistortion"  
SOURCE: Beijing YINGYONG SHENGXUE [APPLIED ACOUSTICS] in Chinese Vol 3 No 4,  
Oct 84 pp 27-30

ABSTRACT: The paper presents a predistortion design by using a variable-track transducer with the interval of the same number of cycles to compensate for the skew passband of a SAW filter. The paper introduces three types of filters designed and manufactured with two types of substrates with experimental results before and after compensation. As shown by results, this is a simple and effective method of compensation design.

One table shows data on three types of filters made of the substrate materials, a transducer side lobe, and characteristics before and after compensation. Three figures illustrate the expected and actual rectangular frequency responses, simulation of the distortion response and mathematical description of the compensation design, and the design structure of devices used in experiments. Five photos show the passband characteristics and passband response of two filters before and after compensation, overall frequency response of another filter, and forked transducer.

The paper was received for publication on 1 April 1984.

10424  
CSO: 4009/49

JPRS-CST-85-008  
27 March 1985

AUTHOR: XIONG Shanwen [3574 0810 2429]

ORG: Beijing Institute of Aeronautics and Astronautics

TITLE: "A Calculation of Slender Delta Wing with Leading-edge Separation by Quasi-Vortex-Lattice Method"

SOURCE: Mianyang KONGQIDONGLIXUE XUEBAO [ACTA AERODYNAMICA SINICA]  
in Chinese No 4, 1984 pp 21-26

TEXT OF ENGLISH ABSTRACT: The Quasi-Vortex-Lattice Method (QVLM) which was used to calculate the thin wing with separation has been extended to calculate the slender delta wing with leading-edge separation. The advantage of this method is that the leading-edge boundary condition can be satisfied exactly. It can be used to predict aerodynamic characteristics of wings having partial leading-edge separation. A calculation has been made here for a slender delta wing with complete leading-edge separation and the results are compared with those of the experimental data. The comparison shows that QVLM can give satisfactory or reasonable results.

## Aerodynamics

AUTHOR: ZHU Peiye [2612 1014 8763]

ORG: Institute of Computing Technology, CAE

TITLE: "Calculation of the Flow Around Thick Wings with Separation Vortices"

SOURCE: Mianyang KONGQIDONGLIXUE XUEBAO [ACTA AERODYNAMICA SINICA]  
in Chinese No 4, 1984 pp 27-33

TEXT OF ENGLISH ABSTRACT: The present paper develops a panel method predicting the nonlinear aerodynamic loads on thick wings with separation vortices. The model used is simple and visual. The method can be used for arbitrary planform wings with different profiles. A planar quadrilateral panel and a panel that consists of a parallelogram and four triangles are used. In order to obtain a high degree of accuracy, the wing is represented by piecewise continuous quadratic doublet sheet distributions. The aerodynamic loads on the rectangular and sweepback wings are computed. They agree well with experimental tests and other theories.

## Aerodynamics

AUTHOR: ZHANG Lumin [1728 7627 3046]  
SHAN Xiaonan [0830 1420 2809]

ORG: Both of the China Aerodynamic Research and Development Center

TITLE: "The Split-Coefficient Matrix Method for Supersonic Three Dimensional Flow"

SOURCE: Mianyang KONGQIDONGLIXUE XUEBAO [ACTA AERODYNAMICA SINICA]  
in Chinese No 4, 1984 pp 41-47

TEXT OF ENGLISH ABSTRACT: The Split Coefficient Matrix (SCM) finite difference method for solving inviscid steady supersonic flow over a non-symmetrical body is presented. This method is based on the mathematical theory of characteristics. In the SCM approach, these coefficients are split according to the sign of the characteristic slopes, and the split coefficients are then multiplied by the appropriate unilateral differences. Forward differences are associated with negative characteristic slopes, while backward differences are associated with positive slope values.

The numerical example of the blunt sphere cones is worked out in this paper and compared with the results of an earlier method cited to demonstrate the good accuracy of SCM in rare mesh.

## Aerodynamics

AUTHOR: GAO Ruifeng [7559 3843 1496]

ORG: China Aerodynamic Research and Development Center

TITLE: "An Experimental Investigation of Flap Turbulent Heat Transfer and Pressure Characteristics in Hypersonic Flow"

SOURCE: Mianyang KONGQIDONGLIXUE XUEBAO [ACTA AERODYNAMICA SINICA]  
in Chinese No 4, 1984 pp 56-60

TEXT OF ENGLISH ABSTRACT: This paper presents experimental results of flap heat transfer and pressure characteristics on a blunt cone in a shock tunnel. Effects of flap deflection angle, angle of attack, Mach number and unit Reynolds number are discussed.

Results show that the flap deflection angle and Mach number are decisive factors which considerably affect the flap heating, pressure characteristics and control effectiveness. This paper gives a correlation between peak heating and peak pressure.  $\frac{\dot{q}_{\max}}{\dot{q}_c} = \left(\frac{P_{\max}}{P_c}\right)^{0.7}$ , also gives an empirical formula for estimating peak heating.

9717

CSO: 4009/94



AUTHOR: XU Zhenyin [1776 2823 3009]  
MA Siliang [7456 7475 5328]

ORG: XU of Northeast Normal University; MA of Jilin University

TITLE: "Generalized Difference Methods for the Problem of Coupled Sound and Heat Flow"

SOURCE: Beijing YINGYONG SHUXUE XUEBAO [ACTA MATHEMATICAE APPLICATAE SINICA]  
in Chinese No 4, Oct 84 pp 385-395

TEXT OF ENGLISH ABSTRACT: The method of constructing a generalized difference scheme ([JILIN DAXUE ZIRAN KEXUE XUEBAO [ACTA SCIENTIARUM NATURALIUM UNIVERSITATIS JILINENSIS] No 1, 1982 pp 26-40]; Abstract in JPRS-80479, 2 Apr 82 p 30) is extended to include coupled sound and heat flow systems, establishing three new schemes. The stability of two new schemes is analyzed. These new schemes have the feature of absolute stability. The third scheme shows how to improve the accuracy.

9717  
CSO: 4009/113

Biochemistry

AUTHORS: JIN Yifeng [6855 0110 6265]  
XU Xianxiu [1776 6343 4423]  
TANG Guozhen [3282 0948 3791]  
ZHU Jiazhen [2612 1367 2182]  
ZHANG Haoyun [1728 7729 0061]

ORG: All of Molecular Biology Laboratory, Department of Biology, Nanjing University

TITLE: "Initiation of DNA Replication and Transcription by PTH in Lymphocytes"

SOURCE: Beijing SHENGWU HUAXUE YU SHENGWU WULIXUE JINZHAN [BIOCHEMISTRY AND BIOPHYSICS] in Chinese No 5, Oct 84 pp 32-34

ABSTRACT: Thymus gland hormone can promote maturation and differentiation of T cells and modify immune cell function, thus having vital significance in immunology. In the maturation process of T cells, such surface configurations as Lyt 1, 2, 3 and sheep blood cell receptor, as well as TDT will appear. With the infiltration test using  $^3\text{H}$ -TdR and  $^3\text{H}$ -Leu, the authors observed a correlation between PTH on one hand, and DNA replication and protein synthesis, on the other; the rosette junction and TDT are used as configurations to study the function of PTH during T cell maturation.

The study leads to the following results: (1) PTH promotes protein and DNA synthesis in T cells; (2) PTH promotes T cell growth, thus affecting biochemical processes in the early growth period; therefore, the medullary cells can synthesize TDT enzyme, leading to a higher TDT stage; and (3) PTH also influences the later growth stage of T cells, promoting further maturation of T cells in producing sheep blood cell receptors. Synthesis of receptor is related to DNA replication. The foregoing shows that PTH can promote the synthesis of new protein during formation of sheep blood cell receptors.

Four figures show promotion by PTH with the infiltration of  $^3\text{H}$ -Leu and  $^3\text{H}$ -TdR; the effect of PTH concentration with infiltration of  $^3\text{H}$ -Leu and  $^3\text{H}$ -TdR; effect of filamentous enzyme on inhibition of DNA replication and protein synthesis, and partial recovery of PTH; and effect on TDT by filamentous enzyme C, actinomycin D and PTH. One table shows the effect of filamentous enzyme C and actinomycin D on the promotion rate of the rosette junction of PTH thymus gland cells.

The paper was received for publication on 20 July 1983.

10424  
CSO ' 4009/85

AUTHOR: DAI Xingyi [2071 5887 5030]  
LU Zhikang [6424 0037 1660]  
ZHANG Yunxiang [1728 0061 4382]  
ZENG Sen [2582 2773]

ORG: All of Shanghai Institute of Organic Chemistry, Chinese Academy of Sciences

TITLE: "Thermoplastic Fluoropolymer Fs-40 G"

SOURCE: Shanghai YOUJI HUAXUE [ORGANIC CHEMISTRY] in Chinese No 3, Jun 84  
pp 224-226

TEXT OF ENGLISH ABSTRACT: A newly-developed melt-processable fluoropolymer Fs-40 G that combines the excellent properties of PTFE (polytetrafluoroethylene) with the versatile processability of PE (polyethylene) is described.

1. The reactivity ratios of ethylene-tetrafluoroethylene (ETFE) copolymerization, as determined by solution precipitation polymerization, are:  
at 40°C,  $\gamma_{C_2F_4} = 0.022 \pm 0.016$ ,  $\gamma_{C_2H_4} = 0.156 \pm 0.001$   
at 70°C,  $\gamma_{C_2F_4} = 0.055 \pm 0.020$ ,  $\gamma_{C_2H_4} = 0.197 \pm 0.001$
2. The properties of ETFE copolymers depend on the E/TFE mole ratio. When the E/TFE mole ratio is nearly equal to 1,  $T_m$  and  $T_c$  reach their maximum values. It is suggested that both the sequences  $-(CF_2CF_2-)_n-$  and  $-(CH_2CH_2-)_n-$  ( $n \geq 2$ ) influence the chain regularity.
3. Fs-40 G is a tricopolymer of ethylene, tetrafluoroethylene and a minor third monomer. The developed Fs-40 G I, II and III can be processed easily by conventional techniques, such as extrusion, injection, molding and powder coating.

9717

CSO: 4009/111

Electronics

AUTHOR: ZHANG Zhizhong [1728 4160 0022]

ORG: Nanjing Institute of Electronic Technology

TITLE: "Development of Low Altitude Defense Radar"

SOURCE: Beijing DIANZI XUEBAO [ACTA ELECTRONICA SINICA] in Chinese No 4, Jul 84  
pp 77-84

ABSTRACT: In the advances made in aviation technology, low altitude defense has gained sharply in importance; the key is reliance on radar to search for and discover incoming low-altitude targets. At present, there are three types of such radars: surface (or ship-borne) low-altitude radar, over-the-horizon radar, and airborne early warning radar. There are disadvantages in the first two types, therefore developments in the 1980's stress airborne early warning radar. The paper presents three types of down-looking airborne radar: low-, medium- and high-pulse repetition frequency (LPRF, MPRF and HPRF) radars. The discussion includes their differences, advantages and disadvantages, technical problems yet to be solved, and the different ground features and clutters these radars are designed for. Their best trade-offs can be made according to different situations and conditions.

As for which type of aircraft with airborne early warning radar is best, apparently this problem reduces to selecting the radar system and the aircraft. Pulse doppler (PD) radar is viewed as better than the airborne mobile target detector (AMTD) radar because PD radar can use high-speed and long-range advanced jets as its carrier, gaining a larger early warning zone and higher survival capability. Five tables show low-altitude search radars in Europe, a comparison of performances between American and British early warning aircraft, performances of American over-the-horizon radar, variation of clutter frequency and spectral width at different orientation angles, and clutter improvement factors of LPRF signal (AMTD) and MPRF and HPRF signals (PD). Eight figures show restrictions by the earth's curvature on the effective distance of radar, radar deployment to cover air territory free of blind spots, clutter spectra of stationary ground radar and airborne down-looking radar, positions in the frequency band of incoming and outgoing targets tracked by HPRF radar, variation of radar effective range by different aircraft altitudes, variation of radar effective ranges on low-altitude flying targets by varying antenna side lobe, and antenna side lobe of AN/APY-1 radar. The first draft was received in January 1984; the final revised draft was completed in April.

Electronics

AUTHORS: LEI Zhenhuan [7191 7201 1403]  
CHI Hongguang [6688 3163 1684]  
WANG Yihua [3769 1355 5478]

ORG: All of Department of Physics, Shandong University, Jinan

TITLE: "Application of Ion Beam Milling Technique for Higher Fundamental Frequency of Quartz Crystal Resonator"

SOURCE: Beijing DIANZI XUEBAO [ACTA ELECTRONICA SINICA] in Chinese No 4, Jul 84 pp 104-105

ABSTRACT: Quartz crystal damage due to ion beam milling is analyzed, appropriate milling conditions and damage-reducing measures are proposed. As a result, the UHF resonators have low equivalent resistance, high Q value, fine frequency response and sufficient mechanical strength; the performances are appreciably enhanced. In 1981, the authors reported studies with fundamental frequency up to 270 MHz. This paper reports on the experimental construction of quartz crystal resonators with the fundamental frequency up to 456 MHz.

The use of low energy, smaller beam current density, appropriate angle of incidence, improvement of cooling conditions, higher milling speed, and chemical etching treatment, among others, can appreciably enhance the performance of resonators thus manufactured.

Two figures show a vertical cross type electrode, and the frequency spectrum property of a No 3 resonator by using TF2370 and TK2373 frequency spectrographs. Two tables show the electrical parameters of three sample resonators, and performance parameters of quartz crystal resonators before and after vibration and impact. The authors express their gratitude to engineer WANG Ronbgin [3769 2837 1755] and senior engineers CHEN Zhiyuan [7115 1807 6678] and QU Xiuge [3255 4423 2706] of Xinan Research Institute of Electronic Technology, and to lecturer LUO Shengxu [5012 0581 2485] and colleague ZHANG Jianhua [1728 1696 5478] of Shandong University for their assistance.

The first draft was received in April 1983; the final revised draft was completed in September.

10424  
CSO: 4009/66

Electronics

AUTHORS: DING Moyuan [0002 1075 0337]  
SHI Yihe [2457 4135 0735]  
WANG Yan [3769 1484]

ORG: All of General Research Institute of Nonferrous Metals, Ministry of Metallurgical Industry

TITLE: "Investigation of LPE-GaAs for X-band Gunn Device"

SOURCE: Beijing DIANZI XUEBAO [ACTA ELECTRONICA SINICA] in Chinese No 4, Jul 84 pp 108-111

ABSTRACT: High quality (epitaxial layers) material for X-band Gunn devices can be grown with the LPE technique at an 80-percent yield; the yield of the device made of this material is higher than 60 percent. Such devices are used in different kinds of microwave equipment. The arrangement for growing the material includes a reaction furnace, reaction tubes, and a hydrogen purifying system, among others. The main characteristics of the arrangement are satisfactory gas tightness, a hard connection system free from oxygen and water contamination (from the atmosphere), simplicity, operating convenience, and reliability without maintenance.

One table shows the experimental results of 10 continuous furnaces. Four figures show a comparison of curves of experimental points conducted by the authors and another researcher, Hsieh, the longitudinal distribution of the carrier concentration of epitaxial layers between the authors and Hsieh, optical fluorescence spectra at 4.2 K, and a DLTS spectral line at 77 K.

The first draft was received in February 1983; the final revised draft was completed in August.

10424  
CSO: 4009/66

AUTHOR: YANG Bi'nan [2799 3880 0589]  
Raymond S. Berkowitz  
Shauh Teh Juang

ORG: YANG of Xiamen Fisheries College; Berkowitz and Juang both of the  
Department of Electrical Engineering, University of Pennsylvania

TITLE: "Study of Time Sampling and Phase Adjustment Beam Steering Technique"

SOURCE: Beijing DIANZI KEXUE XUEKAN [JOURNAL OF ELECTRONICS] in Chinese  
Vol 7 No 1, Jan 85 pp 1-12

TEXT OF ENGLISH ABSTRACT: A computerized technique including time sampling  
and phase adjustment is developed for wideband radar array imaging.  
Algorithms are given for examination of errors due to time sampling. FFT  
is introduced to speed up the imaging processing with a periodic array.  
Simulation results and experimental data are included to show the feasibility  
of the technique.

Electronics

AUTHOR: FENG Guiliang [7458 6311 5328]

ORG: Shanghai Institute of Computing Technology

TITLE: "A New Lower Bound for the Minimum Distance of Binary Goppa Codes"

SOURCE: Beijing DIANZI KEXUE XUEKAN [JOURNAL OF ELECTRONICS] in Chinese  
Vol 7 No 1, Jan 85 pp 13-19

TEXT OF ENGLISH ABSTRACT: Binary Goppa codes are a large and powerful family of error-correcting codes, but how to find the true minimum distance of binary Goppa codes has not yet been solved. Derivation of a new lower bound for the minimum distance of binary Goppa codes is given. This new lower bound improved the results obtained by Y. Sugiyama et al. (1976) and Feng Guiliang (1983). The method described can be generalized for other Goppa codes easily.



AUTHOR: WANG Kairen [3076 0418 0088]

ORG: Fudan University, Shanghai

TITLE: "Tree Decomposition FFT Algorithm"

SOURCE: Beijing DIANZI KEXUE XUEKAN [JOURNAL OF ELECTRONICS] in Chinese  
Vol 7 No 1, Jan 85 pp 20-27

TEXT OF ENGLISH ABSTRACT: The mixed time and frequency decimation FFT algorithm (MDFFT) proposed by K. Nakayama is simplified and expanded, then a new FFY algorithm based on the tree decomposition process is developed. The number of real multiplications of the new algorithm is about

$\frac{65}{64}N\log_2 N - 3N - 4$ , which is less than  $\frac{3}{2}N\log_2 N - 7N + 10\sqrt{N} - 4$  of MDFFT.

Electronics

AUTHOR: ZHOU Wenbiao [0719 2429 5903]

ORG: Institute of Electronics, Chinese Academy of Sciences

TITLE: "Field Distribution in Channel Guide"

SOURCE: Beijing DIANZI KEXUE XUEKAN [JOURNAL OF ELECTRONICS] in Chinese  
Vol 7 No 1, Jan 85 pp 48-55

TEXT OF ENGLISH ABSTRACT: A new method is presented to calculate the field distribution in the channel guide using the Weber-Schafheitlin integral and field matching method. Some numerical results are given for several cases, thus a clear view of the field distribution in the channel guide can be obtained.

Electronics

AUTHOR: KANG Liansheng [1660 6647 3932]  
ZHANG Xizhen [1728 0823 6966]  
QIU Yuhai [6726 5148 3189]

ORG: All of Beijing Observatory, Chinese Academy of Sciences

TITLE: "Interferential Method for Two-dimensional Far-field Pattern Measurement"

SOURCE: Beijing DIANZI KEXUE XUEKAN [JOURNAL OF ELECTRONICS] in Chinese  
Vol 7 No 1, Jan 85 pp 65-68

TEXT OF ENGLISH ABSTRACT: The measurements of a two-dimensional far-field pattern of antennas, to be used in the Miyun synthetic-aperture telescope, are presented. The patterns were measured by means of an inferential method with the quiet sun. The measured results are compared with the calculated ones.

Electronics

AUTHOR: SHU Shiwei [5289 1102 3956]

ORG: Institute of Electronics, Chinese Academy of Sciences

TITLE: "Accuracy and Efficiency of Fourier Transform Iterative Method for Synthesizing Pattern"

SOURCE: Beijing DIANZI KEXUE XUEKAN [JOURNAL OF ELECTRONICS] in Chinese  
Vol 7 No 1, Jan 85 pp 69-73

TEXT OF ENGLISH ABSTRACT: A Fourier transform iterative method for synthesizing a pattern was recently proposed by Feng (1980). The accuracy and efficiency of the method are analyzed, and the results show that in the shaped region the Fourier transform iterative method will converge to a desired shape, but the energy beyond the shaped region will increase as the iterative number becomes larger. As an example, synthesizing the  $\delta$  function by the method is given.

Electronics

AUTHOR: GAO Zhenming [7559 2182 2429]

ORG: Department of Electronics, Shandong University

TITLE: "A Matched Filter Using CCD for PCM"

SOURCE: Beijing DIANZI KEXUE XUEKAN [JOURNAL OF ELECTRONICS] in Chinese  
Vol 7 No 1, Jan 85 pp 74-77

TEXT OF ENGLISH ABSTRACT: A matched filter using CCD for PCM is made. The experimental results of output waveform, transfer function and output signal-to-noise ratio are given and comparisons are made with the theoretical results. The non-return-to-zero codes are realized with the output signal-to-noise ratio being 1 dB below the theoretical value.

9717

CSO: 4009/124

JPRS-CST-85-008  
27 March 1985

AUTHOR: ZHANG Limin [1728 4539 2404]  
WU Hongxing [0702 7703 5281]  
FAN Dianyuan [5400 3329 0337]  
ZHENG Yuxia [6774 3768 7209]

ORG: ZHANG and WU both of the Department of Physics, China University of Science and Technology; FAN and ZHENG both of Shanghai Institute of Optics and Fine Mechanics, Chinese Academy of Sciences

TITLE: "The Output Properties of Nd:YAG Laser Q-Switched by  $\text{LiF:F}_2^-$  Crystal of High Transmittance"

SOURCE: Hefei ZHONGGUO KEXUE JISHU DAXUE XUEBAO [JOURNAL OF CHINA UNIVERSITY OF SCIENCE AND TECHNOLOGY] in Chinese Vol 14 No 3, Sep 84 pp 352-356

TEXT OF ENGLISH ABSTRACT: Experimental research has been made of the single pulse region and the output property of the Nd:YAG laser Q-switched by a high transmittance  $\text{LiF:F}_2^-$  crystal. It is shown that the single pulse region decreases obviously and that the width of the pulse and the modulation possibility of the double axial modes in high transmittance increase. It is also shown that the application of a  $\text{LiF:F}_2^-$  crystal for a passive mode-locked laser is difficult.

Engineering

AUTHOR: YE Yunxiu [0673 0061 4423]  
HAN Rongdian [7281 2837 0368]  
WENG Huimin [5040 1920 3046]  
et al.

ORG: All of the Department of Modern Physics, China University of Science and Technology

TITLE: "The Rebuilding of  $\beta$ -Spectrometer"

SOURCE: Hefei ZHONGGUO KEXUE JISHU DAXUE XUEBAO [JOURNAL OF CHINA UNIVERSITY OF SCIENCE AND TECHNOLOGY] in Chinese Vol 14 No 3, Sep 84 pp 357-361

TEXT OF ENGLISH ABSTRACT: The ironfree double focusing  $\beta$ -spectrometer in our laboratory was designed by Professor Mei, et al., at the end of the 1950's. Due to the move from Beijing to Hefei and long-term storage, it was damaged heavily. Only the pair of main coils remained usable. We have installed new power supplies, a vacuum system, an earth magnetic field compensation system and automatic tracing system and an automatic data collection system. We have also tried dispersion compensation of the source.

Engineering

AUTHOR: LI Yongchi [2621 3057 3069]  
WANG Min [3769 2404]  
ZHOU Guangquan [0719 0342 3123]  
LIU Ruxun [0491 0320 8113]  
XU Bin [1776 1755]

ORG: LI, WANG, ZHOU and XU all of the Department of Modern Mechanics,  
China University of Science and Technology; LIU of the Department of  
Mathematics, China University of Science and Technology

TITLE: "Characteristic Calculations of the Reflection and Transmission of  
an Air Shock on Water Surface"

SOURCE: Hefei ZHONGGUO KEXUE JISHU DAXUE XUEBAO [JOURNAL OF CHINA UNIVERSITY  
OF SCIENCE AND TECHNOLOGY] in Chinese Vol 14 No 3, Sep 84 pp 376-385

TEXT OF ENGLISH ABSTRACT: By introducing the Lagrangian coordinates, a  
computational program is given for non-homoentropic flow fields involving  
multi-discontinuities based on only the  $\alpha$ - and  $\beta$ - characteristics. Calcula-  
tions of air blast shocks with different intensities colliding on the water's  
surface are completed in which a layer-to-layer cycle of the  $\alpha$ -characteristics  
is made and the pressure, as well as particle velocity, is given.



Engineering

AUTHOR: HU Defang [5170 1795 5364]  
TIAN Baoying [3944 1405 3841]

ORG: Both of the National Synchrotron Radiation Laboratory

TITLE: "Three-Dimensional Temperature Field in the 200 MeV Linear Accelerator"

SOURCE: Hefei ZHONGGUO KEXUE JISHU DAXUE XUEBAO [JOURNAL OF CHINA UNIVERSITY OF SCIENCE AND TECHNOLOGY] in Chinese Vol 14 No 3, Sep 84 pp 416-426

TEXT OF ENGLISH ABSTRACT: In this paper, using the finite element method, we calculate the three-dimensional temperature field of a constant impedance disk-loaded wave guide in the 100 MeV linear accelerator for several cooling structures and put forward the optimal feasible cooling structure and engineering design parameters.

9717

CSO: 4009/129

JPRS-CST-85-008  
27 March 1985

AUTHOR: DONG Mingde [5516 2494 1795]

ORG: Institute of Theoretical Physics, Chinese Academy of Sciences,  
Beijing

TITLE: "New Theory for Equations of Non-Fuchsian Type Representation  
Theorem of Tree Series Solution (I)"

SOURCE: Chongqing YINGYONG SHUXUE HE LIXUE [ACTA MATHEMATICS AND MECHANICS]  
in Chinese No 5, Sep 84 pp 647-663

TEXT OF ENGLISH ABSTRACT: In the analytic theory of differential equations the exact explicit analytic solution has not been obtained for equations of the non-Fuchsian type (Poincaré's problem). The new theory proposed in this paper affords for the first time a general method of finding exact analytic expression for irregular integrals.

By discarding the assumption of a formal solution of classical theory, our method consists in deriving a correspondence relationship from the equation itself and providing the analytic structure of irregular integrals naturally by a residue theorem. Irregular integrals are made up of three parts: non-contracted part, represented by ordinary recursion series, all- and semicontracted part, by the so-called tree series. Tree series solutions belong to a new kind of analytic function with the recursion series as a special case only.

AUTHOR: XIE Zhicheng [6200 1807 2052]  
YANG Xuezhong [2799 1331 1813]  
QIAN Zhendong [6929 2182 2639]  
LIU Yan [0491 3601]  
ZHANG Liping [1728 4539 1627]

ORG: All of the Department of Engineering Mechanics, Qinghua University,  
Beijing

TITLE: "Perturbation Finite Element Method for Solving Geometrically Non-linear Problems of Axisymmetrical Shell"

SOURCE: Chongqing YINGYONG SHUXUE HE LIXUE [ACTA MATHEMATICS AND MECHANICS]  
in Chinese No 5, Sep 84 pp 709-723

TEXT OF ENGLISH ABSTRACT: In analyzing the geometrically nonlinear problem of an axisymmetrical thin-walled shell, the paper combines the perturbation method with the finite element method by introducing the former into the variational equation to obtain a series of linear equations of different orders and then solving the equations with the latter. It is well known that the finite element method can be used to deal with difficult problems as in the case of structures with complicated shapes or boundary conditions, and the perturbation method can change the nonlinear problems into linear ones. Evidently the combination of the two methods will give an efficient solution for many difficult nonlinear problems and clear away some obstacles resulting from using either of the two methods solely.

The paper derives all the formulas concerning an axisymmetric shell of large deformation by means of the perturbation finite element method and gives two numerical examples, the results of which show good convergence characteristics.

Mechanics

AUTHOR: LU Yulin [0712 3768 7792]  
LAI Guozhang [6351 0948 3864]

ORG: Both of the Research Institute of Engineering Mechanics, Dalian  
Institute of Technology, Dalian

TITLE: "The Mathematical Modeling of Near Coast Shallow Water Circulation"

SOURCE: Chongqing YINGYONG SHUXUE HE LIXUE [ACTA MATHEMATICS AND MECHANICS]  
in Chinese No 5, Sep 84 pp 731-742

TEXT OF ENGLISH ABSTRACT: A finite element method for solving the shallow  
water circulation problem numerically is presented.

The continuity equation and momentum equation, considering the Coriolis  
effect, bottom friction and eddy viscosity, are integrated vertically. Using  
Galerkin's weighted residual method, the weak variational formulation is  
derived for the finite element analysis. The split-time method is applied  
for the numerical integration instead of iteration for nonlinear terms.  
Moreover, an artificial smooth approach is proposed to suppress the short  
wavelength noise.

In order to save computer storage units, a dense storage scheme is formed  
where all the zero elements in large scaled and sparse matrices are excluded.

9717

CSO: 4009/114

AUTHOR: GUO Kangmin [6665 1660 3046]

ORG: Harbin Turbine Works

TITLE: "A Relation Between the Atomic Radius of Crystal and the Radial Distribution of the Electron in Isolated Atom"

SOURCE: Wuchang FENZI KEXUE YU HUAXUE YANJIU [JOURNAL OF MOLECULAR SCIENCE] in Chinese No 1, Mar 84 pp 65-70

TEXT OF ENGLISH ABSTRACT: Slater's approximation eigenfunction has been used for calculating the maximum radial probability radius  $r_m$  of the electron in the outermost orbital in isolated atom. The relation between the atomic radius  $R_0$  of crystal and the  $r_m$  can be written as:

$$\frac{1}{R_0} = C + D \frac{1}{r_m} .$$

The C value is the same for all crystals of elements in an identical group as the D value.

Molecular Science

AUTHOR: QIU Peihua [6726 0160 5478]  
CHEN Shuchun [7115 6615 2504]

ORG: Both of Shanghai Institute of Optics and Fine Mechanics, Chinese Academy of Sciences

TITLE: "Studies on the Spectra of Infrared Laser-Dyes. I. Molecular Structure and Spectral Properties"

SOURCE: Wuchang FENZI KEXUE YU HUAXUE YANJIU [JOURNAL OF MOLECULAR SCIENCE] in Chinese No 1, Mar 84 pp 93-98

TEXT OF ENGLISH ABSTRACT: The absorption and fluorescence spectra and relaxation time of excited state molecules of several dyes with different structures are investigated experimentally. The spectral properties of infrared laser- and mode-locked dyes are also discussed.

9717

CSO: 4009/97

AUTHOR: WANG Wenzhi [3769 2429 6347]

ORG: South China Sea Institute of Oceanology, Chinese Academy of Sciences

TITLE: "A Spectro-analysis of the Sea Waves in the Gulf of Tonkin after a Cold Air Current"

SOURCE: Beijing NANHAI HAIYANG KEXUE JIKAN [NANHAI STUDIA MARINA SINICA]  
in Chinese No 2, Oct 81 pp 79-92

TEXT OF ENGLISH ABSTRACT: Based on 12 wave records from one station in the Gulf of Tonkin following a cold air current, a spectro-analysis has been made and some correlation function graphs, spectrum patterns and other computations are presented. Discussions of the characteristics of the spectra and of the effects of the "drifting of zero line" on the spectra promise a method to eliminate the mentioned effects. The coefficients of the spectrum width are calculated and compared according to two formulas. Also, the wave heights and mean periods are computed from the spectra, and both computed values are compared with the measured values.

9717

CSO: 4009/119

AUTHOR: CHEN Junchang [7115 0193 2490]

ORG: South China Sea Institute of Oceanology, Chinese Academy of Sciences

TITLE: "The Apparent Ocean Wave Spectrum and Its Estimation"

SOURCE: Beijing NANHAI HAIYANG KEXUE JIKAN [NANHAI STUDIA MARINA SINICA]  
in Chinese No 3, Jul 82 pp 73-80

TEXT OF ENGLISH ABSTRACT: The present paper suggests a concept of an "apparent ocean wave spectrum." The "ocean wave spectrum" is commonly used to describe the distribution rules of ocean wave energy with frequency with respect to the inner structure, while in this paper the "apparent ocean wave spectrum" refers to the distribution rules of apparent ocean wave energy with frequency with respect to the outer appearance. Bretschneider (1963) analyzed the energy distribution of apparent ocean waves, but he mixed up energy distribution of this kind of apparent ocean wave with the commonly used "ocean wave spectrum."

Using a method somewhat different from that of Bretschneider, the author has estimated the "apparent ocean wave spectrum." The paper suggests that there must be some relationship between the inner structure of matter and its outward appearance, although it is difficult to establish this relationship theoretically for the time being. However, based on the actual data of 16 groups, it seems that a certain relationship between the "apparent ocean wave spectrum" and the commonly used "ocean wave spectrum" can be found: their spectrum curves are approximate, their tendencies are basically similar. Therefore, it is considered that the concept established by the author bears at least a value of application, although there are still many problems to be discussed further.

9717

CSO: 4009/120



AUTHOR: LIU Shao [0491 7300]  
QIN Peiling [4440 0160 3781]  
WU Liangji [0702 5328 1015]

ORG: All of the South China Sea Institute of Oceanology, Chinese Academy of Sciences

TITLE: "A Discussion of the Uranium Concentration and Its Isotopic Composition in Seawater Samples from the Northeastern South China Sea"

SOURCE: Beijing NANHAI HAIYANG KEXUE JIKAN [NANHAI STUDIA MARINA SINICA] in Chinese No 5, Apr 84 pp 41-49

TEXT OF ENGLISH ABSTRACT: Uranium concentration and  $U^{234}/U^{238}$  activity ratios have been determined in eight seawater samples (six of which were collected from surface and bottom layers separately) from the northeastern South China Sea, using the alpha-spectrometer method for determinations for the first time. As a result, two mean values are obtained:

- (1) In seawater with higher salinity (33.956 per-thousandth), the uranium concentration is  $3.34 \pm 0.20 \mu g l^{-1}$ .
- (2) The  $U^{234}/U^{238}$  activity ratio is  $1.15 \pm 0.06$ .

9717

CSO: 4009/121

AUTHOR: HE Yueqiang [0149 1878 1730]  
LI Xinlong [2621 2450 7893]

ORG: HE of the South China Sea Institute of Oceanology, Chinese Academy of Sciences; LI of Zhejiang University

TITLE: "Correlated Regression Analyses of the Heavy Metal Elements and Environmental Factors as Media in the Bottom Sediments of Zhujiang Estuary"

SOURCE: Beijing NANHAI HAIYANG KEXUE JIKAN [NANHAI STUDIA MARINA SINICA] in Chinese No 5, Apr 84 pp 121-131

TEXT OF ENGLISH ABSTRACT: Based on the data of samples collected from 29 stations in the Zhujiang (Pearl River) estuary during 1977-1978, we have conducted the correlated regression analyses of the heavy metal elements with the environmental factors as media in the bottom sediments. Conclusions are as follows:

1. The correlation between the heavy metal contents in the bottom sediments and the bottom physical-chemical factors, such as temperature, salinity and pH, are not apparent except for the correlation between Cu, Hg and dissolved oxygen as well as between Hg and salinity.
2. Cn, Pb, Cr, Hg, Cd and As contents in the bottom sediments should correlate positively with the contents of clay, organic substances and sulfide, but not with those of Zn.
3. By using the gradual regression equation, results would better reflect the actual conditions because the calculation of heavy metals is more accurate with this equation than with the monadic regression equation. Therefore, it is preferable to estimate the contents of bottom clay, organic substances and sulfide with the gradual regression equation and to calculate the contents of heavy metals in the bottom sediments.

Oceanology

AUTHOR: LUO Weiquan [5012 0251 2938]  
CHEN Guoqing [7115 0948 3732]

ORG: Both of the South China Sea Institute of Oceanology, Chinese Academy of Sciences

TITLE: "Study of the Forms of Mercury Occurrence in the Guangzhou Section of the Main Stream of the Zhujiang"

SOURCE: Beijing NANHAI HAIYANG KEXUE JIKAN [NANHAI STUDIA MARINA SINICA] in Chinese No 5, Apr 84 pp 133-137

TEXT OF ENGLISH ABSTRACT: The forms of mercury occurrence in the Guangzhou section of the main stream of the Zhujiang (Pearl River) have been studied. The results are as follows:

1. In this section, the surface layer of the water body contains a higher content of suspended mercury than of dissolved mercury. At all stations the former ranges from 0.011-0.060  $\mu\text{g/l}$ , accounting for more than 62.5 percent of the total mercury in the water, while the latter ranges from 0.003-0.009  $\mu\text{g/l}$ . It is therefore concluded that the suspended mercury is the main form of mercury migration in the surface layer of this water body.
2. In the Guangzhou section, the suspended mercury contents decrease going downstream, while those of dissolved mercury decrease going upstream.
3. At most stations, the inorganic dissolved mercury contents in the surface water are higher than those of organic dissolved mercury at the same station.
4. The average suspended mercury (0.023  $\mu\text{g/l}$ ) obtained during the dry season is less than that (0.036  $\mu\text{g/l}$ ) obtained during the rainy season.
5. The total mercury content from all stations is rather low, ranging from 0.016-0.064  $\mu\text{g/l}$ , with an average value of 0.037  $\mu\text{g/l}$ . Therefore, we conclude that the mercury pollution in the Guangzhou section of the Zhujiang is very weak.

9717

CSO: 4009/122

JPRS-CST-85-008  
27 March 1985

AUTHOR: FANG Xinhua [2455 2946 5478]  
WANG Jingming [3769 2529 2494]

ORG: Both of the Department of Physical Oceanology and Marine Meteorology

TITLE: "The Effect of Water Compressibility on Oceanic Internal Waves"

SOURCE: Qingdao SHANDONG HAIYANG XUEYUAN XUEBAO [JOURNAL OF SHANDONG COLLEGE OF OCEANOLOGY] in Chinese No 3, 15 Sep 84 pp 13-18

TEXT OF ENGLISH ABSTRACT: The effect of compressibility on oceanic internal waves is considered by means of order analysis. It is shown that water compressibility must be taken into account even at thermocline in the upper ocean. The effect appears only in the formula calculating  $N$ . In deep water,  $O(N) = 10^{-4} \text{ sec}^{-1}$ , north component of coriolis forces,  $f_2$  should not be omitted and it acts together with  $k_2$ , north component of wave-number, as a complex factor ( $f_2 k_2$ ). Instead of  $f < \omega < N$ , the internal wave frequency interval relates to  $(f_2 k_2)$ .

9717

CSO: 4009/99

AUTHOR: LIU Liren [0491 4539 0086]

ORG: Shanghai Institute of Optics and Fine Mechanics, Chinese Academy of Sciences

TITLE: "Coded-grating Fourier-transformation Diffraction Interferometry with Extended Polychromatic Illumination: Theory"

SOURCE: Shanghai GUANGXUE XUEBAO [ACTA OPTICA SINICA] in Chinese Vol 4 No 11, Nov 84 pp 970-978

TEXT OF ENGLISH ABSTRACT: A new type of interferometry based on Fourier-transformation diffraction of coded gratings with an extended polychromatic illumination is proposed. In the system two coded gratings are inversely imaged to each other by a lens, and the tested phase object is placed between and imaged onto an observation screen. The intensity of a certain image point is related to the phase variations in the corresponding part of the objective Fourier-spectrum of the coded grating encounters. Because of dispersion the resulting interferogram is colored. Thus, various forms of interference can easily be obtained by using different coded gratings. The system is analyzed in detail by the Fresnel first-order diffraction theory, consequently a generalized conclusion is drawn. The relationships among the patterns of coded gratings, their Fourier-transformations and the possible forms of interference are discussed. Experiments are described, too.

## Optics

AUTHOR: WU Zhengliang [0702 2973 0081]  
SHU Juping [5289 5468 0988]  
YE Lin [0673 7207]  
YANG Guang [2799 0342]

ORG: All of Shanghai Institute of Optics and Fine Mechanics, Chinese Academy of Sciences

TITLE: "Study on Spectral and Lasing Characteristics of a New Tautomeric Laser Dye Kiton Red"

SOURCE: Shanghai GUANGXUE XUEBAO [ACTA OPTICA SINICA] in Chinese Vol 4 No 11, Nov 84 pp 990-993

TEXT OF ENGLISH ABSTRACT: A new tautomeric laser dye, Kiton red, has been synthesized. Its spectral and lasing characteristics have been measured. The data obtained in our experiments show that the absorption maximum for Kiton red is at 568 nm, while the fluorescence maximum is at 593 nm. The laser threshold is low and the efficiency is over 40 percent. Therefore, it may be used as a tunable laser dye in the red region of the spectrum.

AUTHOR: YIN Lifeng [3009 4539 1496]  
HU Qiguan [5170 0120 6898]  
SHU Haizhen [5289 3189 3791]  
LIN Fucheng [2651 4395 2052]

ORG: All of the Shanghai Institute of Optics and Fine Mechanics, Chinese Academy of Sciences

TITLE: "The Nonresonant Photoelectric Effect in a Hollow Cathode Discharge Tube Irradiated by Intensive Pulse Laser"

SOURCE: Shanghai GUANGXUE XUEBAO [ACTA OPTICA SINICA] in Chinese Vol 4 No 11, Nov 84 pp 994-1000

TEXT OF ENGLISH ABSTRACT: The characteristics of the nonresonant photoelectric effect signal in a hollow cathode discharge tube irradiated by an intensive laser pulse have been studied theoretically and experimentally. It is shown that this effect can be used to investigate the multiphotoelectric effect and to measure the discharged plasma parameters. It also provides a powerful experimental demonstration for studying the pulse optogalvanic principle.

## Optics

AUTHOR: PAN Shaohua [3382 1421 5478]

ORG: Institute of Physics, Chinese Academy of Sciences

TITLE: "Tuning Range and Critical Behavior of Lasers with Tunability Over Wide Range"

SOURCE: Shanghai GUANGXUE XUEBAO [ACTA OPTICA SINICA] in Chinese Vol 4 No 11, Nov 84 pp 1001-1005

TEXT OF ENGLISH ABSTRACT: By employing the semiclassical theory of lasers, a relationship between the frequency tuning range and various laser parameters is given in this article. It is demonstrated that the width of the tuning range not only depends on the gain profile, but also on the following factors: the sensitivity of frequency selecting elements, relative level of laser output power, the linewidth of selected modes, and the operating configuration of the laser.

The output characteristics of lasers at the critical frequencies, i.e., at the boundary of the tuning range, are analyzed in detail as well. It is shown that the intensity of the selected modes varies slowly when the frequency is tuned in the tuning range, but decreases rapidly when it is tuned out of the boundaries of the tuning range, i.e., the energy of the laser oscillator is rapidly transferred from the selected modes to non-selected modes which will grow around the center of the gain curve. Therefore, the common experimental phenomena mentioned above are explained theoretically.



AUTHOR: XIAO Chaoliang [5135 6389 0081]

ORG: Institute of Physics, Chinese Academy of Sciences

TITLE: "Theory of Width Effect of Isogyres of Crystals with Large Optical Axis Angle and Optical Orienting Method with Fast Rate"

SOURCE: Shanghai GUANGXUE XUEBAO [ACTA OPTICA SINICA] in Chinese Vol 4 No 11, Nov 84 pp 1035-1042

TEXT OF ENGLISH ABSTRACT: In the present paper the width effect of isogyres on the convergence polarization interference diagram of crystals with high refractive index and a large optical angle is considered. By increasing the deviation angle of isogyres from the vision field of the polarization microscope and obtaining the solution of the deviation angle of the isogyres hyperbola from the vision field, the precision of optical orientation is increased significantly. The theory of isogyres involving the width effect is demonstrated and the accurate isogyres equation is derived from a wave surface diagram orthoprojection. The precision solution of the equation of isogyres hyperbola deviating from, leaving or contacting the vision field is obtained and confirmed by experimentation. It is shown that this orientation method for crystals with a large optical angle is convenient, good and valid.

9717

CSO: 4009/93

JPRS-CST-85-008  
27 March 1985

AUTHOR: XUAN Yixiong [8983 0076 7160]  
WU Xiurong [0702 4423 2837]

ORG: Both of the Department of Pharmacology, Zhongshan Medical College,  
Guangzhou

TITLE: "Purification and Toxicological Identification of Fraction VIII-2  
from the Venom of Ophiophagus Hannah"

SOURCE: Beijing YAOXUE XUEBAO [ACTA PHARMACEUTICA SINICA] in Chinese No 10,  
20 Oct 84 pp 721-726

TEXT OF ENGLISH ABSTRACT: The Ophiophagus hannah venom has been fractionated by chromatography on CM-Sephadex C-25 into 20 fractions. Fraction VIII-2 was purified by gel filtration on Sephadex G-50, ion-exchange rechromatography on CM-Cellulose 32 and reuse of Sephadex G-50. Homogeneity was proved by three different kinds of polyacrylamide gel electrophoresis. Its molecular weight, calculated from the measurement in SDS-polyacrylamide gel electrophoresis, is 7,827. The isoelectric point is about 7.6 by isoelectric focusing. The LD<sub>50</sub> for mice (i p) is 0.155 mg/kg (0.146-0.165 mg/kg).

Fraction VIII-2 was shown to block the neuromuscular transmission of chick biventer cervicis muscle and inhibit the acetylcholine response of the muscle after neuromuscular blockade. No effect on the response of the muscle to direct stimulation or to KCL was observed. This indicates that fraction VIII-2 is a postsynaptic neurotoxin. Its blocking action was hardly reversible after repetitive washing for six hours.

From comparison between fraction VIII-2 and  $\alpha$ -Bungarotoxin in the amino acid composition analysis, molecular weight determination, double immunodiffusion, LD<sub>50</sub> and the properties of neuromuscular blockade, it is inferred that fraction VIII-2 is a long postsynaptic neurotoxin which is similar to  $\alpha$ -Bungarotoxin.

Pharmacology

AUTHOR: ZHOU Zhaowu [0719 2507 2976]  
LIU Zhenggu [0491 6966 0942]  
DAI Changshi [2071 2490 0013]  
et al.

ORG: All of the Institute of Radiation Medicine, Academy of Military  
Medical Sciences, Beijing

TITLE: "Studies of Antiradiation Drug: Synthesis of Amino-Lipoates and  
Related Compounds"

SOURCE: Beijing YAOXUE XUEBAO [ACTA PHARMACEUTICA SINICA] in Chinese No 10,  
20 Oct 84 pp 742-747

TEXT OF ENGLISH ABSTRACT: Thirty-five amino-lipoates were synthesized and  
their antiradiation activity was investigated. The polymerizable dithiolane  
ring possibly represents the main effective part, while the side chain is  
the less effective part as it may be altered to a certain extent without  
losing antiradiation activity.

Four different routes are described for synthesizing these amino-lipoates  
with satisfactory results. Improved methods for synthesizing the inter-  
mediates are also reported.

Compounds No 2, 4, 22, 24, 25, 27, 29, 30, 31, 34 and 35, when administered  
intraperitoneally before irradiation, increased the survival rate of mice  
50-70 percent. Compounds No 24 and 27 were found to be effective when  
administered orally before irradiation, increasing the survival rate by  
40 percent. Compounds No 19, 25, 27 and 40, when administered intra-  
peritoneally after irradiation, increased the survival rate by 25-45 percent.  
All these data are statistically significant when the results are compared  
with those of the control. Compound No 10 increased the leucocyte count in  
the peripheral blood in dogs.

9717  
CSO: 4009/127

AUTHOR: CHEN Wenzhi [7115 2429 5268]  
XIE Yuyuan [6200 3022 0337]

ORG: Both of Shanghai Institute of Materia Medica, Chinese Academy of Sciences

TITLE: "Studies on Uranium Mobilization Drugs: Synthesis of Two New Types of Phosphonic Acid Chelating Agents"

SOURCE: Beijing YAOXUE XUEBAO [ACTA PHARMACEUTICA SINICA] in Chinese No 11, 29 Nov 84 pp 865-868

TEXT OF ENGLISH ABSTRACT: Two series of chelating agents containing phosphonic acid and phenolic moieties [III, 2-(bisphosphonomethyl)-aminomethyl-4-substituted phenols] and [IV, N-(substituted phenylcarbamoylemethyl)-N-phosphonomethyl glycines] were synthesized and the effect on the elimination of uranium from the body was evaluated. Three of them (III<sub>f</sub>, IV<sub>h</sub> and IV<sub>j</sub>) were shown to be more effective than tiron or phosphicine in accelerating uranium excretion in rats.

9717

CSO: 4009/126

AUTHOR: QU Wenxiao [2575 2429 1321]

ORG: Southwestern Institute of Physics, Leshan, Sichuan

TITLE: "Effect of the 'Gravitational Force' on Drift Wave Instabilities"

SOURCE: Chongqing HEJUBIAN YU DENG LIZITI WULI [NUCLEAR FUSION AND PLASMA PHYSICS] in Chinese Vol 4 No 4, 15 Dec 84 pp 193-199

TEXT OF ENGLISH ABSTRACT: The effect of the "gravitational force" varying with the poloidal and toroidal angles on drift wave instabilities is analyzed in a cylindrical magnetic configuration using the strong coupling approximation. Although the ripple of the toroidal magnetic field is very small, its effect on drift wave instabilities may not be neglected due to its high frequency. In particular, it is found that the drift waves which are stable when only the poloidal mode coupling is considered may become unstable due to the toroidal mode coupling.

## Physics

AUTHOR: WANG Zhongtian [3769 0022 1131]

ORG: Southwestern Institute of Physics, Leshan, Sichuan

TITLE: "Coil Stabilization of Axisymmetric Modes in Noncircular Tokamak Plasma"

SOURCE: Chongqing HEJUBIAN YU DENG LIZITI WULI [NUCLEAR FUSION AND PLASMA PHYSICS] in Chinese Vol 4 No 4, 15 Dec 84 pp 200-205

TEXT OF ENGLISH ABSTRACT: The axisymmetric instability of tokamak equilibria with a shaping coil system is studied using the energy principle. The problem concerning the effects of the coils on the axisymmetric stability is formulated in terms of a set of singular-differential integral equations. As a trial calculation, the effects of one coil have been studied. The computation shows that a better arrangement of the coil allows the plasma to have a larger elongation. The coil located outside the plasma torus seems to be more effective than when inside. The conducting wall stabilization has also been taken into consideration.

Physics

AUTHOR: ZHANG Cheng [1728 3397]

ORG: Institute of Plasma Physics, Chinese Academy of Sciences, Hefei, Anhui

TITLE: "Slow Compression in Minor Radius on Tokamak"

SOURCE: Chongqing HEJUBIAN YU DENGLIZITI WULI [NUCLEAR FUSION AND PLASMA PHYSICS] in Chinese Vol 4 No 4, 15 Dec 84 pp 213-218

TEXT OF ENGLISH ABSTRACT: The process of slow compression of plasma minor radius on tokamak is studied numerically in a time scale several times longer than the energy confinement time of plasma. A system of 1-D transport equations coupling with toroidal and poloidal magnetic field equations and the MHD equilibrium equation has been developed. The results are compared with those in the ideal MHD model. It is shown that, after the compression, the energy confinement time increases distinctly and the temperature rise is comparable to that evaluated by the adiabatic compression scaling. The effect on compression heating due to magnetic diffusion seems to be insignificant.

Physics

AUTHOR: ZHANG Hongyin [1728 1347 5593]  
XU Deming [1776 1795 2494]  
LI Qirui [2621 0796 3843]

ORG: All of Southwestern Institute of Physics, Leshan, Sichuan

TITLE: "Single Channel 2mm-Band Interferometer with Fundamental-Oversized Waveguide"

SOURCE: Chongqing HEJUBIAN YU DENGGLIZITI WULI [NUCLEAR FUSION AND PLASMA PHYSICS] in Chinese Vol 4 No 4, 15 Dec 84 pp 219-223, 212

TEXT OF ENGLISH ABSTRACT: The development of a single channel 2 mm-band interferometer consisting of fundamental-oversized waveguide is described. In order to reduce the attenuation of transmission in the 2 mm standard waveguide (theoretical value is about 10 dB/m), an oversized waveguide has been adopted. Some of the fundamental and oversized waveguide components used in the interferometer have been developed. They meet the needs of the experiment fairly well. Using this interferometer, the time variation of the average electron density of a low pressure pulsed plasma has been measured and the experimental results are quite satisfactory.



Physics

AUTHOR: ZHAO Xiaochun [6392 2556 4783]  
WANG Jinhe [3769 6855 3109]

ORG: Both of Southwestern Institute of Physics, Leshan, Sichuan

TITLE: "A Large Secondary Electron Emission Detector for Measuring Simultaneously Neutral and Ion Beams"

SOURCE: Chongqing HEJUBIAN YU DENGLIZITI WULI [NUCLEAR FUSION AND PLASMA PHYSICS] in Chinese Vol 4 No 4, 15 Dec. 84 pp 224-227

TEXT OF ENGLISH ABSTRACT: A large secondary electron emission detector used in a magnetic mirror device for measuring automatically and simultaneously neutral and ion injection beams is described. The simple structure of the detector and the dependence of secondary electron emission coefficients for  $H_1^+$ ,  $H_2^+$  and  $H_3^+$  in the energy range of 30 keV to 100 keV on time and energy are given. The measuring circuit and measured results are described.

Physics

AUTHOR: FENG Guangze [7458 0342 3419]  
HONG Wenyu [3163 2429 3768]  
TANG Sujun [0781 4790 4596]  
WANG Wei [3769 0251]  
YAN Derong [2518 1795 2837]

ORG: All of Southwestern Institute of Physics, Leshan, Sichuan

TITLE: "Thermal Desorption from Laser Beam Bombardment on Metal Surface"

SOURCE: Chongqing HEJUBIAN YU DENGZIZITI WULI [NUCLEAR FUSION AND PLASMA PHYSICS] in Chinese Vol 4 No 4, 15 Dec 84 pp 240-242

TEXT OF ENGLISH ABSTRACT: An experiment on thermal desorption induced by bombardment of a laser beam on stainless steel surfaces in a vacuum is described. At a laser pulse width of 50 ns and power flux of  $300 \text{ kW/mm}^2$ , the surface temperature was about 1000 K. The components of the gas from thermal desorption were analyzed by a quadruple mass spectrometer; the sample surfaces after bombardment were studied by means of a double cylindrical microscope.

9717

CSO: 4009/105

Virology

JPRS-CST-85-008  
27 March 1985

AUTHOR: ZHAO Xiaoxia [6392 1420 0204]  
CHANG Chunyan [1603 2504 3601]  
HU Gang [5170 4854]  
et al.

ORG: All of the Institute of Virology, Beijing

TITLE: "Studies of Expression of Human IFN- $\alpha$ D Genome in Mouse L Cells"

SOURCE: Beijing ZHONGGUO YIXUE KEXUEYUAN XUEBAO [ACTA ACADEMIAE MEDICINAE SINICAE] in Chinese No 6, 15 Dec 84 pp 398-401

TEXT OF ENGLISH ABSTRACT: A new plasmid has been constructed for studying expression of human IFN- $\alpha$ D genome in mouse L cells. A fragment of human IFN- $\alpha$ D genome lacking the 3' terminal noncoding sequence and a *Bam*HI fragment of HSV-I DNA containing TK gene have been inserted into plasmid pBR325. Ltk<sup>-</sup> cells were transformed with the recombinant plasmid. Synthesis of human IFN could be induced by NDV. The IFN induced could protect human cells from challenge by VSV and be neutralized by antiserum against human IFN- $\alpha$ D. The results suggest that the 3' terminal noncoding sequence may not be essential for expression and induction of interferon.

9717  
CSO: 4009/132

END